THESIS APPROVAL

GRADUATE SCHOOL, KASETSART UNIVERSITY

Master of Engineering (Civil Engineering)

DEGREE

Civil Engineering	Civil Engineering
FIELD	**DEPARTMENT**

TITLE: Strength and Fire-Resistance of Class C and Class F Fly Ash Geopolymer Paste

NAME: Mr. Tikumporn Thubpo

THIS THESIS HAS BEEN ACCEPTED BY

(Associate Professor Prasert Suwanvitaya, Ph.D.) **THESIS ADVISOR**

(Associate Professor Trakool Aramraks, Ph.D.) **THESIS CO-ADVISOR**

(Assistant Professor Wanchai Yodsudjai, Ph.D.) **DEPARTMENT HEAD**

APPROVED BY THE GRADUATE SCHOOL ON _____

(Associate Professor Gunjana Theeragool, D.Agr.) **DEAN**

THESIS

STRENGTH AND FIRE-RESISTANCE OF CLASS C AND CLASS F FLY ASH GEOPOLYMER PASTE

TIKUMPORN THUBPO

A Thesis Submitted in Partial Fulfillment of
the Requirements for the Degree of
Master of Engineering (Civil Engineering)
Graduate School, Kasetsart University
2013

Tikumporn Thubpo 2013: Strength and Fire-Resistance of Class C and Class F Fly Ash Geopolymer Paste. Master of Engineering (Civil Engineering), Major Field: Civil Engineering, Department of Civil Engineering.
Thesis Advisor: Associate Professor Prasert Suwanvitaya, Ph.D. 115 pages.

The research presents the results of a study on the compressive strength of geopolymers produced using Class C fly ash (CFA) and Class F fly ash (FFA) when subjected to elevated temperatures. The geopolymers used were synthesized with sodium silicate (Na_2SiO_3) and sodium hydroxide (NaOH) solutions, and specimens included three concentrations of NaOH (4, 8, and 12 M); the fly ash content ranged from 50, 55, 60, 65 and 70 percent by weight. A 10 mm-thick geopolymer panel was used for the fire resistance tests.

From the experimental results reported in this study, it can be concluded that the thermal stability of fly ash-based geopolymer is dependent on the concentration of NaOH and the fly ash content. The thermal stability of the geopolymer materials prepared with high concentrations of NaOH was quite low. Materials prepared using high fly ash content had better thermal stability than geopolymers prepared using low fly ash content. Geopolymer materials prepared using low concentrations of NaOH and high fly ash content showed good fire resistance as well as low heat conduction through the geopolymer, especially in temperatures above 800°C. The strength loss and fire resistance characteristics showed improvement when the NaOH concentration was decreased and the fly ash content increased. This study demonstrated that the loss of compressive strength of fly ash-based geopolymer when exposed to firing was associated with a significant increase in average pore size, and that, consequently, elevated temperature strength is dependent on pore size and the total porosity percentages of geopolymer paste specimens.

_____ _____ __ / __ / __

Student's signature Thesis Advisor's signature

ACKNOWLEDGEMENTS

This research would not have been successful without the help, support and guidance rendered by many people who were directly or indirectly involved in this work. I would like to express my sincere gratitude and appreciation to my thesis advisor Assoc.Prof.Dr. Prasert Suwanvitaya for his advice at all stages of work, strong support and insight provided throughout the research period. My sincere appreciation is also due to Associate Professor Dr.Trakool Aramraks for his invaluable suggestions. The acknowledgements are also extended to Assoc.Prof. Patcharaporn Suwanvitaya of faculty of Environmental Engineering, Kasetsart University for sharing their ideas, suggestions and support with the experimental facilities.

I would like to thank the Civil Engineering Laboratory, Kasetsart University and the Laboratory, Royal Irrigation Department.who provided the experimental equipment for this research and also the staff of the International Graduate Program in Civil Engineering (IPCE), Kasetsart University for the opportunity to study, and for the continuous finacial support. The author also wishes to express his thanks to Kasetsart University for the great opportunity over the years.

Finally, the author is deeply grateful to his parents and his friends, whom continuously gave great support of all kinds and inspiration, especially Miss. Phimluk Sapsongsaeng and Mr. Panya Klongassornkul for coperation and help during experimental work.

Tikumporn Thubpo

May 2013

TABLE OF CONTENTS

Page

TABLE OF CONTENTS	i
LIST OF TABLES	ii
LIST OF FIGURES	v
LIST OF ABBREVIATIONS	x
INTRODUCTION	1
OBJECTIVES	3
LITERATURE REVIEW	5
MATERIALS AND METHODS	28
Materials	28
Methods	29
RESULTS AND DISCUSSION	40
CONCLUSION AND RECOMMENDATION	70
Conclusion	70
Recommendation	72
LITRATURE CITED	73
APPENDICES	76
Appendix A Tables	77
Appendix B Figures	101
CURRICULUM VITAE	115

LIST OF TABLES

Table		Page
1	Chemical requirements for fly ash classification	12
2	Composition of fly ash as determined by XRF (mass %)	28
3	Details of mix proportions for geopolymer made with fly ash classes F and C.	30
4	Proportional of NaOH	32
5	Ratio mixtures of geopolymer paste, tested for porosity and pore-size distribution using MIP experimentation.	60
6	Total porosity and pore size distribution of geopolymer paste	61

Appendix Table

A1	Mixture composition in terms of molar ratio	78
A2	Compressive strength of specimens after thermal exposure for class F fly ash	78
A3	Compressive strength of specimens after thermal exposure for class C fly ash	80
A4	Residual strength of specimens after thermal exposure for class F fly ash	81
A5	Residual strength of specimens after thermal exposure for class C fly ash	82
A6	Result of thermal conductivity testing after exposure for geopolymer-paste panels. Mix F1, 4M, Class F fly ash 50%	82
A7	Result of thermal conductivity testing after exposure for geopolymer-paste panels. Mix F2, 8M, Class F fly ash 50%	83
A8	Result of thermal conductivity testing after exposure for geopolymer-paste panels. Mix F3, 12M, Class F fly ash 50%	85

LIST OF TABLES (Continued)

Appendix Table		Page
A9	Result of thermal conductivity testing after exposure for geopolymer-paste panels. Mix F4, 4M, Class F fly ash 55%	86
A10	Result of thermal conductivity testing after exposure for geopolymer-paste panels. Mix F5, 8M, Class F fly ash 55%	87
A11	Result of thermal conductivity testing after exposure for geopolymer-paste panels. Mix F6, 12M, Class F fly ash 55%	88
A12	Result of thermal conductivity testing after exposure for geopolymer-paste panels. Mix F7, 4M, Class F fly ash 60%	89
A13	Result of thermal conductivity testing after exposure for geopolymer-paste panels. Mix F8, 8M, Class F fly ash 60%	90
A14	Result of thermal conductivity testing after exposure for geopolymer-paste panels. Mix F9, 12M, Class F fly ash 60%	91
A15	Result of thermal conductivity testing after exposure for geopolymer-paste panels. Mix C1, 4M, Class C fly ash 60%	92
A16	Result of thermal conductivity testing after exposure for geopolymer-paste panels. Mix C2, 8M, Class C fly ash 60%	93
A17	Result of thermal conductivity testing after exposure for geopolymer-paste panels. Mix C3, 12M, Class C fly ash 60%	94
A18	Result of thermal conductivity testing after exposure for geopolymer-paste panels. Mix C4, 4M, Class C fly ash 65%	95
A19	Result of thermal conductivity testing after exposure for geopolymer-paste panels. Mix C5, 8M, Class C fly ash 65%	96
A20	Result of thermal conductivity testing after exposure for geopolymer-paste panels. Mix C6, 12M, Class C fly ash 65%	97
A21	Result of thermal conductivity testing after exposure for geopolymer-paste panels. Mix C7, 4M, Class C fly ash 70%	98

LIST OF TABLES (Continued)

Appendix Table		Page
A22	Result of thermal conductivity testing after exposure for geopolymer-paste panels. Mix C8, 8M, Class C fly ash 70%	99
A23	Result of thermal conductivity testing after exposure for geopolymer-paste panels. Mix C9, 12M, Class C fly ash 70%	100

LIST OF FIGURES

Figure		Page
1	Temperature versus time relationship of a standard fire. (ASTME119, ISO 834, Eurocode EN1991-1-2).	15
2	ASTM E 119 Time temperature curve	17
3	SEM micrographs of the fractured surface of a fly ash geopolymer before and after high-temperature exposure.	22
4	Mercury intrusion porosimetry data showing pore size, distributions of metakaolin and fly ash geopolymers at 3 days	23
5	One-dimensional heat conduction through a plane wall	25
6	Prepared fly ash, Class C and Class F	31
7	Prepared sodium hydroxide solution, stored until required for use.	31
8	Prepared sodium silicate solution	32
9	Procedure for mixing: (a) The NaOH and fly ash first mixed together in a bowl; (b) the addition of sodium silicate solution.	33
10	Geopolymer paste cast in moulds. (a) Geopolymer paste placed in PVC pipe moulds for thermal stability tests; (b) Geopolymer paste placed in wooden frame moulds for fire resistance tests.	34
11	Specimens carefully marked and sealed before curing and analysis. (a) The cylindrical samples kept for thermal stability tests; (b) The panel samples kept for fire resistance tests.	35
12	Experimental set up for thermal stability tests: (a) Specimens prior to placement in the furnace; (b) Start of the test; (c) The furnace extinguished after 3hrs; (d) After thermal exposure compressive-strength tests performed on specimens.	37
13	Experimental set up for fire resistance test	39
14	Compressive strength test results for geopolymer-paste specimens made using Class F fly ash at content ratios of 50, 55 and 60% with various NaOH concentrations, post thermal exposure at 28 days	42

LIST OF FIGURES (Continued)

Figure		Page
15	Compressive strength test results for geopolymer-paste specimens made using Class C fly ash at content ratios of 60, 65 and 70% with various NaOH concentrations, post thermal exposure at 28 days	43
16	Residual strength results for geopolymer-paste specimens made using Class F fly ash at content ratios of 50, 55 and 60% with different NaOH concentrations, post thermal exposure at 28 days	46
17	Residual strength results for geopolymer-paste specimens made using Class C fly ash at content ratios of 60, 65 and 70% with different NaOH concentrations, post thermal exposure at 28 days	46
18	Fire resistance test results for geopolymer-paste panels made using Class F fly ash at 28 days	48
19	Fire resistance test results for geopolymer-paste panels made using Class C fly ash at 28 days	49
20	Geopolymer-paste fire-resistance test results for specimens made using Class F fly ash at ratios 50, 55 and 60% with various NaOH concentrations, after firing	51
21	Geopolymer-paste fire-resistance test results for specimens made using different quantities of Class F fly ash with NaOH concentrations at 4, 8 and 12M, after firing	52
22	Fire-resistance test results after firing for geopolymer-paste specimens made using Class C fly ash at content ratios 60, 65 and 70% with various NaOH concentrations	54
23	Fire-resistance test results after firing for geopolymer-paste specimens made using Class C fly ash at various content ratios with NaOH solution concentrations at 4, 8 and 12M	56

LIST OF FIGURES (Continued)

Figure		Page
24	Thermal conductivity test results after exposure for geopolymer-paste panels made with various concentrations of NaOH, and using Class F fly ash (FFA) at content ratios of 50, 55 and 60% respectively, at 28 days	58
25	Thermal conductivity test results after exposure for geopolymer-paste panels made with various concentrations of NaOH, and using Class C fly ash (CFA) at content ratios of 60, 65, and 70% respectively, at 28 days	59
26	Cumulative volume of intrusion vs pore diameter in the MIP tests for the geopolymer class F fly ash before and after exposure to firing at 400°C	65
27	Cumulative volume of intrusion vs pore diameter in the MIP tests for the geopolymer class C fly ash before and after exposure to firing at 400°C	66
28	Total porosity and average pore diameter in the MIP tests for the geopolymer class F fly ash before and after exposure to firing at 400°C	67
29	Total porosity and average pore diameter in the MIP tests for the geopolymer class C fly ash before and after exposure to firing at 400°C	68
30	XRD patterns of fly ash-based geopolymer prepared using Class F and C fly ash, before and after exposure to 400°C. Q= quartz, M= mullite and C = calcite	69

LIST OF FIGURES (Continued)

Appendix Figure		Page
B1	Pore size distribution in the MIP tests for the 4M geopolymer class F fly ash 60% before exposure to firing.	102
B2	Pore size distribution in the MIP tests for the 4M geopolymer class F fly ash 60% after exposure to firing at 400°C.	103
B3	Pore size distribution in the MIP tests for the 8M geopolymer class F fly ash 60% before exposure to firing.	104
B4	Pore size distribution in the MIP tests for the 8M geopolymer class F fly ash 60% after exposure to firing at 400°C.	105
B5	Pore size distribution in the MIP tests for the 4M geopolymer class C fly ash 70% before exposure to firing.	106
B6	Pore size distribution in the MIP tests for the 4M geopolymer class C fly ash 70% after exposure to firing at 400°C.	107
B7	Pore size distribution in the MIP tests for the 12M geopolymer class C fly ash 70% before exposure to firing.	108
B8	Pore size distribution in the MIP tests for the 12M geopolymer class C fly ash 70% after exposure to firing at 400°C.	109
B9	Materials for experiment	110
B10	Hobart mixer.	110
B11	CWF1200 carbolite furnace	111
B12	Thermometer measurement and Regulator Flow-meter (LPG)	111
B13	Result of thermal stability tests for class F fly ash mixed with 4M, 8M and 12M NaOH, post thermal exposure at 200°C.	112
B14	Result of thermal stability tests for class F fly ash mixed with 4M, 8M and 12M NaOH, post thermal exposure at 300°C.	112
B15	Result of thermal stability tests for class F fly ash mixed with 4M, 8M and 12M NaOH, post thermal exposure at 400°C.	112

LIST OF FIGURES (Continued)

Appendix Figure		Page
B16	Result of thermal stability tests for class C fly ash mixed with 4M, 8M and 12M NaOH, post thermal exposure at 200°C.	113
B17	Result of thermal stability tests for class C fly ash mixed with 4M, 8M and 12M NaOH, post thermal exposure at 300°C.	113
B18	Result of thermal stability tests for class C fly ash mixed with 4M, 8M and 12M NaOH, post thermal exposure at 400°C.	113
B19	Result of fire-resistance tests after exposure for class F fly ash geopolymer-paste panels.	114
B20	Result of fire-resistance tests after exposure for class C fly ash geopolymer-paste panels.	114

LIST OF ABBREVIATIONS

Al	=	Aluminum
ASTM	=	American Standard Testing Method
Ca	=	Calcium
CFA	=	Class C fly ash
FA	=	Fly ash
FFA	=	Class F fly ash
ksc	=	Kilogram per square centimeter
Kg.	=	Kilogram
M	=	Molarity
MIP.	=	Mercury Intrusion Porosimetry
min	=	Minute
mm	=	Millimeter
NaOH	=	Sodium Hydroxide
Na_2SiO_3	=	Sodium Silicate
Si	=	Silicon
SiO_2	=	Silica
Std	=	Standard
T.C.	=	Thermal conductivity
XRD	=	X-ray Diffractometer
XRF	=	X-Ray Fluorescence
^{o}C	=	Celsius degree temperature
w/b	=	Water to binder ratio

STRENGTH AND FIRE-RESISTANCE OF CLASS C AND CLASS F FLY ASH GEOPOLYMER PASTE

INTRODUCTION

Currently, Portland cement is used widely in the construction industry; however, it releases large amounts of greenhouse gases, such as carbon dioxide (CO_2), into the atmosphere during its manufacture. Another important property of construction products is their fire resistance-fire is one of the main menaces to modern buildings and its incidence has increased in recent years. Therefore, there is a need to find alternative types of binders to produce a more environmentally-friendly product which prevents fire spreading and keeps certain elements from reaching temperatures which put the stability of buildings at risk.

In 1978 Joseph Davidovits developed a binder he called geopolymer, an alternative cementitious material which exhibits ceramic-like properties. Geopolymer can be produced by combining a pozzolanic compound or aluminosilicate source material with highly alkaline solutions. Geopolymers do not combust when exposed to fire, are durable, wear-resistant and inexpensive when compared with ordinary Portland cement (OPC). It is also well known that geopolymers have excellent performance and possess good fire resistance due to their ceramic-like properties. Consequently, geopolymers are generally believed to perform better than conventional concretes when exposed to fire.

This study aims to explore the possibility of recycling different types of fly ash, and using them as the main component in new fire-resistant block products. Fire-resistant blocks are manufactured using various combinations of fly ashes and alkaline solutions, and are considered to have an insulating capacity, in so far as they are able to contain the fire within a protected environment. In the study the new materials will be subjected to several thermal and mechanical tests in order to find their thermal stability, fire-resistance, mechanical properties, and thermal conductivity. Changes in mechanical strength, both during and after thermal

exposure, are of critical importance and will be scrutinised as part of assessing the high-temperature performance of these geopolymer blocks, especially considering these materials have structural application.

This study will concentrate on geopolymers prepared using either class F fly ash (FFA) or class C fly ash (CFA), which have different compositions and properties. The main difference between CFA and FFA is calcium content, and knowledge of the use of high-calcium fly ash (CFA) and low-calcium fly ash (FFA) produced geopolymers will benefit our understanding of their possible applications for construction purposes, as they have great potential for engineering projects in Thailand.

OBJECTIVES

The aims of this study are to investigate the thermal stability and fire-resistance of geopolymer materials–up to 800°C- when prepared using Class F fly ash (FFA) and Class C fly ash (CFA), at different NaOH mix ratios, and compare their thermal behaviour with geopolymers prepared using only those types of fly ash.

The building industry requires materials with fire resistance which prevent fires and resist heat for a minimum of three hours. It is important, therefore, to find a mix proportion which achieves the highest compressive strength, while satisfying these criteria. It is vital, then, to analyse the fire conductivity of each mix-proportion relative to its maximum compressive strength.

The specific objectives of this study are:

1. To find the effects of concentrations of NaOH solution and fly ash quantities on thermal stability.

2. To find the effects of concentrations of NaOH solution and fly ash quantities on fire-resistance and thermal conductivity characteristics.

3. To find the effects on thermal resistance caused by differences in the porosity of geopolymers, as determined by the varying concentrations of NaOH solution used in their manufacture.

Scope of Study

This research study will be performed within the scope listed below:

1. The concentrations of NaOH solution, 4, 8 and 12M NaOH, are used, and the sodium silicate/NaOH ratio kept constant at 1.00.

2. The fly ashes used in this study are of classes C and F.

3. X-Ray diffraction (XRD) and mercury intrusion porosimetry (MIP) analysis will be performed on the fly ash-based geopolymers.

4. The fire tests will be performed according to the internationally standardised (ASTM E 119) time-temperature relationship, set at 3 hours.

5. The study regarding thermal conductivity will only consider a one-dimensional heat flow in a perpendicular direction to the plane wall.

LITERATURE REVIEW

1. Geopolymer

1.1 The Term of Geopolymer

The new term, Geopolymer, is defined by Davidovit (1979) as a mineral based on a poly-sialate (Si-O-Al-O) framework structure, with alternating Si or Al tetrahedrons join in three directions through sharing all the oxygen atoms. The replacement of Al^{3+} (four-fold coordination) for Si^{4+} causes a negative charge, which needs alkalis or alkali-earths to balance, like Na^{+} ,K^{+} ,Ca^{2+} or Mg^{2+} .

Their composition can be represented by the formula:

$$M_n[-(Si\text{-}O)_z\text{-}Al\text{-}O]_n wH_2O$$

Where z is 1, 2 or 3;
M is an alkali cation, such as Potassium (K) or Sodium (Na);
and n represents the degree of polymerization.

Secondary H_2O may be formed during polymerization. Amorphous (gel-like), partially-amorphous or crystalline substances may originate depending on the character of the starting raw material and the conditions of the reaction.

The geopolymer binder is a polymer material with a chain-like molecular structure. The binders are linked by silicon and oxygen in tetrahedral form, SiO_4; and aluminum and oxygen in tetrahedral form AlO_4. This formation is called “sialate (-Si-O-Al-O-)”. It is the core structure of geopolymer, with the ordering of silica to alumina in a linked 1:1 ratio, known as “poly-sialate”. The ordering of silica to alumina in a 2:1 ratio is called “poly-sialate-siloxo”. The chain bonds are continuously linked to form a three-dimensional framework.

The Si-O-Al linkages were further defined as follows:

PS (-Si-O-Al-O-) Poly(sialate) Si:Al = 2

PSS (-Si-O-Al-O-Si-O-) Poly(sialate-siloxo) Si:Al = 4

PSDS (-Si-O-Al-O-Si-O-Si-O-) Poly(sialate-disiloxo) Si:Al = 6

In this system, the ratio of Si /Al equals two (Si:Al = 2), and the core structure is PS (Poly-sialate), called "M-PS" (M= Alkali species) . If an Na ion is used to balance the system, the resulting geopolymer –generally used in thermal insulation- is called "Na-PS". A system with a ratio of Si/Al equal to four (Si:Al = 4) has a core structure PSS (Poly-sialate siloxo), known as "M-PSS"; a K ion used to balance the system results in a geopolymer called "K-PSS", customarily used in refractory.
(Davidovits, 1991)

If Al (+3) ions replace Si (+4) ions, the silica structure needs one cation for bonding and to balance the molecule. In this case an alkaline cation with a valency of +1 is used. If the replacement equals two aluminum ions, an alkaline-earth is used as the balancing ion. The new composition material is called "Feldspar", and has a chemical structure of $M_2O.Al_2O_3.6SiO_2$ (M = alkaline species) and $MO.Al_2O_3.6SiO_2$ (M = alkaline-earth species), with a ratio of silicon/aluminum equal to six (Si:Al = 6). The crystallization of feldspar is triclinic, being linked by $(Si_3Al)O_6$ or $(Si_2Al_2)O_8$ in a

constant structure. It has less strength than the silica structure because the replacement of aluminum destroys the old strength bonding and rebuilds with one of lesser strength; in other words it weakens the covalent bond due to increased gaps in the molecular structure. To break down silica bonding a temperature of 800–1000^{o}C is required, whereas feldspar synthesis needs only 400^{o}C. The difference between geopolymer and the feldspar mineral is that geopolymer has better mechanism characteristic.

1.2 Geopolymerisation

Geopolymerisation involves a chemical reaction between various alumino-silicate oxides (in an Al^{+} four-fold coordination) and silicates under highly alkaline conditions, yielding polymetric (Si-O-Al-O) bonds. This can be presented schematically as follows:

$$n(Si_2O_5,Al_2O_2)+2nSiO_2+4nH_2O+NaOH \longrightarrow Na^{+} + n(OH)_3\text{-}Si\text{-}O\text{-}Al^{-}(OH)_2\text{-}O\text{-}Si\text{-}(OH)_3$$

(Geopolymer Backbone)

Equation 1

$$n(OH)_3\text{-}Si\text{-}O\text{-}Al^{-}(OH)_2\text{-}O\text{-}Si\text{-}(OH)_3 + NaOH \longrightarrow (Na^{+}, K^{+})\text{-}Si\text{-}O\text{-}Al^{-}O\text{-}Si\text{-}O\text{-}) + 4n\ H_2O$$

(O O O)

Equation 2

The above two reaction paths indicate that any Si-Al materials might become sources of geopolymerisation, Van Jaarveld *et al.* (1997). The structure of geopolymers could be either amorphous or crystalline, depending on the condensation temperature. Amorphous polymers are obtained at temperatures ranging from 20 to 90^{o}C, while crystalline polymers are obtained between 150- 200^{o}C. The structure of crystalline geopolymers resembles that of zeolite, Davidovits (1991).

The below reactions, (1) and (2), show that the amount of Al-Si material used depends on particle size, the extent of dissolution of the Al-Si materials, and the concentration of the alkaline solution. The geopolymer's amorphous structure is formed during the reaction (3). In most cases, however, the alumino-silicate particles are not converted totally from the solid to the gel phase. Undissolved alumino-silicate solids contained in a geopolymer could act as matrix reinforcement, Palomo *et al*. (1992).

$$\text{Al-Si materials(s)} + \text{MOH(aq)} + Na_2Sio_3\text{(s or aq)} \quad (1)$$

$$\downarrow$$

$$\text{Al-Si materials(s)} + [Mz(AlO_2)x(SiO_2)y.n\text{MOH}.mH_2O]\text{gel} \quad (2)$$

$$\downarrow$$

$$\text{Al-Si materials(s)} + [Ma((AlO_2)a(SiO_2)b.n\text{MOH}.mH_2O) \quad (3)$$

Geopolymers with an amorphous structure.

The overall process is described in four steps, Xu *et al*. (2001)

1. The dissolution of alumino-silicate in alkaline environment occurs first. When alumino-silicate minerals are subjected to a high pH environment the bonds between interlinked silicate and aluminate tetrahedrons are broken.

2. The dissolved aluminum and silicon complexes diffuse from the solid alumino-silicate surface to the inter-particle space.

3. The gel phase is formed, resulting from polymerisation between an added silicate solution and aluminum and silicon complexes.

4. The gel phase hardens due to the exclusion of spare water to form ageopolymer product.

1.3 Effect of source material on geopolymerisation

Consideration should be given to the volume of calcium, as CaO content in the source material can improve the strength of geopolymer by forming amorphously structured Ca–Al–Si gel, Yip and Van Deventer (2001) and studies Xu and Van Deventer (2000a); and Yip *et al.* (2005) found that calcium has a positive effect on the compressive strength of geopolymeric binders. When the CaO content is high the micro-structural porosity decreases, and the resulting formation of the amorphous gel (Ca–Al–Si) strengthens the final product, Van Jaarsveld *et al.* (1998); Xu and Van Deventer (2002b); Phair and Van Deventer (2001) supported the idea that compressive strength development by calcium is more likely to be achieved through enhancing silicate and polysialate network formation and hardening throughout the matrix. Liu (2005) used milled Australian slag with a high CaO content (41%) for geopolymerisation, and cured at 60^{o}C for 24h. The compressive strength did not exceed 30Mpa, but when they reduced the water ratio in sodium silicate solution the compressive strength increased. Zaharaki *et al*. (2006) used low Ca electric-arc ferronickel slag in geopolymerization and found the particle size of slag mostly effective for final compressive strength of geopolymer similat to Rahier *et al*. (2003), that decreased particle size of precursor powder increased compressive strength. Palomo *et al*. (1999), and Xu and Van Deventer (2000a), proved that calcined materials such as slag, fly ash and metakaolinite are mostly amorphous, and usually accelerate the reaction of geopolymer when compared with non-calcined materials. This can be explained in that calcined materials change from a crystalline to an amorphous structure with the subsequent storage of the extra energy. Fernandez-Jimenez *et al*. (2006) found Al and Si enrichment- in fly ash-based geopolymer can develop compressive strength. Therefore, it is critical to control Al and Si dissolution from raw materials.

1.4 Effect of alkali metals on geopolymerisation

The selection of alkali-earth cations for synthesizing geopolymer depend on various factors. The most important is the source of material used and its

application. According to Van Jaarsveld (2000) alkali-metal cations control and affect almost all stages of geopolymerisation, particularly during gel hardening and crystal formation when they contribute to the structure and formation of geopolymers. Furthermore, Duxson *et al*. (2007b) showed that the addition of potassium-hydroxide (KOH) tended to increase the degree of polycondensation in alkali-metal silicate solutions, while the addition of NaOH increased the quantity of monomeric-silicate. Phair and Van Deventer (2002); Khale and Chaudhary (2007), suggest that the limits of synthesis for strong geopolymer products are in the ranges of 0.2–0.48, 3.3–4.5, 10–25 and 0.8–1.6 for M_2O/SiO_2, SiO_2/Al_2O_3,H_2O/M_2O and M_2O/Al_2O_3 ratios respectively. However, high concentrations of silicates are required during the synthesis of geopolymers, especially when sodium-silicate is used. The concentration of soluble silicon was found to affect the distribution of porosity in metakaolin-based geopolymers; using low concentrations resulted in the formation of a dense gel, while high concentrations resulted in reduced-gel skeletal densities, Duxson *et al*. (2005b); Dombrowski *et al*. (2007) assessed the effect of calcium and its dosage on structure formation and property development; fly ash-based geopolymers showed an increased reaction degree and thus acquired higher strength. According to Lee (2002), the amount of calcium present in a geopolymeric reaction system, regardless of its initial source, is important in determining the nature of the alumino-silicate gel formed.

1.5 Factors affecting compressive strength

Compressive strength depends on various factors, as detailed below:

- Strength of the gel phase.

- The ratio of the gel phase/undissolved Al–Si particles.

- The distribution and the hardness of the undissolved Al–Si particle sizes.

- The amorphous nature of geopolymers or the degree of crystallinity.

- The surface reaction between the gel phase and the undissolved Al–Si particles.

- The % CaO, % K2O and the type of alkali.

The significance of the molar Si/Al ratio during alkaline dissolution of the individual minerals indicates that compressive strength is acquired through complex reactions between the mineral surface and the concentrated sodium silicate solution. After geopolymerisation, the undissolved particles which remain bonded in the matrix affect the final compressive strength due to the hardness of each undissolved mineral. Duxson *et al*. (2005b) believed that the amount of un-reacted material in specimens with higher silica content acted as a defect with a negative effect on strength; higher strength was recorded when the ratios SiO_2/Al_2O_3 and Na_2O/Al_2O_3 were 3.0–3.8 and about 1 respectively. Lee and Van Deventer (2002) proved that higher alkali content can promote solid dissolution but also cause alumino-silicate gel precipitation at very early stages, thus resulting in lower compressive strength. Moreover, the calcium content in fly ash-based geopolymers, as well as the water to fly ash ratio, seems to be of high importance.

2. Classification of fly ash

The American Society for Testing and Materials, ASTM C618 is used for classified coal combustion products, including fly ash. Ashes produced from coal are separated into two classes, namely C and F, with their distinction based on the total amount of SiO_2, Al_2O_3 and Fe_2O_3 present. When the sum of these components is greater than 70 (mol) %, the ash is classified as a Class F. Their properties depend on the nature of the coal and the combustion process. Class F is mostly produced from bituminous coals which have low concentration of calcium compounds. Sub-bituminous coals have higher concentrations of calcium carbonate ($CaCO_3$) and, thus, produce Class C fly ash. To classify these two classes of fly ash, the chemical requirement in Table 1 should be followed:

Table 1 Chemical requirements for fly ash classification

Chemical requirements for fly ash classification	**Class of fly ash**	
	Class F	**Class C**
Silicon dioxide (SiO_2) + aluminium oxide (Al_2O_3) + iron oxide (Fe_2O_3), min %	70	50
Sulfur trioxide (SO_3), max, %	5	5
Moisture Content, max, %	3	3
Loss on ignition, max, %	6	6

3. Properties and potential applications of fly ash-based geopolymers

Duxson *et al*. (2007c) said that the microstructure and geopolymer characteristics depend on the source of material, even though the alumino-silicate geopolymer form seems similar because the silicon bonding and aluminum binders are the same in the gel phase. Subaer and Van Riessen (2007) said the microstructure of geopolymer obviously depends on the ratio of source material, which affects the homogeneity of the geopolymer microstructure, as well as impacting thermal conductivity and compressive strength. The microstructure and properties of geopolymers depend strongly on the nature of the initial raw materials, even though the macroscopic characteristics of alumino-silicate-based geopolymers may appear similar, since the same silicon and aluminum bonding and the same gel phase binder are present, Duxson *et al*. (2007c). Through micro-structural investigations it becomes clear that the ratio of the starting materials influences the homogeneity of the geopolymer microstructure, which in turn affects thermal conductivity and compressive strength, Subaer and Van Riessen (2007).

4. The importance of analytical techniques

4.1 X-ray fluorescence (XRF) spectrometry

X-ray fluorescence (XRF) spectrometry may be used for elemental analysis of Al–Si minerals. This is a technique for classifying and assessing the volume of elements in a specimen, including solid, liquid and emulsion. A principle function of this equipment is the use of X-rays on high energy-exposed specimens, which then release photons. The photons released depend on type of elements in the specimen, which radiate specific wavelengths.

4.2 X-ray diffraction (XRD)

X-ray diffraction (XRD) provides information regarding the extent to which crystalline starting materials have reacted. X-ray diffraction (XRD) uses X-ray radiation in known wavelengths from the exposed specimen.The component and structure in specimen create diffraction of X-ray in various angle that we can analyze and classify element in specimen.

4.3 Mercury Intrusion Porosimetry (MIP)

Mercury Intrusion Porosimetry (MIP) is a well-know technique based on one property of non-wetting liquids (like mercury), namely of their not being adsorbed on the surface of solids or inside their pores. MIP can determine volume of porosity in materials such as ceramic, rock, clay and cement paste. MIP shows results, including volume and diameter of pore, pore size distribution, total porosity, theoretical pore diameter, maximum continuous pore diameter and mean pore diameter.

5. Fire resistance

Kong *et al*. (2007) found that, unlike other construction materials, the strength of some geopolymers increases after elevated temperature exposure. In fire, the materials not only get exposed to elevated temperatures, but also a certain rate of temperature increase over time, and is this also to be accommodated. The time versus temperature variation of a fire depends on the type of fire and where it occurs.

5.1 Standard fire curves

Building and structural components are generally required to be shown to withstand accidental fire. For this purpose it is necessary to adopt a standard fire curve, so that there is a common benchmark test to compare different options for building components. The most commonly adopted fire curve is the ISO 834, which differs slightly from the, also common, ASTM E119 curve. The ISO 834 curve is based on cellulose fire, and has also been adopted as the Australian (AS1530.4), Norwegian (Nordtest NT Fire 046) and Eurocode (EN1991-1-2:2002) standards. The time versus temperature relationship of the standard (cellulose) fire is shown in Fig. 1.

For many materials, the performance of the material in a fire can be determined by knowing the maximum temperature exposure of the material. However, materials which are relatively brittle, such as geopolymers and Portland cement-based concretes, are also affected by the thermal gradient developed in the material and building component. One significant parameter that affects the thermal gradient is the rate of temperature rise of the fire during the initial stages.

Hydrocarbon fire is particularly damaging for materials such as Portland cement concrete, because the rapid temperature rise causes a steep thermal gradient and the steam pressure build up in the pores can lead to explosive spalling. Therefore, unlike materials such as steel, where the actual temperature and duration of exposure are the primary factors influencing fire response, in relatively brittle materials, the rate of temperature rise is an important factor.

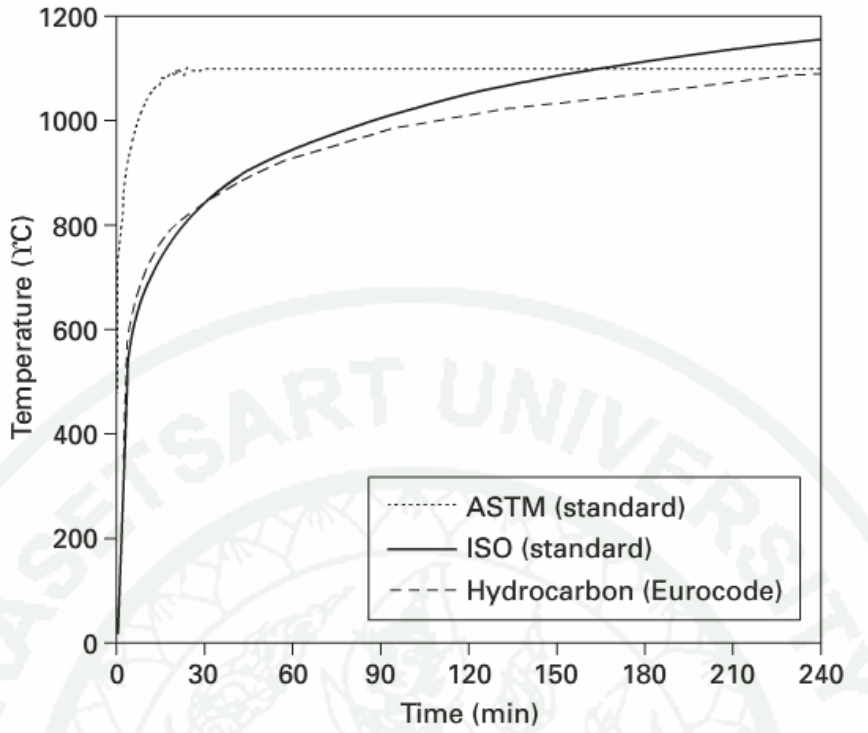

Figure 1 Temperature versus time relationship of a standard fire. (ASTME119, ISO 834, Eurocode EN1991-1-2).

5.2 Fire endurance of structure

The reinforcement of concrete and steel will decrease as temperatures increase. It can take up to three hours for heat to penetrate through the concrete cover to the steel reinforcement. It is important to point out that time required for a fire to reach the point where the reinforcing steel reaches critical strength, is dependent on the protection to the reinforcement provided by the concrete cover.

5.3 Fire resistance rating

The fire resistance rating (FRR) is used when assigning barrier or construction elements to determine and or extend the period of time -usually in hours or parts of hours- in which the building elements can meet certain criteria when exposed to the standard fire test. The criteria in tests, which determine an element's fire resistance when exposed to fire, are stability, integrity and insulation. A fire

resistance rating (or fire rating) is determined by the duration of time an assembly (roof, floor, beam or column) can endure a “standard fire” following ASTM E119.

5.4 Fire Severity

Fire severity is a measure of the destructive potential of fire; but fire severity on each occasion can be quite different, due to the many variables a combustible has, such as volume of fuel, type of fuel, volume of oxygen in each area, type of area and volume of burning area. So we used theory, utilizing the standard fire curve to compare structural characteristics and created a standard fire model to gauge specific structural fire resistances for various types of material.

5.5 History of the standard fire curve

The first standard of this curve was introduced in 1917 by the American Society for Testing and Materials (ASTM). The modified standard became ASTM E119 in 1918 (now ASTM E119, 1995).

Fire test methods are used to determine the fire-resistant properties of building components and structural assemblies. ASTM (American Society of Testing and Material) is a widely used and nationally accepted test procedure. It is designated as ASTM E119, Standard Methods of Fire Test of Building Construction and Materials, and is conducted by placing a full size assembly in a test furnace. The standard fire exposure is a defined time-temperature relationship of the fire shown in Fig. 2, and is required by ASTM E119.

This specified time-temperature relationship provides a furnace temperature of 538^{o}C five minutes from beginning the test, 704^{o}C at 10 minutes, 843^{o}C at 30 minutes, 927^{o}C at one hour, 1010^{o}C at two hours, and 1093^{o}C at four hours.

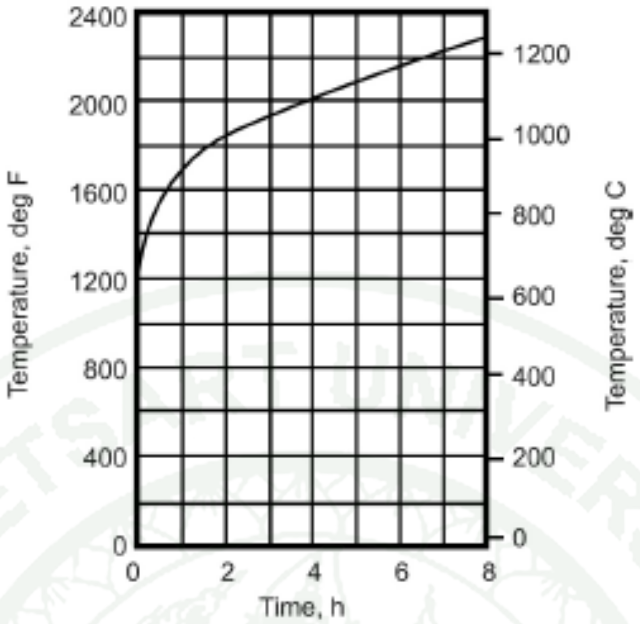

Figure 2 ASTM E 119 Time temperature curve

5.6 High temperature and fire resistance

Previous investigations by Davidovits et al. (1991, 1994, 1999) reported very good heat resistance properties in materials prepared using sodium-silicate, potassium-silicates and metakaolin, their having thermal stability up to 1200-1400°C. Barbosa and MacKenzie (2003) found that increased amounts of water and/or sodium-silicate could cause a reduction in the thermal resistance of geopolymer material when exposed to firing. In this investigation, geopolymer specimens experienced re-crystallisation to feldspars, leucite and kalsilite at 1000°C. For alkali-activated fly ashes Bakharev (2006) found that materials alkali-activated with K-containing alkaline solution presented better fire resistance than those activated with Na. Fly ash samples activated with Na-containing activators developed shrinkage, cracking and a rapid deterioration of strength at 800°C, which was connected to a dramatic increase in average pore size. Loss of strength on firing was possibly connected to the deterioration of the alumino-silicate gel. Decomposition of the alumino-silicate gel freed sodium, silicon and aluminum, producing Na-feldspars. The melting point occurred at a lower temperature if the sodium content of the specimens increased.

With respect to the behaviour of alkali-activated alumino-silicates at high temperature, geopolymers show better resistance to fire than Portland cement mortars or concrete. Gourley and Johnson (2005) indicated that as geopolymer is a network structure similar to glass, unlike OPC, which is a hydrate, resistance to heat is greatly improved. The absolute volume of water contained in the pore structure is low, and the pore structure is continuous. Thus, the mode of decomposition of geopolymers is to melt at temperatures in excess of 1000°C, rather than to explosively release water or dehydrate to a powder.

Bakharev (2006) concluded that geopolymer materials were found superior to Portland cement concretes in their thermal properties when exposed to 700-1000°C. However, according to the literature (Bakharev 2006; Krivenko and Kovalchuk 2002, 2007; Fernández-Jiménez. *et al*. 2008; Palomo *et al*. 2008; Skvara *et al.*, 2005), materials utilizing class F fly ash are not suitable for refractory applications due to high shrinkage and dramatic changes in compressive strength, possibly caused by the negative influence of large amount of iron impurities present. However, in a fire-protection context, studies show that these materials have relatively good stability and strength after firing, which is indicative of good fire resistance. More study is needed to determine heat conduction through a sample when exposed to the standard fire defined by ISO 834, as well as the relation between the thermal resistance of the protection layer and the thickness of equivalent concrete protection.

5.7 Mechanical strength evolution

The mechanical strength of geopolymer changes due to high temperature-induced structural and phase composition changes in the material. Structural changes include sintering, densification, melting, cracking and pore size/volume/ interconnectivity changes. Phase composition changes include crystal growth, crystal destruction, dehydration and geopolymer-paste decomposition to release free Si, Al and alkali.

Densification of the geopolymer results in fewer voids and allows for more uniform stress gradients during an applied load, enabling greater mechanical strength. Sintering of the un-reacted material, such as crystalline fly ash particles, provides increased mechanical strength due to stronger bonding between particles. This is especially important in geopolymers containing aggregates. The temperature of the densification and sintering is dependent on the sample's composition and the type of secondary phases.

Kong *et al.* (2007) found that pore structure changes have a mixed effect on the mechanical strength of geopolymers. Pores act as defects, and, in general, mechanical strength decreases as pore size and volume increases. However, this is not always the case. Increased pore interconnectivity allows for greater water mobility during heating, which reduces structural damage caused by vapour pressure on the pore walls. Thus geopolymers with a more interconnected pore structure will experience lower strength loss than comparable geopolymers with isolated pore structures. Pore structure is known to vary in geopolymers during thermal exposure which causes nonlinear variations in mechanical strength during heating.

Geopolymers with high shrinkage will tend to have lower mechanical strength after heating due to crack formation. Cracking increases in samples with high water content.

Geopolymers prepared with different alkali activators perform differently when exposed to elevated temperatures. Bakharev (2006) found that geopolymers prepared with a potassium activator exhibited increased compressive strength after heating to 800°C, whereas it was greatly reduced in geopolymers prepared with a sodium activator.

Dombrowski (2007) found that the addition of calcium to fly ash geopolymers increased initial compressive strength. However, it reduced the amount of strength gain upon heating to 1000°C when compared to samples without added calcium.

5.8 Phase changes at elevated temperatures

Crystallisation and phase changes have been observed to occur in geopolymers exposed to elevated temperatures. The analysis can be performed qualitatively (peak identification) or quantitatively conducted by analysis of x-ray diffraction (XRD) data. High temperatures provide the energy to induce a wide range of changes to the crystal structure and phase abundance in geopolymers. The three main changes are crystal formation, crystal destruction and crystal structure changes.

5.8.1 Phase changes in the geopolymer paste (formation and destruction)

During heating to high temperatures, decomposition of the geopolymer-paste frees Na, Si and Al species to crystallize to various zeolitic phases and alkali feldspars. The temperature for the onset of crystal growth in geopolymer-paste is variable. For example, Brabosa and MacKenzie (2003) found that geopolymers remain totally amorphous up to 1200°C, whereas Duxson (2006) observed crystallization to begin as low as 600°C.

Brabosa and MacKenzie (2003), and Bakharev (2006), found that the degree and type of crystallization in geopolymers depends on sample composition and heating conditions. Poorly reacted geopolymers have additional Na or K, Si or Al monomers not incorporated in the paste and consequently exhibit higher crystal growth during heating. Duxson *et al*. (2006) demonstrated that increased heat rates during testing, reduced the amount of crystal growth of some phases.

5.8.2 Phases formed form secondary material

Geopolymers are a composite material with crystalline phases present among the amorphous paste. The crystalline material initially present in the geopolymers can either come from the source material or the aggregate. This material is subject to phase changes during high temperature exposure, which can affect the bulk thermal properties of the geopolymer. Bakharev (2006) observed a similar

increase in hematite peak-intensity in fly ash geopolymers after exposure to 1200°C. Quartz is commonly found in geopolymers, not only as part of the aggregate but as a fine impurity in the source material, which adversely influences bulk properties such as mechanical strength.

5.9 Microstructural changes

Changes in geopolymer microstructure have been observed to affect the bulk thermal properties. Pore analysis is of interest to researchers to further understand its implications for mechanical strength and thermo-physical properties. There are a wide range of pore analysis techniques including mercury intrusion porosimetry (MIP).

Thermal exposure alters the microstructure of geopolymers in a number of ways. Sintering, crystallization and eventual melting alter the morphology of the paste at high temperatures, while dehydration and densification affect the size and distribution of the pore structure.

Dehydration causes the first microstructural change, beginning at just above ambient temperature and continuing to above 200°C. Vapour pressure from escaping water causes damage to the structure of geopolymer and alters the pore interconnectivity by creating pathways to the surface of the material. Kong *et al*. (2007) reported that metakaolin geopolymers experience more damage to the microstructure during evaporation than fly ash geopolymers due to the lower interconnectivity of the pore structure.

At higher temperatures, sintering and densification of the geopolymer paste alter the morphology as shown in Fig. 3. The post-exposure geopolymer-paste has fewer inclusions and exhibits a smoother texture than unexposed geopolymer. This is caused by the viscous sintering of the paste during high temperature exposure, which also leads to crack healing. This was also observed by Duxson *et al*. (2006) in

metakaolin geopolymers, and Bakharev (2006) and Kong *et al*. (2007) reported that the partially-dissolved fly ash particles are seen to have a porous internal structure.

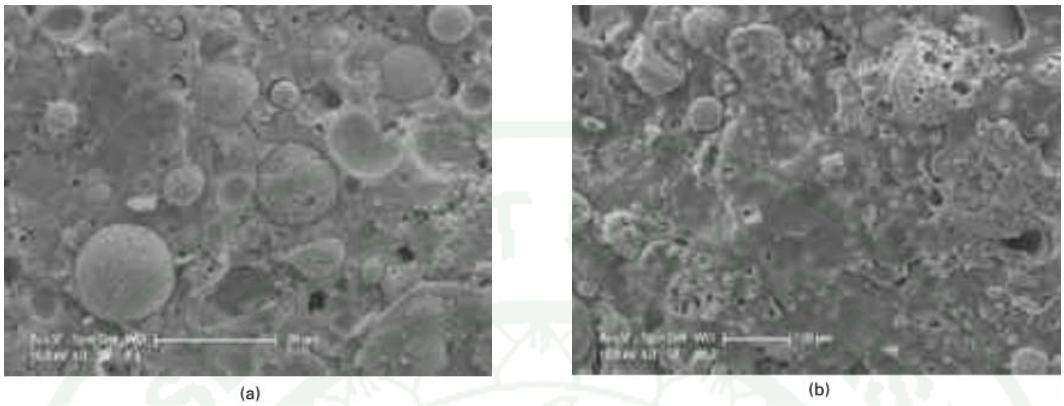

(a)Unexposed. (b) After exposure to 900°C

Figure 3 SEM micrographs of the fractured surface of a fly ash geopolymer before and after high-temperature exposure.

Source: Bakharev (2006); Kong *et al.* (2007)

5.9.1 Pore Structure evolution

Fly ash geopolymers exhibit quite different changes in pore structure compared to metakaolin geopolymers during heating. Fly ash geopolymers have smaller, more connected pores than metakaolin geopolymers that better allow water to permeate to the surface, as shown in Fig. 4.

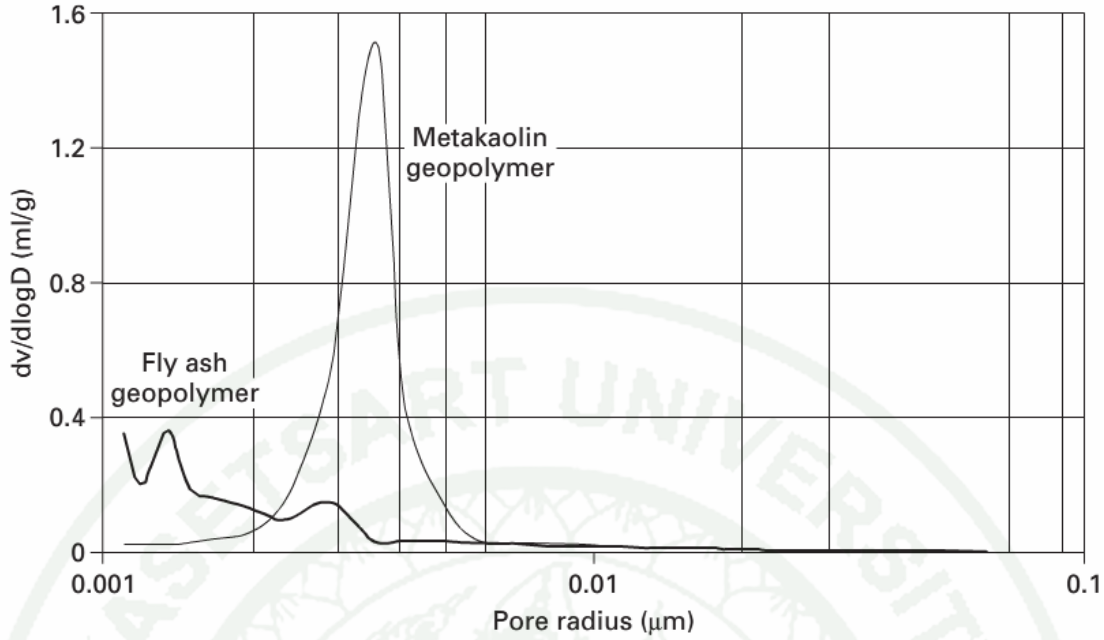

Figure 4 Mercury intrusion porosimetry data showing pore size, distributions of metakaolin and fly ash geopolymers at 3 days

Source: Kong *et al*. (2007)

Fly ash geopolymers also contain un-reacted fly ash particles that can also contain pores. During heating, the pore volume of all geopolymers increases initially as any water-filled voids empty. At higher temperatures, multiple factors influence the size and distribution of pores. Melting of the amorphous material from fly ash particles during heating exposes additional pores from within the un-reacted fly ash particles Kong *et al.* (2007). This can be seen in Fig. 4.

Bakharev (2006) found that in fly ash geopolymers the cumulative pore volume, when compared to unheated samples, increased by 26% and 29% after exposure to 800 and 1000°C respectively, and that the average pore size increased significantly.

6. Heat transfer mechanisms

Heat is defined as energy transferred by virtue of temperature difference; it flows from regions of higher temperature to regions of lower temperature. It is customary to refer to different types of heat transfer mechanism as modes. The basic modes of heat transfer are conduction, radiation, and convection.

Conduction is the transfer of heat from one part of a body at a higher temperature to another part of the same body at a lower temperature, or from one body at a higher temperature to another body in physical contact with it at a lower temperature. The conduction process takes place at the molecular level and involves the transfer of energy from the more energetic molecules to those at a lower energy level.

At the macroscopic level the heat flux (i.e., the heat transfer rate per unit area normal to the direction of heat flow) q" is proportional to the temperature gradient:

$$q'' = -k\frac{dT}{dx} \qquad (6.1)$$

where the proportionality constant k is a transport property known as the thermal conductivity and is a characteristic of the material. The minus sign is a consequence of the fact that heat is transferred in the direction of decreasing temperature. Equation 6.1 is the one-dimensional form of Fourier's law of heat conduction.

If we consider a one-dimensional heat flow in x direction, in the plane wall shown in Fig. 5, a direct application of Eq. 6.1 can be made. Integration then yields

$$q = \frac{kA}{\Delta x}(T_2 - T_1) \qquad (6.2)$$

where the thermal conductivity is considered constant, Δx is the wall thickness, and T1 and T2 are the wall-face temperatures. Note that q/A = q", where q is the heat transfer rate through an area A. Eq. 6.2 can be written in the form

$$q = \frac{T_2 - T_1}{\Delta x / kA} = \frac{T_2 - T_1}{R_{th}} = \frac{thermal}{thermal} \frac{potential}{resis\tan ce} \frac{difference}{} \qquad (6.3)$$

Where $\frac{\Delta x}{kA}$ assumes the role of a thermal resistance R_{th}.

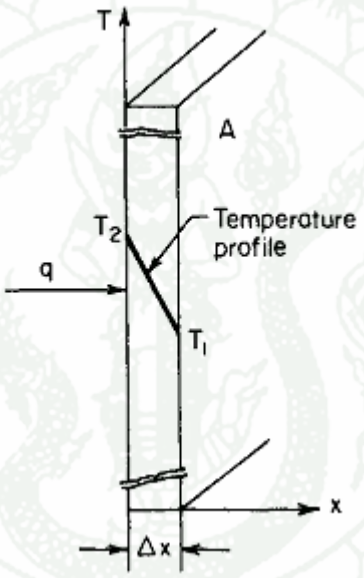

Figure 5 One-dimensional heat conduction through a plane wall

The thermal conductivity of geopolymers is measured to assess their potential application as an insulating product or a concrete building material. Insulators require a low thermal conductivity because they are designed to reduce the conduction of heat, whereas concretes require a relatively high thermal conductivity as this reduces expansion stresses within the material, Subaer (2005).

Low density geopolymer foams, designed as thermal insulators, have been produced with a thermal conductivity of 0.037 $Wm^{-1}K^{-1}$ Liefke (1999). Duxson *et al*. (2006) reported the thermal conductivity of metakaolin geopolymers as approximately

0.8 $Wm^{-1}K^{-1}$. Subaer and van Riessen's (2006) results were slightly lower than the Duxson study, ranging between 0.55 and 0.65 $Wm^{-1}K^{-1}$. The thermal conductivity values reported by Subaer and Duxson are higher than that of OPC paste which has a thermal conductivity of 0.53 $Wm^{-1}K^{-1}$, Demiborga (2003). The Subaer (2006) study found that the addition of 40 wt% quartz aggregate increased the thermal conductivity by 40% relative to metakaolin geopolymers. This is in agreement with the density dependency hypothesis, as the addition of aggregate increases the sample's bulk density.

7. Related Research

Chindaprasirt *et al*. (2006) studied on the workability and strength of geopolymer mortar made from coarse-lignite high-calcium fly ash, with sodium-hydroxide (NaOH), sodium-silicate and heat as an activator. The test result indicated that to produce a high strength geopolymer the optimum sodium-silicate to NaOH ratio was 0.67-1.00.

Leelathawornsuk (2009) researched the role of sodium-hydroxide concentration in fly ash-based geopolymer. The sodium-hydroxide used as an activator was fixed at a 4M concentration. The results depended on the proportion and properties of the fly ash. Class C fly ash-based geopolymer produced a higher compressive strength than geopolymer made using Class F.

Cheng and Chiu (2002) studied the fire-resistance of geopolymer produced by granulated blast-furnace slag. The result shows the K_2O content in the geopolymerization plays an important role. With increased K_2O content the setting time, and, consequently, the compressive strength, can be increased, and the fire-resistance characteristic improved.

Hardjito (2008) found the strength and thermal stability of fly ash-based geopolymer mortar dependent on the concentration of KOH. The result revealed that as the concentration of KOH increased, the compressive strength of the geopolymer

mortar increased; it was also found that geopolymer poses superior thermal stability at least up to 800^{o}C.

Daniel *et al*. (2007) studied effect of elevated temperature on geopolymer produced from metakaolin and fly ash of various mixture proportions. The sodium silicate and potassium hydroxide solutions were used for synthesis. This research found the strength of fly ash-based geopolymer increased after exposure to elevated temperature (800^{o}C) but the strength of metakaolin-based geopolymers decreased after similar exposure.

Arenas *et al*. (2011) studied high fire resistance in blocks containing coal-combustion fly ashes and bottom ash. They found that the replacement of fine aggregate with fly ash, and coarse aggregate with bottom ash, had a remarkable influence on fire resistance and caused no detriment to mechanical properties.

Demirboga's (2002) study on the thermo-mechanical properties of sand and high-volume mineral admixtures found thermal conductivity decreased with an increase in fly ash and blast-furnace slag as replacement for cement. Fly ash and blast-furnace slag decreased compressive strength and increased water absorption, but after a 120 day curing period saw an increase in compressive strength of 6%.

MATERIALS AND METHODS

Materials

1. The work described in this paper utilised fly ash derived from two sources: Fly ash 1 was sourced from Rayong province in the east of Thailand, and is a Class F fly ash (ASTM C618); fly ash 2 was sourced from Mae Moh Power Station in the north of Thailand, and is a Class C fly ash (ASTM C618). The chemical compositions and loss on ignition (LOI) of fly ash, as determined by X-ray Fluorescence (XRF), are given in Table 2.

Table 2 Composition of fly ash as determined by XRF (mass %)

Oxide	SiO_2	Al_2O_3	Fe_2O_3	CaO	MgO	K_2O	Na_2O	TiO_2	P_2O_5	MnO	SO_3	LOI
Fly ash1	66.07	22.68	3.28	1.23	0.57	0.94	0.33	1.3	0.31	0.03	0.21	2.61
Fly ash2	33.55	19.01	14.50	20.78	1.88	2.37	1.36	0.46	0.22	0.11	4.79	0.27

Fly ash1- Bituminous, Rayong province, Thailand

Fly ash2- Lignite, Mae Moh, Thailand

2. Sodium silicate solution, grade B (Na_2O=10.12%, SiO_2=31.19%, and water=58.69% by mass.)

3. Sodium Hydroxide (NaOH) in flake from (98% purity)

4. Water: Tap water.

5. Hobart mixer.

6. PVC pipe moulds (40x80mm)

7. Wooden frame (300x300mm)

8. Compressive strength testing machine.

9. Regulator: Flow-meter (LPG)

10. Gas cylinder (LPG)

11. Thermometer measurement with infrared thermometer.

12. Glass bowl.

13. Digital scale, 2 kg capacity with accuracy of 0.01kg

14. A stainless-steel type-K thermocouple.

15. A ceramic type-K thermocouple.

16. X-ray diffractometer (XRD)

17. Mercury intrusion porosimetry (MIP)

18. CWF1200 carbolite furnace

Methods

1. Preparation of geopolymer specimens

In this study 18 mixes -shown in Table 3-were investigated in order to optimize components using different fly ashes and alkali content in different proportions. The initial compressive strength of mixes, which may be considered as an optimum composition of the ingredients was tested.

1.1. The study divided the fly ash element into two main classes (Class F and Class C), and samples were made as shown in Fig.6, each differing in their composition. Geopolymer paste samples of both fly ash classes were prepared by varying their mix composition in order to study the effects of alkali content and varying fly ash content, and were produced as shown in Table 3.

Table 3 Details of mix proportions for geopolymer made with fly ash classes F and C.

Mix No.	Designation	Fly ash	NaOH		$Na_2O.SiO_3$ (kg/m^3)	Fly ash (kg/m^3)	Water/ binder ratio
			Molar	Mass (kg/m^3)			
F-1	4F-50	50% FFA	4	462.50	462.50	925.00	0.38
F-2	8F-50	50% FFA	8	462.50	462.50	925.00	0.35
F-3	12F-50	50% FFA	12	462.50	462.50	925.00	0.31
F-4	4F-55	55% FFA	4	416.25	416.25	1017.5	0.34
F-5	8F-55	55% FFA	8	416.25	416.25	1017.5	0.31
F-6	12F-55	55% FFA	12	416.25	416.25	1017.5	0.28
F-7	4F-60	60% FFA	4	370.00	370.00	1110.0	0.30
F-8	8F-60	60% FFA	8	370.00	370.00	1110.0	0.28
F-9	12F-60	60% FFA	12	370.00	370.00	1110.0	0.25
C-1	4C-60	60% CFA	4	370.00	370.00	1110.0	0.31
C-2	8C-60	60% CFA	8	370.00	370.00	1110.0	0.29
C-3	12C-60	60% CFA	12	370.00	370.00	1110.0	0.26
C-4	4C-65	65% CFA	4	323.75	323.75	1202.5	0.28
C-5	8C-65	65% CFA	8	323.75	323.75	1202.5	0.25
C-6	12C-65	65% CFA	12	323.75	323.75	1202.5	0.23
C-7	4C-70	70% CFA	4	277.50	277.50	1295.0	0.24
C-8	8C-70	70% CFA	8	277.50	277.50	1295.0	0.22
C-9	12C-70	70% CFA	12	277.50	277.50	1295.0	0.20

Remark: Mixture composition (kg/m^3)

Figure 6 Prepared fly ash, Class C and Class F

1.1.1 For both fly ashes, the sodium hydroxide solution 4M, 8M and 12 M was prepared by dissolving sodium hydroxide pellets in tap water, and were kept, premixed, in flasks, as show in Fig. 7. The proportion of NaOH is shown in Table 4.

Figure 7 Prepared sodium hydroxide solution, stored until required for use.

Table 4 Proportional of NaOH

NaOH concentration (M)	98% purity (g/L)
4	160
8	320
12	480

1.1.2. With Class F fly ash, the sodium hydroxide solution was prepared in terms of morality (M), in the ranges of 4, 8 and 12M of the mix, and with water/binder ratios of 0.25 to 0.38. The Class F fly ash content ratios were 50, 55 and 60 percent by weight of mix. In each fly ash mix a mass ratio Na_2SiO_3/ NaOH of 1.0 was used. The Sodium silicate solution, which has the same weight percentage of sodium hydroxide, is shown in Fig.8.

1.1.3. With Class C fly ash, the sodium hydroxide solution was prepared in terms of morality (M), in the ranges of 4, 8 and 12M of the mix, and with water/binder ratios of 0.20 to 0.31. The Class C fly ash content ratios were 60, 65 and 70 percent by weight of mix. In each fly ash mix a mass ratio Na_2SiO_3/ NaOH of 1.0 was used, the same as with Class F fly ash.

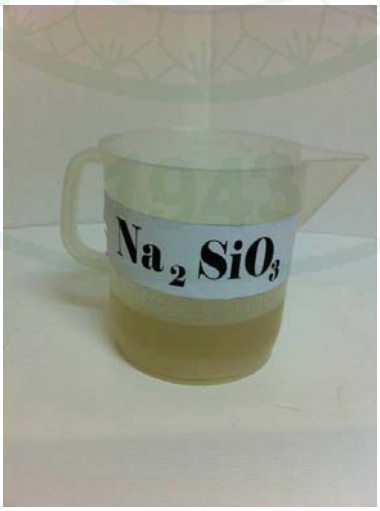

Figure 8 Prepared sodium silicate solution

2. Procedure for mixing geopolymer paste

2.1. The NaOH concentration solution for each mix was prepared at least 24 hours prior to use. The solution of NaOH and Fly ash (either Class F or Class C) - shown in Table 3-was placed in the mixing bowl and mixed by hand for 10 min, until a homogeneous mixture was achieved. This is shown in Fig.9a.

2.2. The sodium silicate solution was then added to the mixture and the bowl contents mixed for further 5 min with a mixer, until a homogeneous paste was obtained. This is shown in Fig. 9b.

2.3. The paste obtained was then placed in moulds. The paste was divided into two parts: the first was cast in 40x80 mm PVC pipe moulds in order to investigate thermal stability; the second was cast in 300x300mm wooden frame moulds, together with a type-K thermocouple, in order to record the results of fire-resistance tests. This is shown in Fig.10.

(a) (b)

Figure 9 Procedure for mixing: (a) The NaOH and fly ash first mixed together in a bowl; (b) the addition of sodium silicate solution.

2.4. The samples were taken out of the moulds after 24 hours and left to cure at an average room temperature of 30^{o}C for 27 days. Subsequently, the samples were

sealed with a film, with cylindrical samples kept in zip-lock bags to prevent moisture loss before being subjected to high temperature. This is shown in Fig. 11.

3. Test methods

In Thailand there is no current specific test or standard for evaluating the fire resistance of fly ash-based geopolymer material. However, the ASTM E119-00a standard of fire test for building construction and its materials is accepted and was used to carry out the fire testing of the geopolymer-paste specimens, along with associated laboratory testing. The time/temperature curve from the ASTM E119 test standard was used to compare the performance of currently accepted geopolymer materials in each mix.

(a)

(b)

Figure 10 (a-b): Geopolymer paste cast in moulds.
(a) Geopolymer paste placed in PVC pipe moulds for thermal stability tests; (b) Geopolymer paste placed in wooden frame moulds for fire resistance tests.

a) b)

Figure 11 (a-b): Specimens carefully marked and sealed before curing and analysis. (a) The cylindrical samples kept for thermal stability tests; (b) The panel samples kept for fire resistance tests.

3.1 Thermal stability test

Geopolymer-paste specimens were produced using the 40x80mm diameter cylinder moulds, in order to test thermal stability. All specimens were measured for compressive strength before and after exposure to fire; they were exposed to furnace fires with temperatures in the ranges of 200°C to 400°C for 3 hours at a heating rate 27 °C/min from room temperature. The compressive strength tests were performed in accordance with ASTM C109, after ageing the specimen to 28 days, using a 2,000 KN 400RD compression test machine with a loading rate of 0.33 mm/minute. At least four samples were used for each data point in these tests. A diagram of the experimental set-up for the measurement of the thermal stability is shown in Fig.12. The procedure is as follows:

After 27 days, the samples were be taken out of zip-lock bags after curing. The samples were divided into three parts. Eight samples were prepared for each mix study (i.e. 4 unexposed and 4 for elevated temperature exposure). In the first part samples were exposed to a furnace fire with a temperature of 200°C, at a heating rate 27 °C/min. After the target temperature was accomplished it was maintained for 3

hours before the specimens were allowed to cool naturally to room temperature inside the furnace. This cooling was expected to take more than 12 hours, and compressive strength tests were conducted the following day. In the second and third parts, the specimens were tested as per the above procedure, but with furnace temperatures of 300 and 400°C respectively. Meanwhile, the unexposed samples were left undisturbed at room temperature for 28 days.

3.1.1 Microstructure changes and analysis

Subsequent to the optimum mix ratios –those with the preferred thermal and compressive strength results- being chosen, the resultant specimens were then microscopically examined with X-ray diffraction (XRD) and mercury intrusion porosimetry (MIP). This procedure was as follows:

a) The X-ray diffraction (XRD) method was used to perform a phase analysis of the crystalline material initially present in the geopolymers, subject to phase changes during exposure to high temperature. The polished specimens were used. To prepare the polished specimens, 1mm thick slices were cut from cylinder samples and mounted in aluminium holders.

Diffraction patterns were acquired on a Siemens D500 Bragg-Brentano diffractometer. Operating conditions were set to 30 kV and 30 mA, Cu-K wavelengths: 1.54060 and 1.54439 A. In collecting data sets, the 2θ step size was 0.02˚, the counting time per step 0.6 s, and the 2θ range from 10 – 80. The software MDI-Jade (version 5) for peak identification and automated search and match was used to analyze the results of diffraction patterns.

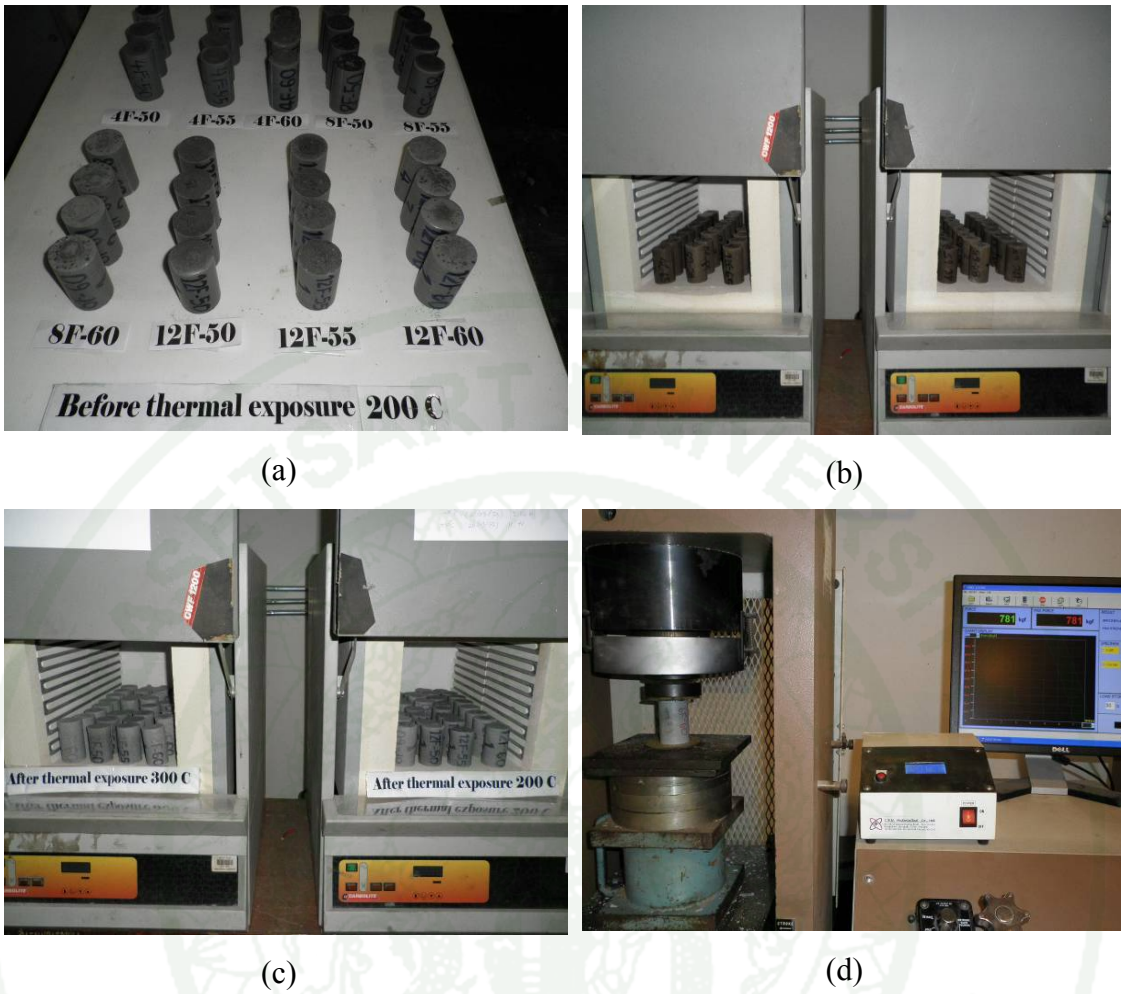

Figure 12 (a-d) Experimental set up for thermal stability tests:
(a) Specimens prior to placement in the furnace;
(b) Start of the test;
(c) The furnace extinguished after 3hrs;
(d) After thermal exposure compressive-strength tests performed on specimens.

b) Mercury intrusion porosimetry (MIP) was used to study porosity and average pore diameter before and after the firing test. Pore analysis is of interest in understanding its involvement in relation to mechanical strength and thermo-physical properties.

3.2. Fire resistance tests

For the fire-resistance tests, geopolymer panels were exposed to an 800°C flame. A diagram of the experimental set-up for the measurement of fire resistance is shown in Fig.13. All the geopolymer panels, for every composition tested, were 10mm thick, 30mm high and 30mm wide. They were placed in special furnace and subjected to a heating program that provided a fire-resistance temperature curve in accordance with the standard temperature curve, ASTM E119. A gas-fired furnace was used to study the fire-resistance of the geopolymer panels. This furnace allowed the surface temperature of the geopolymer panel's exposed surface (T_{in}) to be recorded through the use of a ceramic type-S thermocouple and a stainless steel type-K thermocouple, which were also used as controllers to produce the standard temperature curve. The temperature within the gas-fired furnace was determined using the mathematical average of the thermocouples located on the exposed surface within the gas-fired furnace and closer to horizontal face of the geopolymer test panel. On the unexposed surface (T_{out}), the temperature was registered using the average value of the type-K thermocouple and the infrared thermometer.

An additional type-K thermocouple was embedded in the geopolymer panel at the mid-point and middle thickness from the unexposed surface. The geopolymer panel was surrounded by mineral wool on its exterior perimeter to avoid the transmission of heat from the sides of the panel. Three thermocouples on the exposed and unexposed surface were connected to the thermometer system to record both temperatures (T_{in}, T_{out}). During the fire exposure tests the temperature was recorded every minute by the thermocouples in order to monitor temperature distribution. The geopolymer panel remained exposed to fire until the specimen withstood the test conditions for 35 minute. Also, the heat capacity process from the furnace was regulated using a flow meter operating at 0.0056 litres per minute.

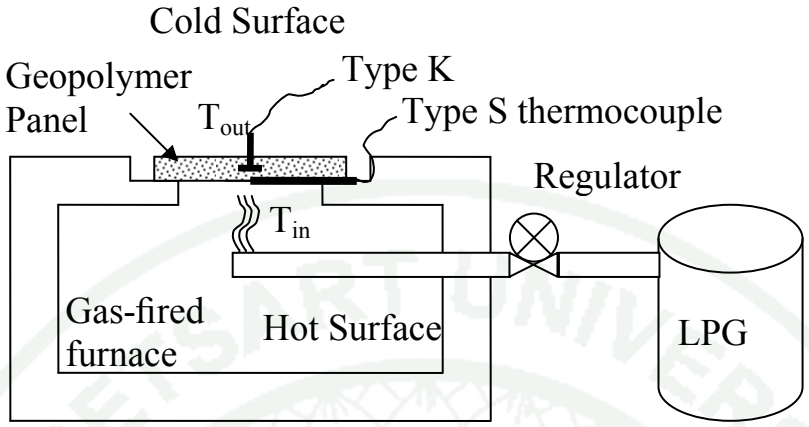

Figure 13 Experimental set up for fire resistance test

RESULTS AND DICUSSION

1. Thermal stability

Here follows the results of stability tests on the compressive strength of geopolymer-paste samples made from fly ash classes F and C. For this purpose, two identical specimens were produced and left for a period of 28 days. One specimen was then fired to temperatures of 200, 300, and 400 ^{o}C for three hours, and its compressive strength compared with the remaining, control, specimen, which had been kept at room temperature. A table is presented in Appendices Table A2 and A3.

1.1 Compressive strength at room temperature

The results of stability tests on the compressive strength of 28-day-old geopolymer-paste samples made from fly ash classes F and C are shown in Figures 14 and 15.Of the geopolymer-paste samples tested, those made using fly ash classes F and C at ratios 8F–60 and 12C–70 showed the highest compressive strength, with respective results of 296.23 and 501.23 ksc. In comparison, samples made using fly ash at ratios 4F–60 and 4C–60 showed the lowest compressive strength results, at 120.97 and 201.93 ksc respectively. The compressive strength of geopolymer-paste specimens made using these fly ash types was also influenced by other variables, including concentration of NaOH solution, and percentage of fly ash in the mix. The details of these influences are discussed below.

1.1.1 Effect of NaOH concentration

The results of stability tests on the compressive strength of geopolymer-paste samples revealed a relationship between the content ratios of fly ash classes F and C, and various concentrations of NaOH solution, with regard to their fire-resistance efficacy. In short, the concentration of the NaOH solution directly affected the performance of geopolymer-paste specimens. This is shown in Figures 14 and 15. With both Class F and C fly ash-based geopolymer-paste samples, an increase

in NaOH concentration, from 4 to 8 to 12M, tended to induce comparative increases in compressive strength when made using the same fly ash content ratio. The Class F specimen showed 159.90 to 202.41 ksc using 55% fly ash by weight of mix; and the Class C specimens showed 201.93 to 320.85 ksc, 272.39 to 326.26 ksc and 292.87 to 591.23 ksc, with 60, 65 and 70% fly ash respectively. Geopolymer-paste specimens incorporating an NaOH concentration of 8M showed the highest compressive strength when made using Class F fly ash at content ratios of 50 and 60%. Deviations from this ratio always resulted in lower compressive strengths. The samples tested, at ratios 8F-50 and 8F-60, gave results of 179.60 and 296.23 ksc respectively, as shown in Figure 14.

1.1.2 Effect of fly ash content

The results of compressive strength tests on geopolymer-paste samples made using variable quantities of fly ash classes F and C are shown in Figures 14 and 15 respectively.

The results of geopolymer-paste tests using Class F fly ash: Tests on specimens made by incrementing the quantity of Class F fly ash from 50 to 60% by weight of mix showed higher compressive strength when the NaOH concentration was decreased from 12 to 8M, giving respective results of 104 to 241.27 ksc, and179.60 to 296.23 ksc. Samples made with an NaOH concentration of 4M showed reduced compressive strength when increasing fly ash content, going from 162.06 to 120.97 ksc. This is shown in Figure 14.

It can be deducted that the specimens made using fly ash at a content ratio of 50% showed a decrease in compressive strength when the NaOH concentration was increased from 4 to 12M; samples made with an NaOH concentration at 8M, however, showed the highest compressive strength at this ratio. Tests on specimens at a content ratio of 60% showed a significant increase in compressive strength when the NaOH concentration was increased from 4 to 12M; samples made with an NaOH concentration at 8M again showed the highest

compressive strength. Finally, tests on specimens at a content ratio of 55% showed a uniform increase in compressive strength dependent on the NaOH concentration, rising from 4 through 12M, with the latter giving the highest compressive strength.

The results of geopolymer-paste tests using Class C fly ash: Tests on specimens made using different content ratios of Class C fly ash (60, 65 and 70%) this time produced uniform results, with increases in compressive strength comparative with both fly ash content and NaOH concentration, giving results of 201.93 to 292.87 ksc, 232.64 to 356.25ksc, and 320.85 to 501.23ksc respectively. This can be seen in Figure 15.

It can be seen from the above results that both fly ash content ratio and concentration of NaOH are conclusively linked to the compressive strength of the sample produced: both fly ash content and NaOH concentration together influenced compressive strength in the specimen, the greater the fly ash content and the higher the concentration the greater the compressive strength. For example, the lowest compressive strength was obtained using a fly ash content ratio of 60% with an NaOH concentration of4M, while the highest strength came from a content ratio of 70% with an NaOH concentration of 12M.

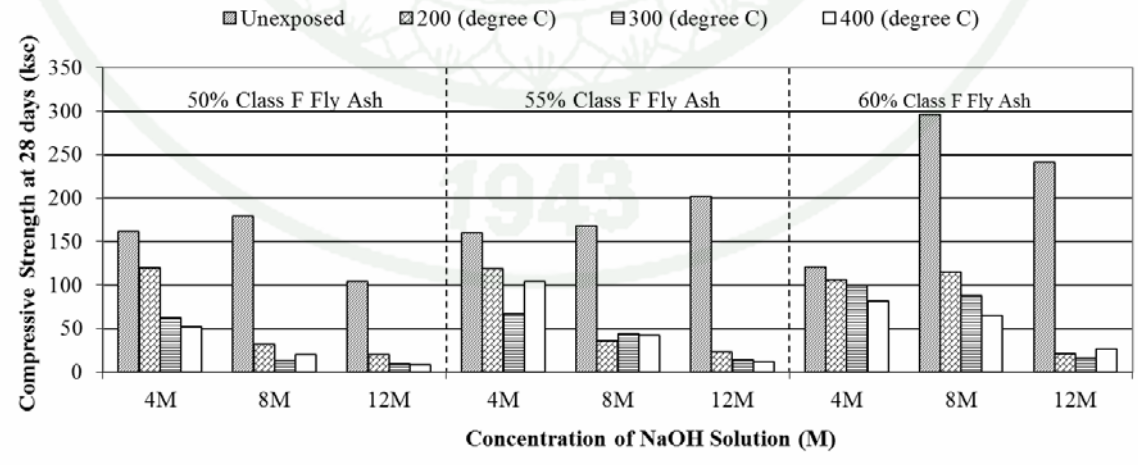

Figure 14 Compressive strength test results for geopolymer-paste specimens made using Class F fly ash at content ratios of 50, 55 and 60% with various NaOH concentrations, post thermal exposure at 28 days

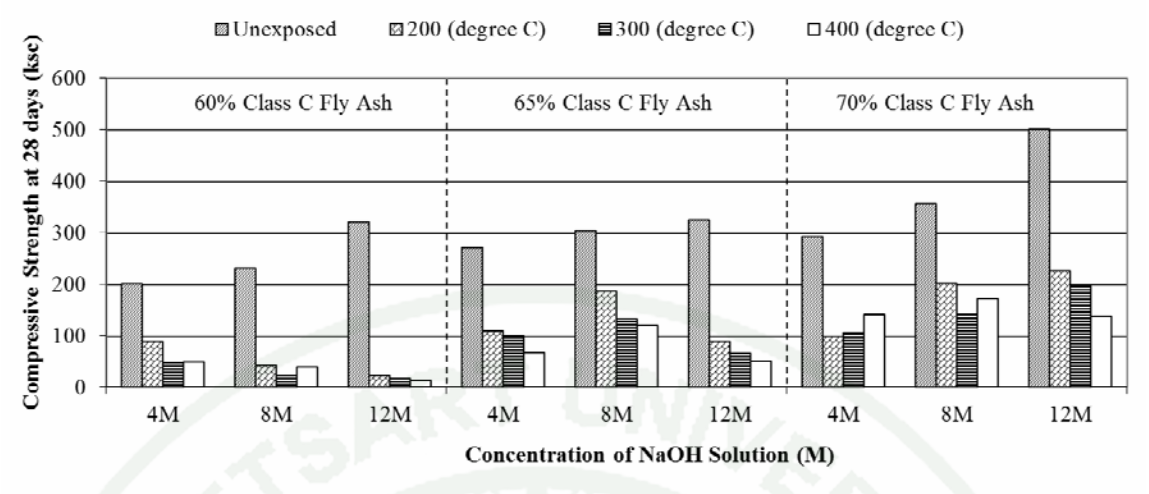

Figure 15 Compressive strength test results for geopolymer-paste specimens made using Class C fly ash at content ratios of 60, 65 and 70% with various NaOH concentrations, post thermal exposure at 28 days

1.2 Compressive strength at elevated temperature

The results of compressive strength tests on geopolymer-paste samples made using fly ash classes F and C after thermal exposure showed that specimens produced using fly ash at content ratios of 60% (Class F) and 70% (Class C) by weight of mix, then left for a period of 27 days before exposure, gave the highest initial compressive strength. This is shown in Figures 14 and 15. Each specimen was fired for 3 hours at temperatures of 200, 300, or 400^{o}C, as individual tests required. These results are shown in Figures 14 to 17.

The results of tests conducted on geopolymer-paste samples made with fly ash Class F fired at 400^{o}C showed that specimens made at the ratio 4F-60 were more stable than those made at 8F-60. This was because although 4F-60 specimens had a lower initial compressive strength (120.97ksc), the residual strength after firing was 67.22%; in contrast, specimens made at the ratio 8F-60 had the highest initial compressive strength (296.23ksc), but after firing experienced significant strength loss, leaving them with a residual strength of only 22%; in fact, a 4F-60 specimen was shown to be stronger than an 8F-60 after firing to 400^{o}C. This is shown in Figures 14 and 16.

The results of tests conducted on geopolymer-paste samples made with Class C fly ash fired at 400°C indicated that, as with Class F fly ash, specimens made with a lower NaOH ratio, in this case 4C-70, were more stable than higher-ratio specimens, for example 12C-70. Again, the lower-ratio specimen recorded a lower initial compressive strength (292.87ksc), but also benefited from reduced strength loss after firing, leaving a residual strength of 47.96%; in contrast, specimens made at the ratio 12C-70 had the highest initial compressive strength (501.23ksc), but experienced significant strength loss after firing, leaving a residual strength of only 27.36%. This is shown in Figures 15 and 17.

From the results of experiments detailed below it will be shown how differing NaOH concentrations (4, 8 and 12M), and classes F and C fly ash content ratios influence the residual strength of geopolymer-paste specimens after firing at temperatures of 200, 300 and 400°C.

1.2.1 Effect of NaOH concentration

Figures 14 to 17 show the results of and relationships between tests conducted on geopolymer-paste specimens made with fly ash classes F and C and varying concentrations of NaOH (4, 8 and 12M), after firing at temperatures ranging from 200 to 400°C.

The results of tests done on geopolymer-paste specimens made with Class F fly ash showed that increases in temperature, from 200 to 400°C, gave specimens a reduced residual strength when compared with unfired specimens. With samples fired at 400°C, increased concentrations of NaOH, from 4 through 12M, produced samples with reduced residual strength when made with fly ash at content ratios of 50, 55, and 60%, giving results of 31.96 to 7.97%, 64.97 to 6.16%, and 67.22 to 11.11% respectively. Reduced concentrations of NaOH showed improved residual strength, especially at NaOH 4M, which gave the highest residual strengths: 31.96, 64.97 and 67.22%, when made with fly ash at content ratios of 50, 55 and 60% respectively. This is shown in Figures 14 and 16.

Figure 17 shows the percentage of residual strength of geopolymer-paste specimens made with Class C fly ash specifically. Increased temperatures, from 200 to 400^{o}C, reduced the residual strength, as with Class F fly ash, when compared with unfired specimens, but only with a content ratio of 60%. Specimens with a fly ash content ratio of 60% by weight of mix and with increased concentrations of NaOH, from 4 through 12M, after being fired at a temperature of 400oc, showed a lower residual strength, going from 24.09 to 3.87%.

It was when samples were made with higher fly ash content ratios and NaOH concentrations that residual strength results began to show improvement. Specimens made using a fly ash content of 65%, while increasing the NaOH concentration to 8M, gave specimens the highest residual strength, at 39.22%, compared with those made with NaOH concentrations of 4 and 12M, which gave lower residual strengths of 24.41 and 15.24% respectively. Using a fly ash content of 70% and increasing the concentration of NaOH from 4 to 8M tended to induce a marginally improved residual strength, from 47.96 to 48.26%; whereas a concentration of NaOH at 12M gave a lower residual strength of 27.36%.

1.2.2 Effect of fly ash content

Figures 16 and 17 show the relationship between the percentage of residual strength and fly ash content ratios in geopolymer-paste for fly ash classes F and C.

Geopolymer-paste specimens made using Class F fly ash, when fired at a temperature of 400^{o}C, induced generally higher residual strengths when the fly ash content ratio was increased from 50 to 60% by weight of mix. The results were 31.96 to 67.22%, 11.31 to 22.00% and 7.97 to 11.11%, when made with respective fly ash content ratios, and with NaOH concentrations at 4, 8 and 12M. This is shown in Figures 14 and 16.

Geopolymer-paste specimens made using Class C fly ash tended to induce higher residual strengths when the fly ash content ratio was increased from 60 to 70% by weight of mix. The results were 24.09 to 47.96%, 16.77 to 48.26% and 3.87 to 27.36%, when made with respective fly ash content ratios, and with NaOH concentrations at 4, 8 and 12M. This is shown in Figures 15 and 17.

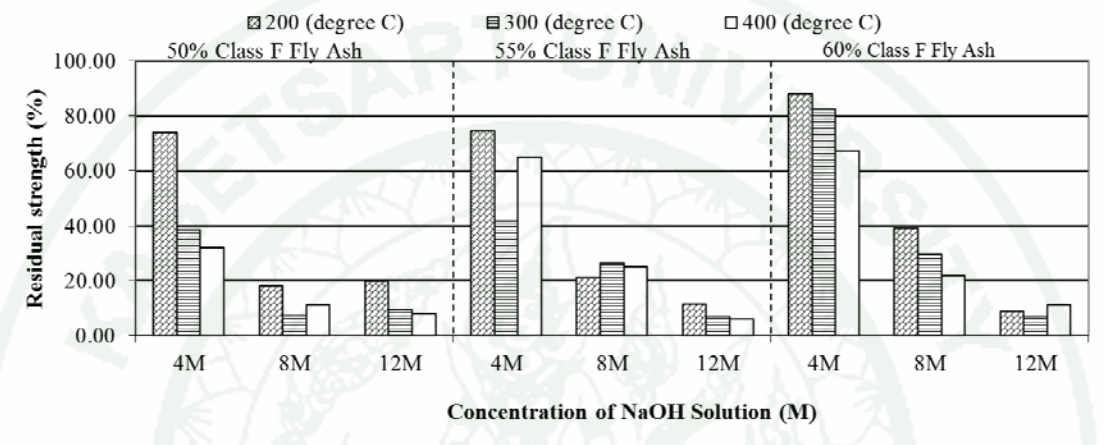

Figure 16 Residual strength results for geopolymer-paste specimens made using Class F fly ash at content ratios of 50, 55 and 60% with different NaOH concentrations, post thermal exposure at 28 days

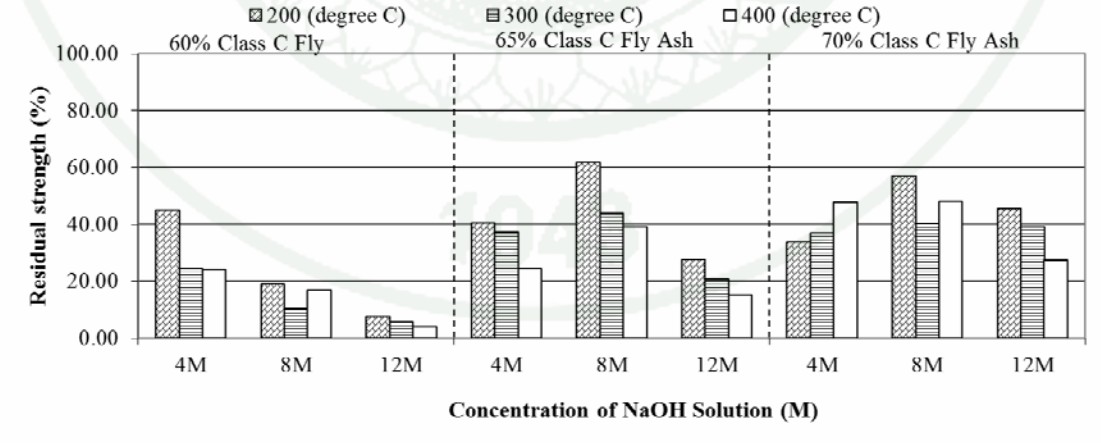

Figure 17 Residual strength results for geopolymer-paste specimens made using Class C fly ash at content ratios of 60, 65 and 70% with different NaOH concentrations, post thermal exposure at 28 days

Tests on the thermal stability of geopolymer-paste specimens made using fly ash classes F and C, after firing at temperatures ranging from 200 to 400^{o}C, showed a decrease in residual strength compared to unfired samples. The initial strength of geopolymer-paste specimens before firing indicated a reverse effect on thermal stability post firing, dependent on NaOH concentration. That a geopolymer-paste specimen with a high initial strength tended to induce lower results clearly suggested that NaOH affects residual strength, as when residual strength increased, thermal stability also increased.

The results of tests showed that the themal stability of geopolymer-paste Class F specimens was further improved by reducing the NaOH concentration and increasing fly ash content. It was also shown that reducing the concentration of NaOH was more effective in improving thermal stability than increasing fly ash content alone. Geopolymer-paste samples made using Class C fly ash with an NaOH concentration at 8M showed improved thermal stability, except when made with a fly ash content ratio of 60% by weight of mix. Results showed that increases in fly ash content produced greater thermal stability when compared against samples made using the same concentration of NaOH.

2. Fire resistance

Figures 18 and 19 show thermocouple temperature readings as a function of time for all specimens during the fire tests on a 10mm-thick geopolymer-paste panel made using fly ash classes F and C. A gradual increase in temperature was observed as a function of test duration, with a heat-front moving progressively through the specimen as the furnace temperature increased, reaching 847^{o}C after 30 minutes. Each data-set (shown in Figs. 18 and 19, and a table presented in Appendix Table A6 to A23) was recorded via type-K thermocouples located at the mid-depth point (5mm) of the panel. Figures 18 and 19 show that for the first 5 minutes the temperature on the panel's unexposed side remained constant, and that it then rose in linear fashion until approximately the 20th minute, after which time it remained almost constant. This behaviour was caused by the pressure of the water present in the sample's pores, as it conducted heat through to the unexposed side.

First the specimen was fired on one side, with the heat then passing through to the unfired side. The heat moved through the specimen's wall by process of heat conduction. However, it should be noted that when the exposed side was subjected to the standard fire temperature curve, the unexposed-side temperature depended on properties granted by NaOH concentration and fly ash content.

Different concentrations of NaOH and quantities of fly ash in the mix influenced the fire-resistance characteristics in both geopolymer-paste panels made with fly ash classes F and C.

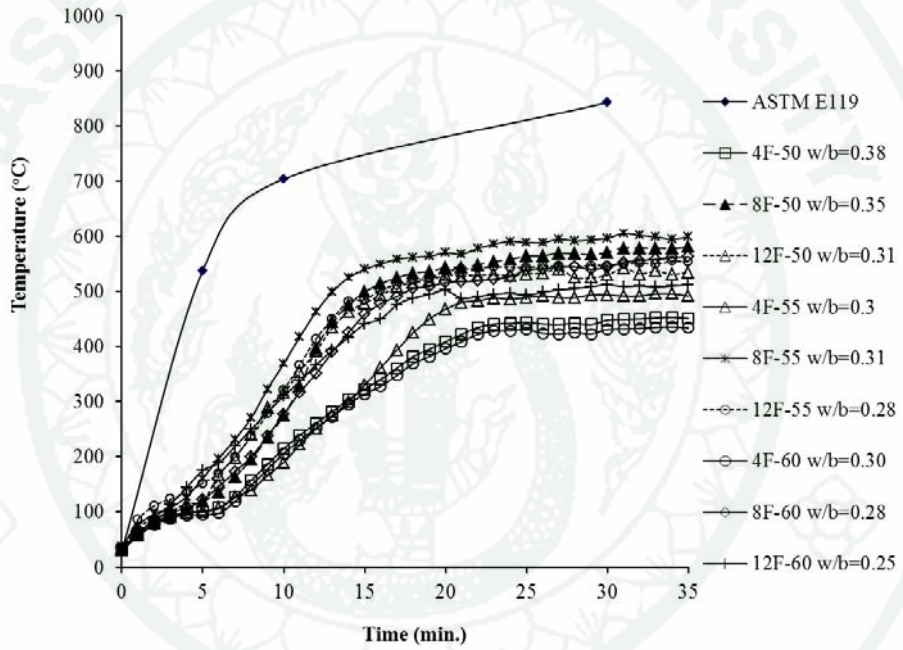

Figure 18 Fire resistance test results for geopolymer-paste panels made using Class F fly ash at 28 days

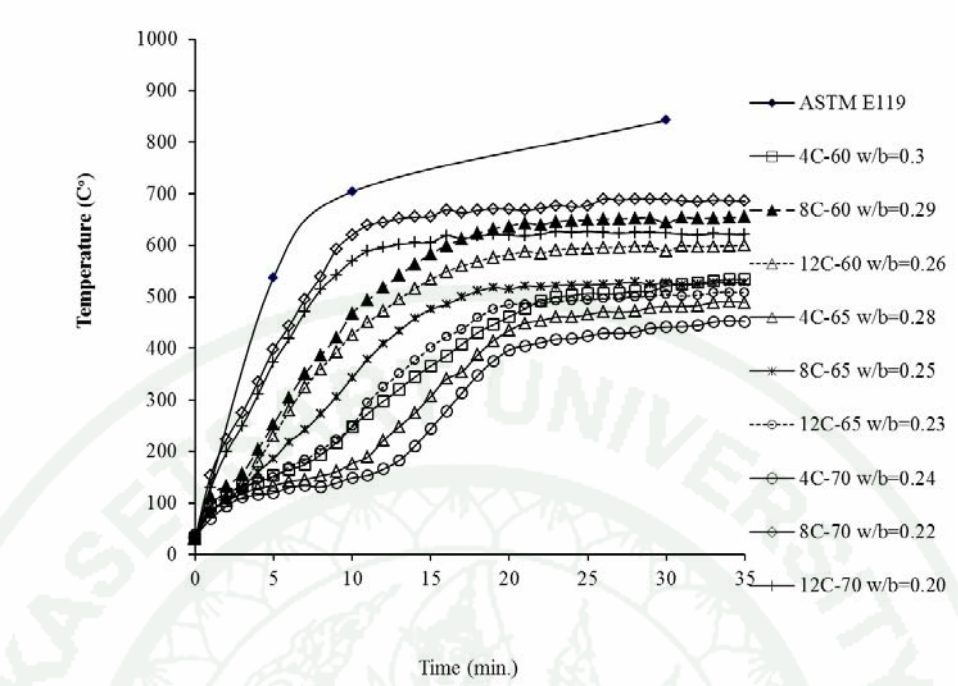

Figure 19 Fire resistance test results for geopolymer-paste panels made using Class C fly ash at 28 days

2.1 Effect of NaOH solution concentration and Class F fly ash (FFA) content

Figure 20 shows that changes in NaOH concentration influence the fire-resistance of geopolymer-paste panels made using Class F fly ash. Specimens fired at temperatures above 800°C for 35 minutes, which were made with NaOH concentrations at 4M and fly ash content ratios of 50, 55, and 60% by weight of mix, gave the highest fire-resistance. This was observed in specimen samples at ratios 4F-50, 4F-55, and 4F-60, which, after exposure for 35 minutes, had temperatures on the unexposed side of 451, 492 and 434 °C respectively.

Increasing concentrations of NaOH from 4 to 8M in the mix produced reduced fire-resistance in example specimens at ratios 8F-50, 8F-55 and 8F-60. The temperatures on the unexposed side increased from 451 to 581°C, 492 to 599°C, and 434 to 563°C respectively. Increasing the NaOH concentration from 8 to 12M, at ratios 12F-50, 12F-55, and 12F-60, induced marginal improvements in fire resistance, with temperatures recorded on the unexposed side decreasing from 581 to 535 °C, 599

to 554°C and 563 to 512°C respectively. Increasing the concentration of NaOH to 12M gave higher fire-resistance, but it was still less than with specimens made with an NaOH concentration at 4M, which gave the highest fire resistance.

Figure 21 shows that changing the Class F fly ash content ratio to 60% by weight of mix gave the highest fire-resistance when compared with specimens made using the same concentrations of NaOH (4, 8 and 12M). This was evidenced using geopolymer-paste specimens at ratios 4F-60, 8F-60, and 12F-60. The temperatures on the unexposed side were recorded as 434, 563 and 512 °C respectively.

Reducing the quantity of fly ash from 60 to 55% gave specimens the lowest fire-resistance, again compared with those made using the same concentrations of NaOH. The temperatures on the unexposed side increased, rising from 434 to 492 °C, 563 to 599 °C and 512 to 554 °C, as shown using example specimens at ratios 4F-55, 8F-55, and 12F-55.

Interestingly, reducing the quantity of fly ash still further, from 55 to 50%, tended to induce marginally higher fire-resistance, as the temperatures recorded on the unexposed side were lower, going from 492 to 451°C, 599 to 581°C, and 554 to 535 °C. This was discovered using samples at ratios 4F-50, 8F-50, and 12F-50, again when compared with those made using the same concentrations of NaOH.

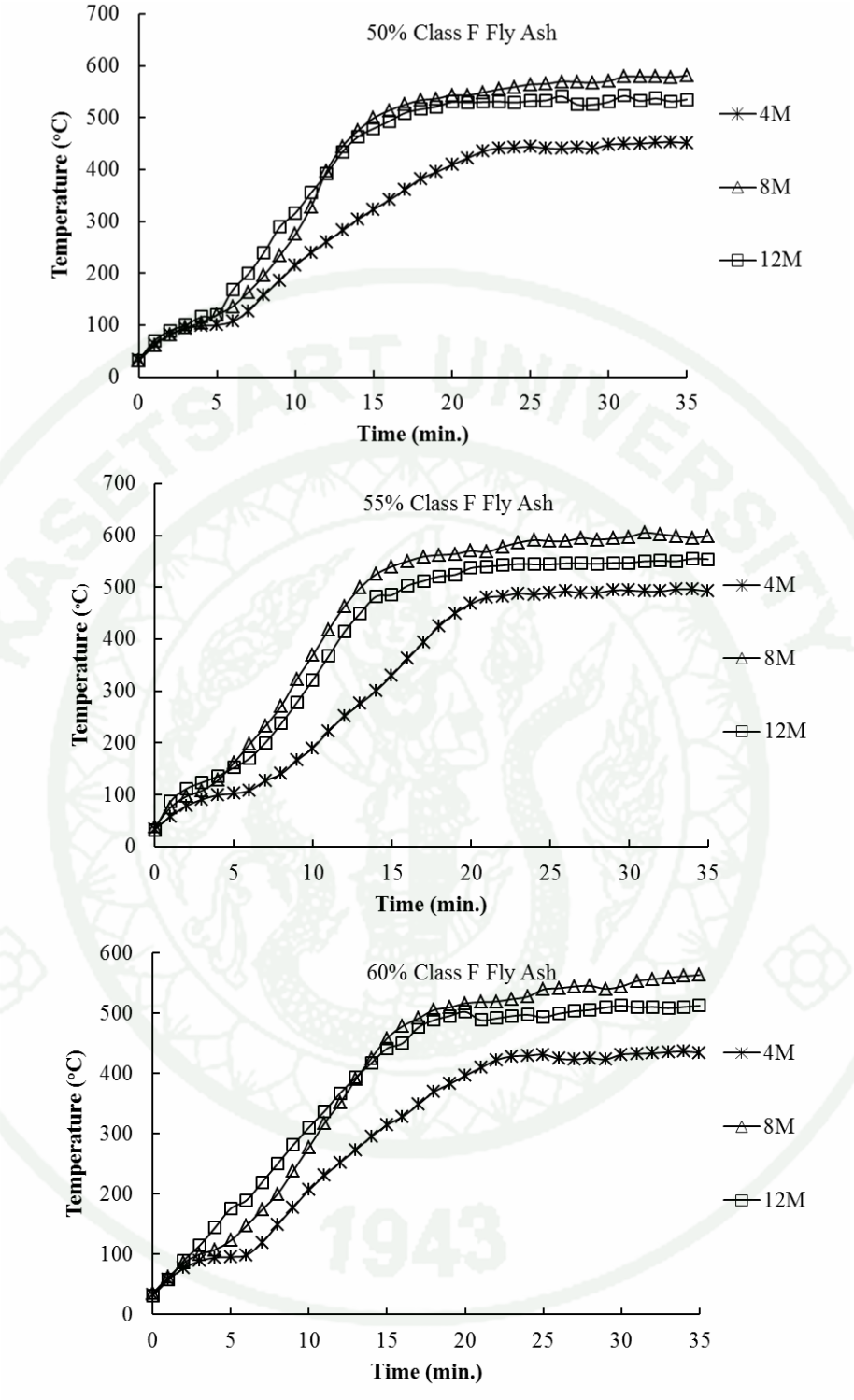

Figure 20 Geopolymer-paste fire-resistance test results for specimens made using Class F fly ash at ratios 50, 55 and 60% with various NaOH concentrations, after firing

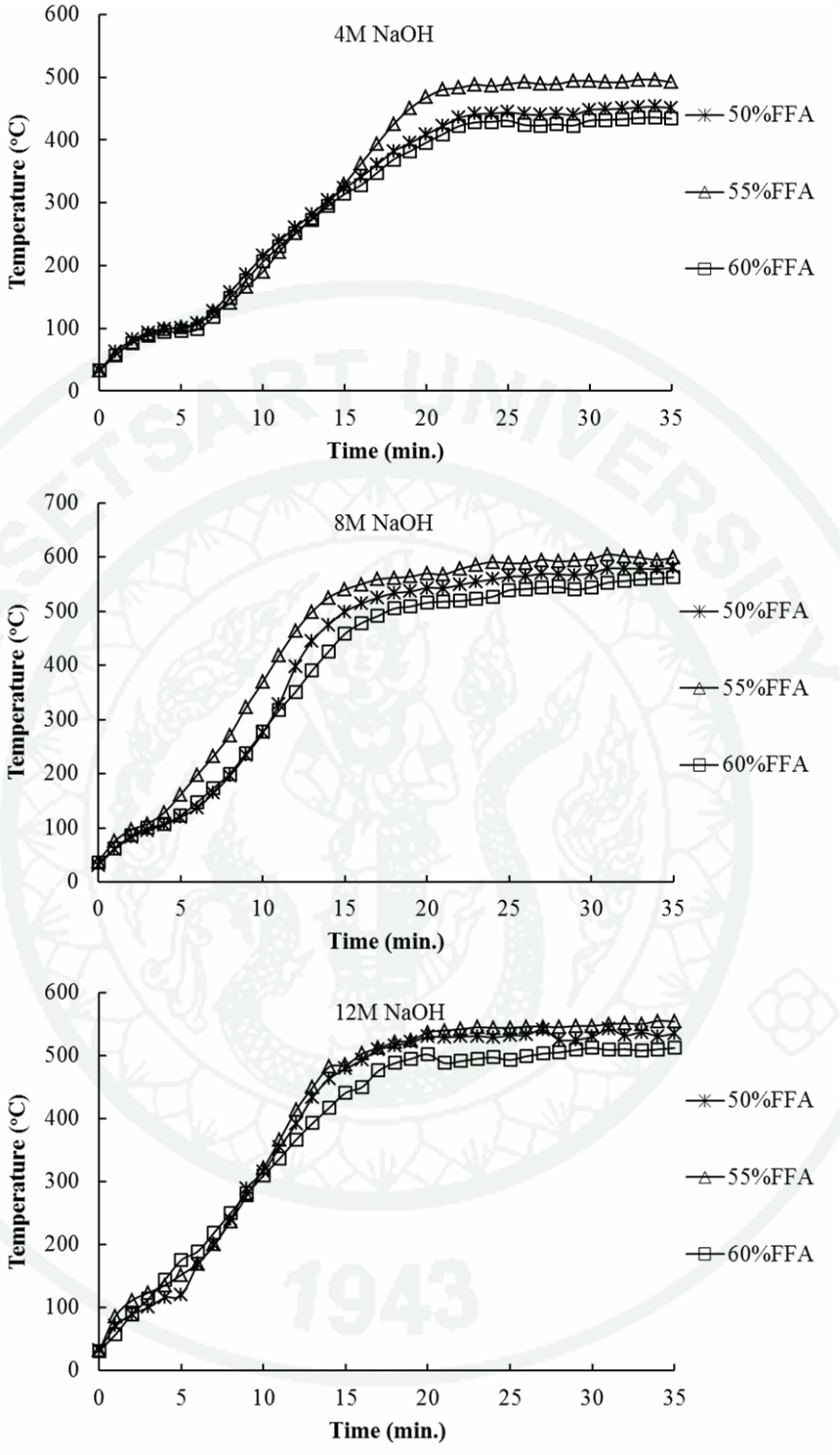

Figure 21 Geopolymer-paste fire-resistance test results for specimens made using different quantities of Class F fly ash with NaOH concentrations at 4, 8 and 12M, after firing

2.2 Effects of concentration of NaOH Solution and Class C fly ash (CFA) content

Figure 22 shows that changes in NaOH concentration influence the fire-resistance of geopolymer-paste panels made using Class C fly ash. Specimens fired at temperatures over 800^{o}C for 35 minutes, which were made using NaOH concentrations at 4M, and with fly ash at content ratios of 50, 55, and 60% by weight of mix, gave the highest fire-resistance. This was shown using specimen examples at ratios 4C-60, 4C-65, and 4C-70. After being heated for 35 minutes the temperatures recorded on the unexposed side were 451, 492 and 434 ^{o}C respectively.

Increasing concentrations of NaOH in the mix, from 4 to 8M, gave the lowest fire resistance when compared to specimens made using the same fly ash content. When tested, the temperatures on the unexposed side of the specimens were higher, rising from 534 to 655 ^{o}C, 489 to 527 ^{o}C and 452 to 686 ^{o}C, as shown using samples at ratios 8C-60, 8C-65, and 8C-70 respectively. Increasing the NaOH concentration from 8 to 12M induced marginal improvements in fire resistance, when compared with specimens made using an NaOH concentration at 4M, as shown using samples at ratios 12C-60, 12C-65, and 12C-70. In these instances the recorded temperatures were lower, falling from 655 to 600 ^{o}C, 527 to 508 ^{o}C and 686 to 621 ^{o}C respectively, when compared with specimens made using the same fly ash content.

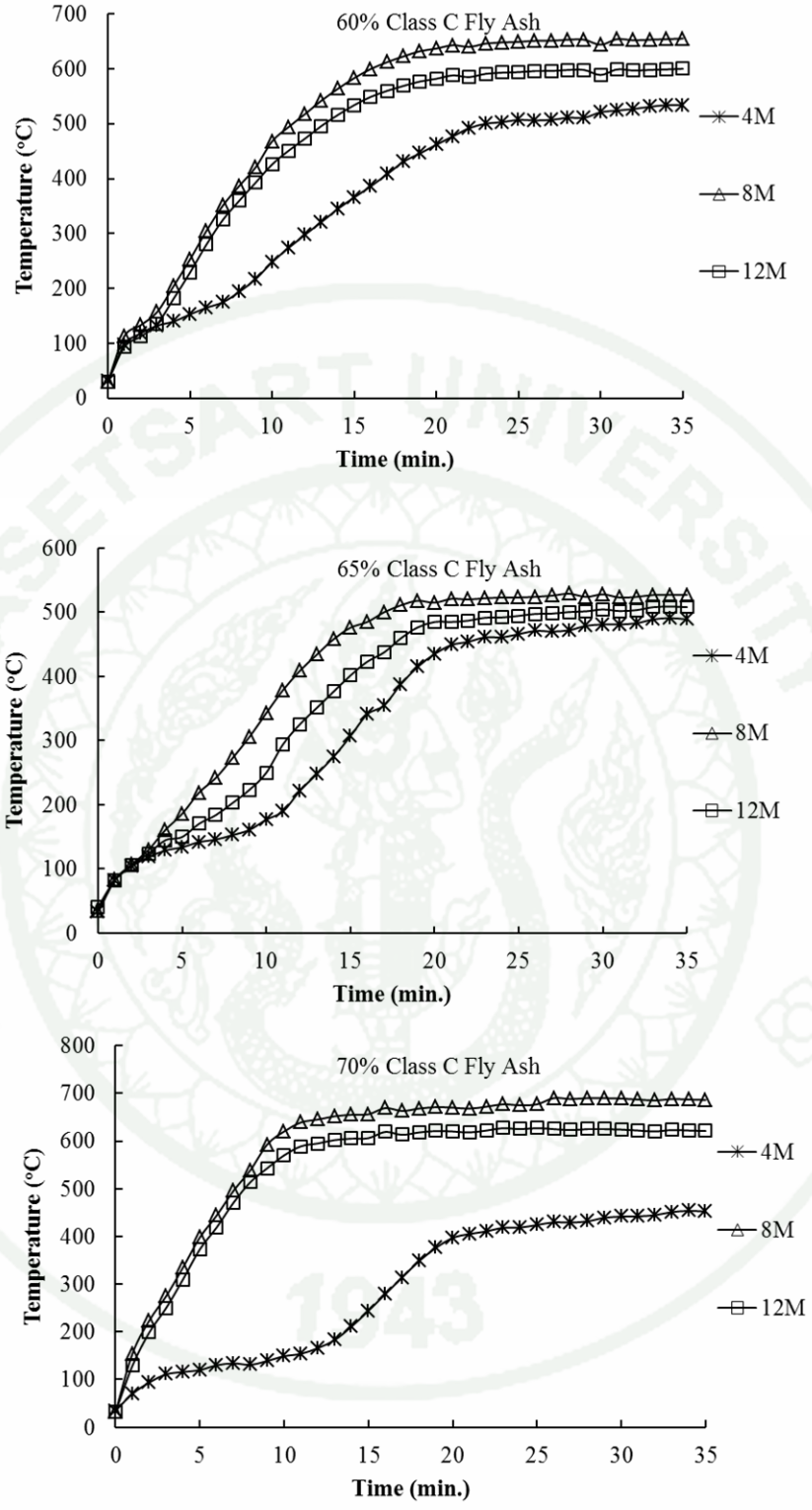

Figure 22 Fire-resistance test results after firing for geopolymer-paste specimens made using Class C fly ash at content ratios 60, 65 and 70% with various NaOH concentrations

Figure 23 shows that changes in NaOH concentration influence the fire-resistance of geopolymer-paste panels made using Class C fly ash. Specimens made with a fly ash content of 70% by weight of mix with NaOH concentrations at 8 and 12M, which were then fired at temperatures over 800^{o}C for 35 minutes, gave the lowest fire-resistance when compared with samples made with fly ash content ratios of 60 and 65%. Geopolymer-paste samples produced at the ratios 8C-70 and 12C-70 recorded temperatures on the unexposed side of 686 and 621^{o}C, a fire-resistance generally lower than specimens made at ratios 8C-60, 12C-60, 8C-65, and 12C-65, whose unexposed side temperatures were 655, 600 ^{o}C, and 527, 508 ^{o}C respectively.

Reducing the quantity of fly ash from 70 to either 65 or 60% by weight of mix, tended to induce a higher fire-resistance, especially with a fly ash content ratio of 65%. This median ratio induced the best fire-resistance, greater than specimens made using content ratios of 60 or 70%. Specimens made using fly ash at a content ratio of 70% by weight of mix gave the lowest fire-resistance, marginally worse than those made using a content ratio of 60%. In contrast, increasing the content ratio of fly ash from 60 to 65 to 70% gave specimens a respectively higher fire-resistance when made with NaOH at a concentration of 4M. Geopolymer-paste example specimens made at ratios 4C-60, 4C-65, and 4C-70 recorded unexposed side temperatures of 534, 489 and 452 ^{o}C respectively.

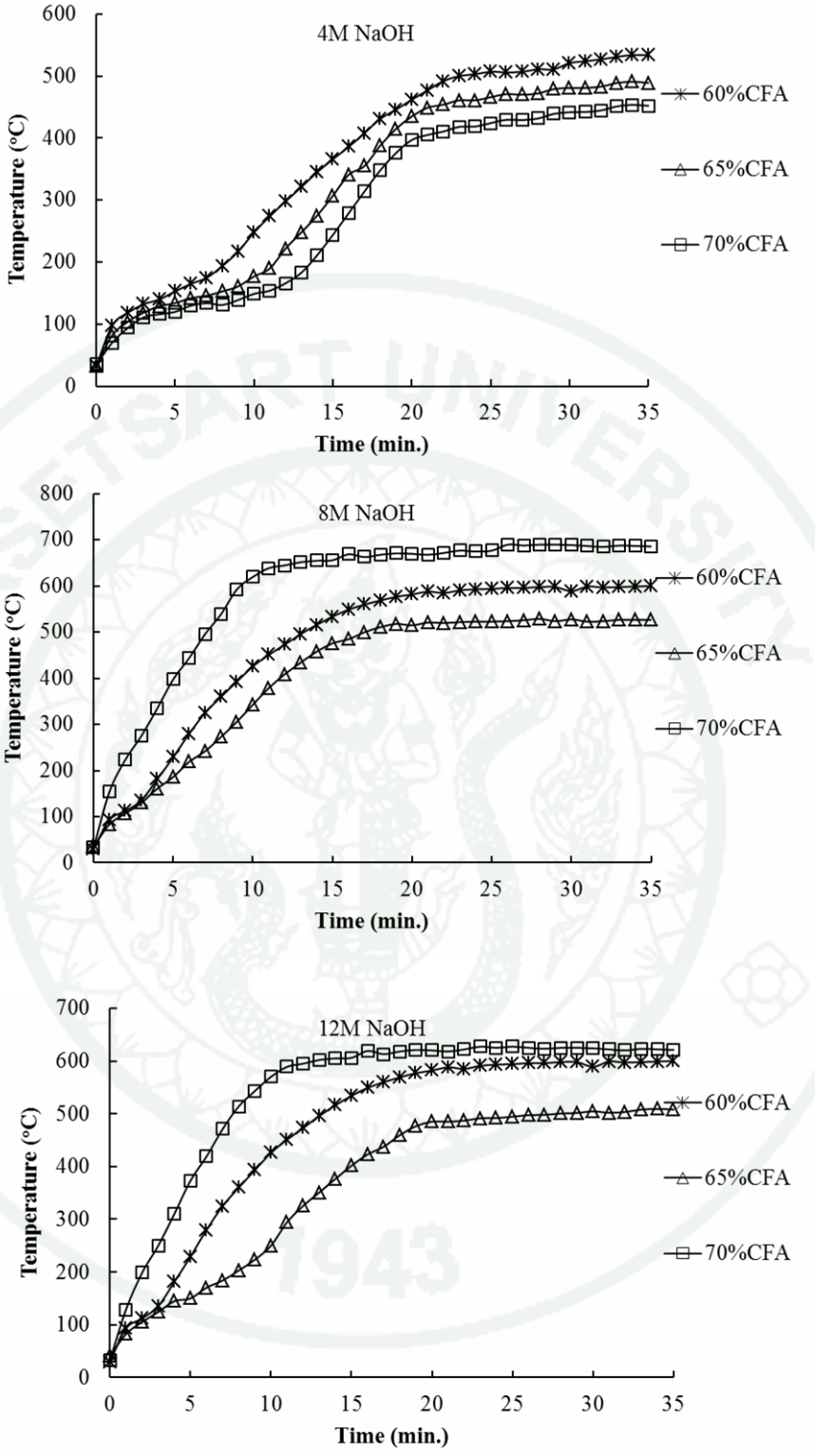

Figure 23 Fire-resistance test results after firing for geopolymer-paste specimens made using Class C fly ash at various content ratios with NaOH solution concentrations at 4, 8 and 12M

From the results obtained, the best fire-resistance characteristics in geopolymer-paste panels made with fly ash classes F and C were found in samples produced at ratios 4F-50, 4F-55, 4F-60, and 4C-60, 4C-65, 4C-70 respectively. The corresponding temperatures on the unexposed sides of tested panels measured 451, 492 and 434°C, and 534, 489 and 452°C after 35 minutes exposure. Specimens with an NaOH concentration of 4M and a high fly ash content gave the highest fire-resistance characteristics when compared with all other mixes.

3. Thermal conductivity

Figure 24 shows the average thermal conductivity of geopolymer-paste specimens made using Class F fly ash. Geopolymer-paste panels made using fly ash at content ratios 50, 55, and 60% by weight of mix and an NaOH concentration at 8M, when fired at temperatures over 800°C, gave the highest average thermal conductivity.

Geopolymer-paste samples made at ratios 8F-50, 8F-55 and 8F-60 had the highest average thermal conductivities of 0.284, 0.313 and 0.277 respectively. Using NaOH concentrations at either 4 or 12M gave a low average thermal conductivity, as evidenced with geopolymer-paste samples made at ratios 4F-50, 4F-55, 4F-60 and 12F-50, 12F-55, and 12F-60, which gave respective average thermal conductivity results of 0.273, 0.281, 0.274 and 0.284, 0.276, 0.271.

In this study, increasing the quantity of fly ash in the mix tended to induce a lower average thermal conductivity in samples made with an NaOH concentration of 12M. This was shown using geopolymer-paste samples produced at the ratio 12F-50, which had an average thermal conductivity of 0.284, a result higher than both 12F-55 and 12F-60, with values of 0.276 and 0.271 respectively.

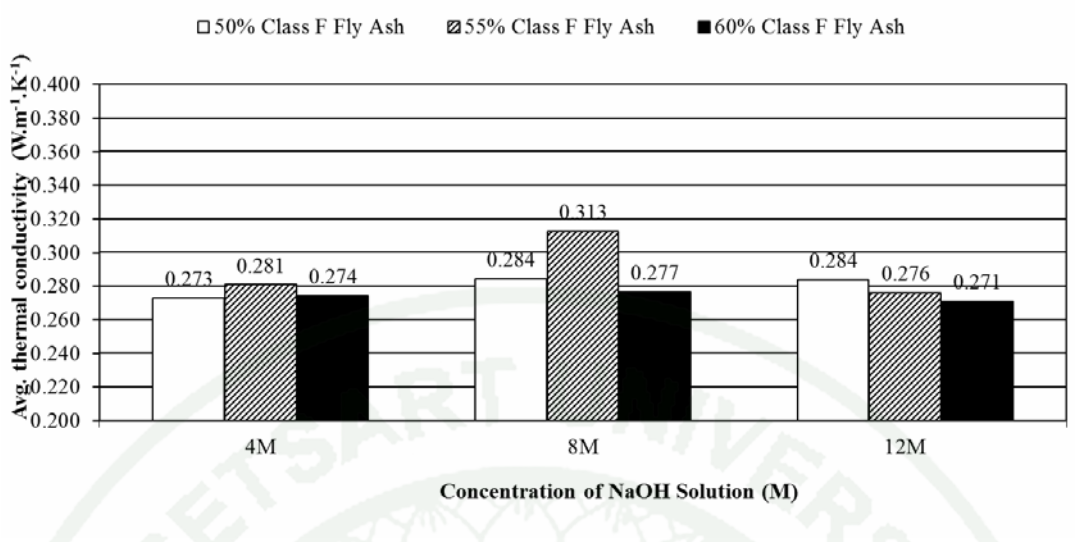

Figure 24 Thermal conductivity test results after exposure for geopolymer-paste panels made with various concentrations of NaOH, and using Class F fly ash (FFA) at content ratios of 50, 55 and 60% respectively, at 28 days

Figure 25 shows the average thermal conductivity of geopolymer-paste specimens made using Class C fly ash. Geopolymer-paste specimens made using fly ash at content ratios 60, 65 and 70% by weight of mix, with an NaOH concentration at 8M, and fired at temperatures over 800°C, gave the highest average thermal conductivity.

Geopolymer-paste samples at ratios 8C-60, 8C-65 and 8C-70 had average themal conductivities of 0.329, 0.294 and 0.377 respectively. Using NaOH concentrations at either 4 or 12M gave low average thermal conductivity results, especially at 4M, which gave the lowest average conductivity. This was evidenced using geopolymer-paste samples at ratios 4C-60, 4C-65 and 4C-70, and 12C-60, 12C-65, and 12C-70, which gave respective average thermal conductivities of 0.281, 0.271 and 0.265, and 0.286, 0.288 and 0.337.

In this study, increasing the quantity of fly ash in the mix tended to induce a higher average thermal conductivity than with comparative samples made using the same concentration of NaOH, except at 4M. In this case, increasing the quantity of fly ash tended to induce lower themal conductivity.

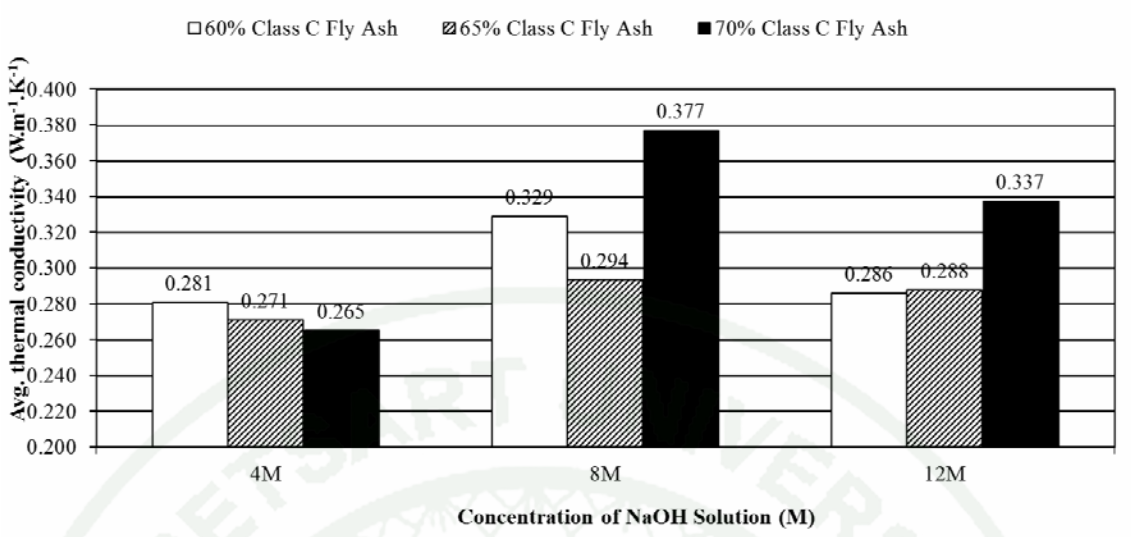

Figure 25 Thermal conductivity test results after exposure for geopolymer-paste panels made with various concentrations of NaOH, and using Class C fly ash (CFA) at content ratios of 60, 65, and 70% respectively, at 28 days

The effects of thermal conductivity on geopolymer-paste panels made using various fly ash content ratios and NaOH concentrations are shown in Figures 24 and 25.

The highest thermal conductivity value (K) for geopolymer-paste panels made using Class F fly ash was obtained from specimens composed of fly ash at a content ratio of 55% with an NaOH concentration at 8M; the use of NaOH concentrations at 4 and 12M resulted in decreased thermal conductivity; a decrease in thermal conductivity was also observed when the fly ash content was increased in samples made with an NaOH concentration at 12M.

For geopolymer-paste panels made with Class C fly ash, the highest and lowest thermal conductivity (K) values were obtained from specimens with NaOH concentrations at 8 and 4M respectively, which included the same fly ash content. In samples made with an NaOH concentration at 4M, thermal conductivity decreased when increasing fly ash content; contrastingly, increasing fly ash content with NaOH concentrations at 8 and 12M gave samples greater thermal conductivity. This was significant with 8M, but only slight with 12M.

4. Microstructural Characterization

As previously described, tests done on geopolymer-paste specimens comprised of fly ash classes F and C showed the influence of fly ash ratio variation and NaOH concentration on the initial compressive strength and thermal stability of samples.

As part of this experiment, geopolymer-paste samples were selected at ratios 4F-60, 8F-60, 4C-70 and 12C-70, as these had given the highest and lowest initial compressive strength and thermal stability results after firing to 400^{o}C for 3 hours. This is shown in Table 5.

The above samples were used in order to study porosity and pore-size distribution, as obtained using the mercury intrusion porosimetry (MIP) method. The crystallinity of samples was also investigated using the x-ray diffraction method (XRD), along with the influence of different NaOH concentrations. Specimens were compared with pre-burn, control, samples, as shown in Figure 23-28.

Table 5 Ratio mixtures of geopolymer paste, tested for porosity and pore-size distribution using MIP experimentation.

Mixture No.	Designation	NaOH (M)	Fly ash (%)	Before test	After firing 400°C
				Compressive strength at 28-day (ksc)	Residual strength at 28-day (%)
1	4F-60	4	60%FFA	120.97	67.22
2	8F60	8	60%FFA	296.23	22.00
3	4C-70	4	70%CFA	292.87	47.96
4	12C-70	12	70%CFA	501.23	27.36

4.1 Porosity and pore-size distribution using MIP

Table 6 and Figures 26-29 show the results of this analysis, including the amount of total porosity, cumulative pore volume, and average pore diameter of geopolymer-paste samples made using fly ash classes F and C.

Heating to 400°C tended to induce an increase in total porosity, cumulative pore volume and average pore diameter. Increasing the concentration of NaOH tended to induce a decrease in total porosity and cumulative pore volume, but increased average pore diameter. The result was different, however, with pre-fired geopolymer-paste samples made using Class C fly ash, as with this mixture increasing the NaOH concentration resulted in an increase in total porosity. This is detailed below.

Table 6 Total porosity and pore size distribution of geopolymer paste

	Before Test			After Firing 400°C		
Designa-tion	Total Porosity	Cumulative Volume	Avg. Pore Dia.	Total Porosity	Cumulative Volume	Avg. Pore Dia.
	(%)	(cc/g)	(μm)	(%)	(cc/g)	(μm)
4F-60	42.80	0.362	0.051	48.89	0.435	0.070
8F-60	31.95	0.275	0.060	43.36	0.341	0.082
4C-70	5.47	0.038	0.107	30.62	0.224	0.172
12C-70	12.60	0.099	0.107	25.39	0.158	0.330

Figures 26 and 27 show the relationship between pore diameter and cumulative pore volume, and Figures 28 and 29 show the relationship between total porosity and average pore diameter in geopolymer paste made using fly ash classes F and C.

It was found that using NaOH concentrations at 4 and 8M in geopolymer-paste samples, made using Class F fly ash and fired to 400°C, tended to give the same result: they both increased cumulative pore volume, while marginally increasing pore size. These are shown in Figure 26, in graphs a and b, as replica curves, raised and to the right of those indicating the unfired samples.

The 4M sample showed an increase in cumulative pore volume, and gave the highest value, as shown in Figure 26(a). The total porosity increased slightly from 42.80 to 48.89%, and the average pore diameter increased from 0.051 - 0.07 μm, as shown in Figure 28. The 8M sample also showed an increase in cumulative pore volume, but only when the pore diameter was smaller than 1 μm. This is shown in Figure 26(b). The total porosity increased significantly from 31.95 to 43.36%, and the average pore diameter increased from 0.062 - 0.082 μm, as shown in Figure 28.

Increasing the concentration of NaOH from 4 to 8M in pre-exposure samples resulted in a reduced rate of cumulative pore volume increase. There was also an increase in average pore diameter, but a decrease in total porosity. This can be seen with samples made at the ratio 8F-60.This result relates to the increase in initial compressive strength because of the decrease of total porosity as shown in Table 5,which is consistent with the early compressive strength increases. After firing samples to temperatures of 400^{o}C, it was shown that increasing the concentration of NaOH during composition resulted in an increase in average pore diameter, but a decrease in cumulative pore volume and total porosity. The effect was a decrease in residual strength. This was demonstrated using samples at the ratio 8F-60, as shown in Table 5.

Geopolymer-paste samples made using Class C fly ash after firing to 400^{o}C, with NaOH concentrations at 4 and 12M, realised the same effect as geopolymer-paste samples made using Class F fly ash, which was an increase in cumulative volume and total size of pores. This is shown in Figure 27. However at the concentration 4M, after firing at 400^{o}C, the sample's cumulative pore volume and total porosity significantly increased, the latter going from 5.47% to 30.62%, compared with the pre-expose sample. This is shown in Figures 27 (a) and 29 (a), respectively. It was also shown that the average pore diameter increased slightly from 0.107-0.172 μm, as shown in Figure 29 (b). Samples made using concentrations of NaOH at 12M, which were subsequently fired at 400^{o}C, showed increases in cumulative pore volume when the pores were smaller than 10μm, as shown in Figure 27 (b) Also, the total porosity increased from 12.60% to 25.39%, but the average

pore diameter increased significantly, from 0.107-0.330 μm, when compared with the pre-burn sample. This is shown in Figure 29.

When increasing the concentration of NaOH from 4 to 12M in pre-fired samples, the result was an increase in cumulative pore volume when the pore size was smaller than 1μm; the total porosity increased, but the average pore diameter was relatively unchanged. This is evidenced by samples made at the ratio 12C-70, as shown in Figures 27 (a) and 29. The result of this is the highest initial compressive strength, as shown in Table 5.

Increases in the concentration of NaOH in geopolymer-paste samples after firing to 400^{o}C resulted in a lower rate of cumulative pore volume, and a decrease in total porosity and average pore diameter, especially when the pore size was smaller than 1um. This was evidenced using samples at the ratio 12C-70, as shown in Figures 27 and 29, and supported the results of compressive strength tests which showed a lower percentage residual strength. It was apparent the increasing strength loss percentage was due to the decrease in total porosity and increase in average pore diameter in post-fired samples. This is shown in Table 5.

The same sample, after firing at 400^{o}C, with increase in the concentration of the solution NaOH, especially when the pore size is smaller than 1μm, will result in an increase in the cumulative pore volume being low and total porosity decreases. While the size of the average pore diameter increases the ratio 12C-70 as shown in Figure 27 and 29, which correspond to the test, compressive strength and percentage compressive residual strength is lower as the percentage loss of compressive strength increased due to a decrease in the total porosity and an increase in the average pore size of the samples after the burn as shown in Table 5.

From the test results it can be deduced that increasing the concentration of NaOH solution in fly ash-based geopolymer samples increased the initial compressive strength. However, it reduced the strength after firing to 400^{o}C when compared to samples lacking that NaoH concentration. That was due to the fact fly ash-based

geopolymer-paste was discovered to have large numbers of interconnected pores which facilitate the escape of moisture when heated, causing minimal damage to the geopolymer matrix. As Kong, D., Sanjayan, J., and Sagoe Crentsil (2007) said: a geopolymer-paste specimen with a structure containing more interconnected pores will experience a reduced strength loss during heating compared with a geopolymer sample with an isolated pore structure; and, more generally, that mechanical strength decreases as pore size and volume increases. This, however, is not always the case: Increased pore interconnectivity allows for greater water mobility.

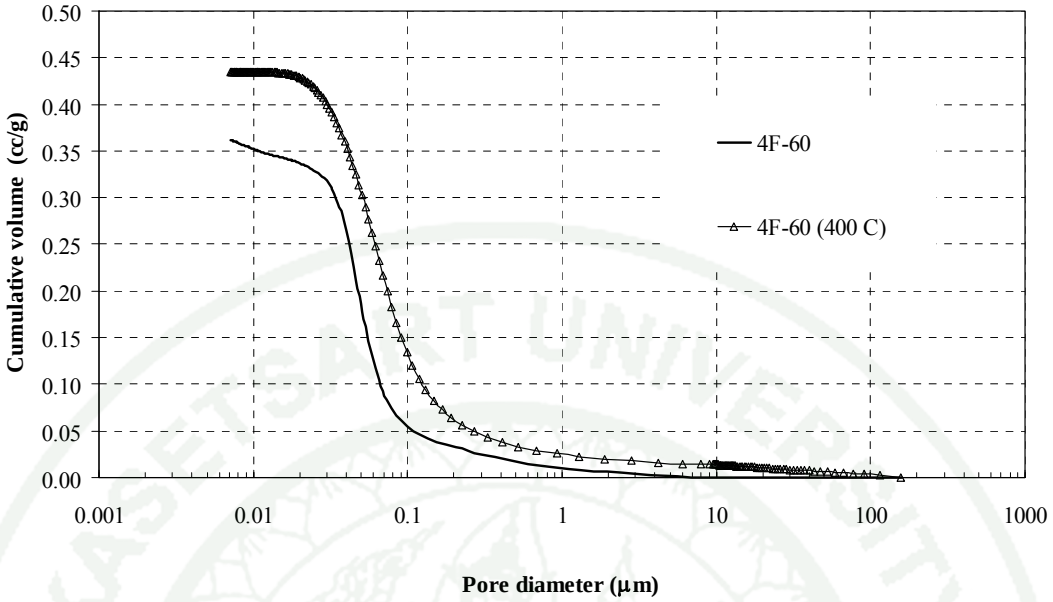

(a) Geopolymer MIP test results with 4M of NaOH solution

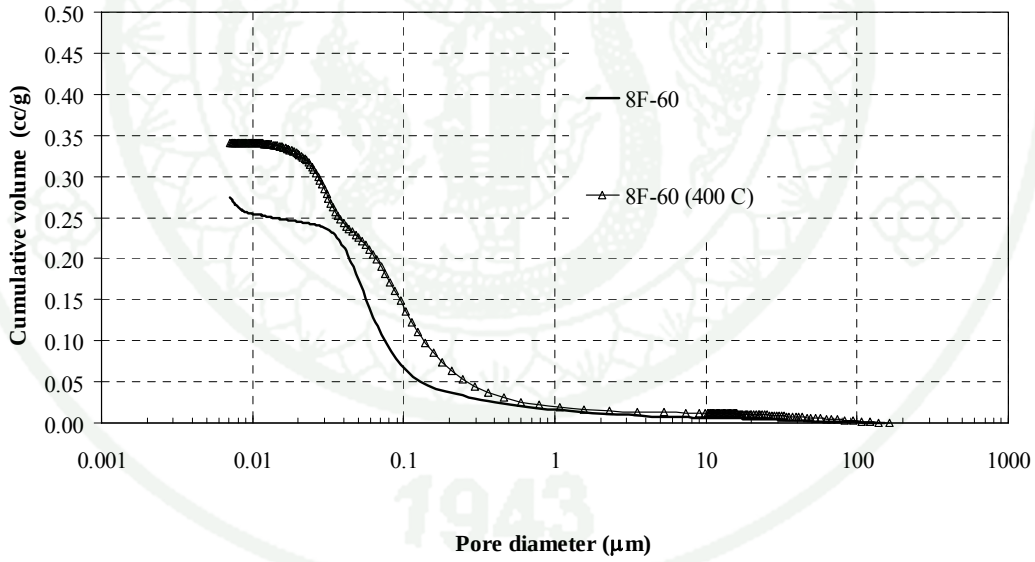

(b) Geopolymer MIP test results with 8M of NaOH solution

Figure 26 Cumulative volume of intrusion vs pore diameter in the MIP tests for the geopolymer class F fly ash before and after exposure to firing at 400°C

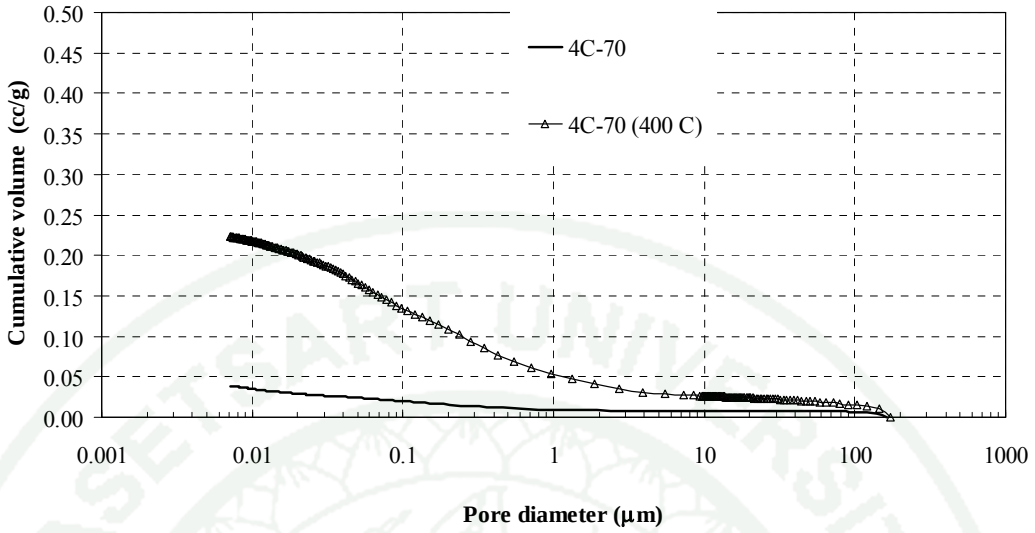

(a) Geopolymer MIP test results with 4M of NaOH solution

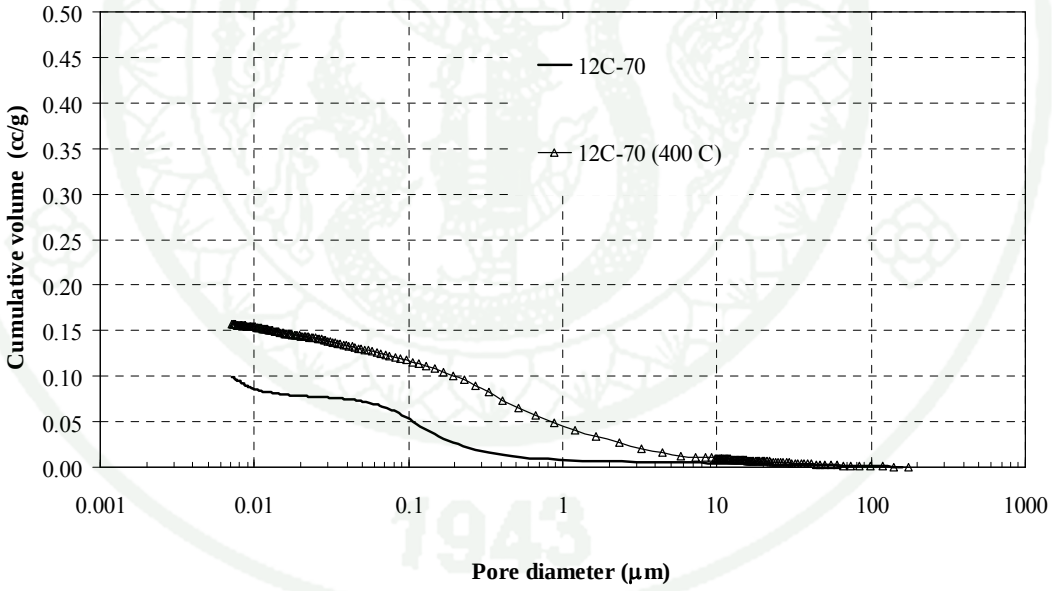

(b) Geopolymer MIP test results with 12M of NaOH solution

Figure 27 Cumulative volume of intrusion vs pore diameter in the MIP tests for the geopolymer class C fly ash before and after exposure to firing at 400°C

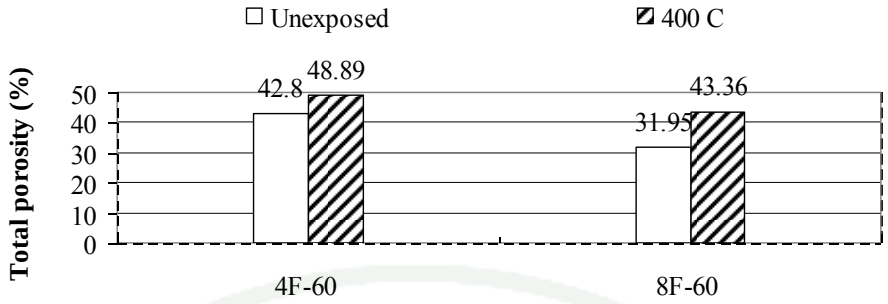

(a) The development of porosity (%)

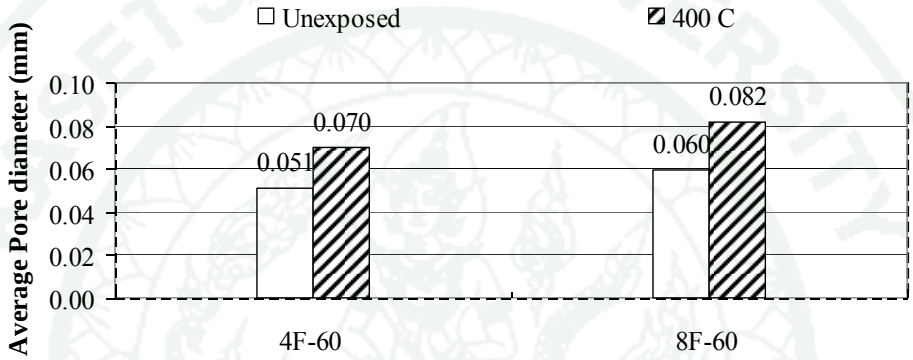

(b) The development of average pore diameter (μm)

Figure 28 Total porosity and average pore diameter in the MIP tests for the geopolymer class F fly ash before and after exposure to firing at 400°C

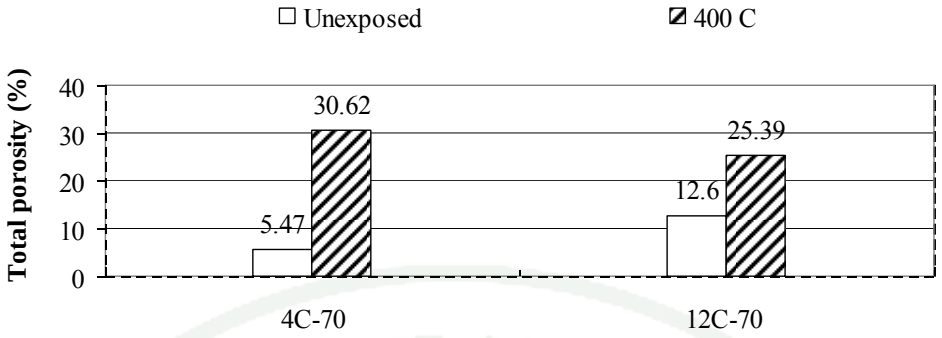

(a) The development of porosity (%)

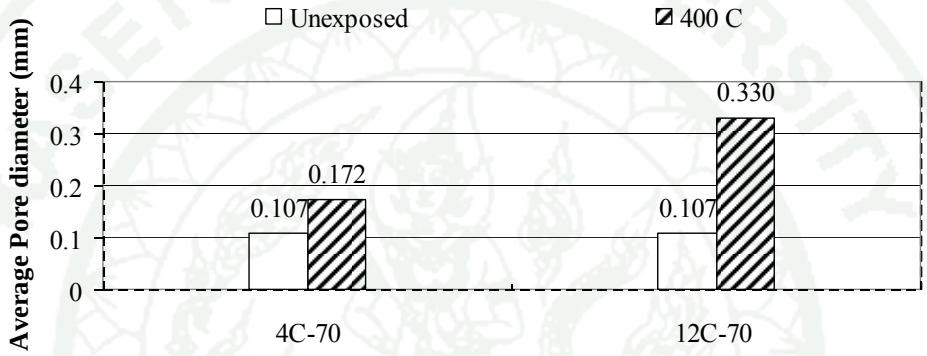

(b) The development of average pore diameter (μm)

Figure 29 Total porosity and average pore diameter in the MIP tests for the geopolymer class C fly ash before and after exposure to firing at 400°C

4.2 XRD

Crystallisation and phase changes have been observed to occur in geopolymers exposed to elevated temperatures. Phase identification is usually conducted by analysis using x-ray diffraction (XRD) data. The results of XRD analysis of geopolymer-pastes are shown in Fig. 30. Fig. 30 presents XRD patterns of geopolymer material prepared using fly ash classes F and C before and after exposure to firing at 400°C, and which used 4M NaOH in the mix. The main crystalline phases of fly ash detected from XRD (Fig. 30) were quartz (Q, SiO_2), mullite (M, $Ai_6Si_2O_{13}$) and calcite (C, $CaCO_3$). The crystalline phases, quartz, mullite and calcite were detected in the initial material before and after the fire test. After exposure to firing at 400°C, the diffraction pattern showed no apparent changes to the initial samples,

when compared to same type fly ash. Further heating of the geopolymer to 400°C caused the sample to melt. From the patterns, the XRD for unheated samples (4F-60, 4C-70) and heated samples were similar, indicating that geopolymerization did not significantly alter the degree of amorphousness and crystallization when exposed to fire at 400°C. The crystalline phase, quartz (SiO_2), is commonly found in fly ashes, and calcite($CaCO_3$) was found during mixing due to the fact that Ca^{2+} reacts with OH^- in the alkaline aqueous system to form $Ca(OH)_2$, which then reacts with CO_2 in the atmosphere forming calcite, $CaCO_3$.

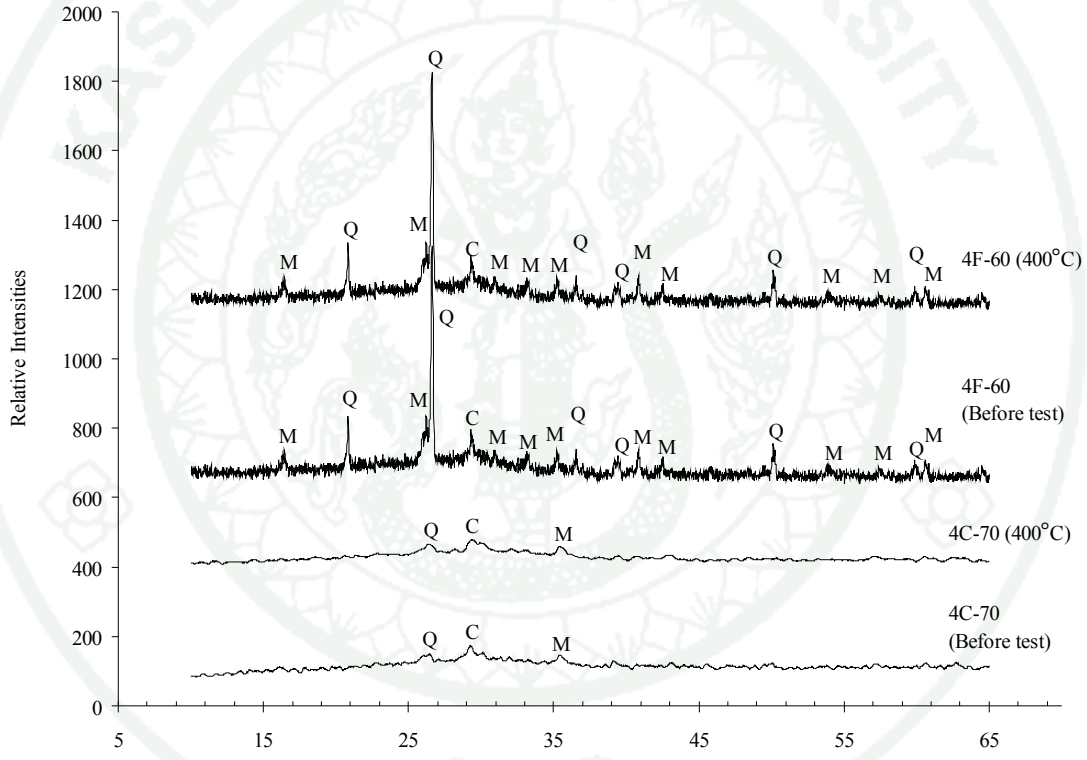

Figure 30 XRD patterns of fly ash-based geopolymer prepared using Class F and C fly ash, before and after exposure to 400°C. Q= quartz, M= mullite and C = calcite

CONCLUSION AND RECOMMENDATIONS

Conclusion

From the data obtained, it can be concluded that the concentration of NaOH solution and fly ash content have a direct bearing on the compressive strength, thermal stability and fire-resistance of geopolymer, and that in the correct proportions they can offer improvements and advantages over conventional binders. The effect of NaOH concentration and fly ash content can be clarified by examining the results obtained from this study, and from which the following conclusions can be drawn:

1. The thermal stability of geopolymer materials prepared using high concentrations of NaOH was quite low. Materials prepared using high fly ash content ratios had better thermal stability than those prepared using low content ratios. The thermal stability of geopolymer-paste made using Class F fly ash was further improved by reducing the NaOH concentration and increasing fly ash content, although reducing the concentration of NaOH was more effective in improving thermal stability than increasing fly ash content alone. Analysis of the data indicated that the most suitable mix-ratio for geopolymers made using Class F fly ash was 4F-60. Geopolymer-paste made using Class C fly ash with an NaOH concentration at 8M showed improved thermal stability, except when made with a fly ash content ratio of 60% by weight of mix. Increasing the fly ash content produced greater thermal stability. The most suitable mix-ratio for geopolymers made using Class C fly was found to be 8C-70.

2. Geopolymer materials prepared using low concentrations of NaOH and a high fly ash content showed good fire resistance and low thermal conductivity values (K) in geopolymer-paste panels made with both classes of fly ash, F and C, in mixture ratios of 4F-60 and 4C-70 respectively. These were the best ratios when exposed to firing above 800°C.

3. The Mercury Intrusion Porosimetry (MIP) results confirmed that a reduction in concentration of NaOH solution resulted in a decrease in average pore diameter. However, it also increased cumulative pore volume and total porosity, both of which effected increases in residual strength after heating. The porosity of the geopolymer rose on firing at 400°C, and the material density decreased. This was caused due to the melting of amorphous material from fly ash particles during heating, as this exposed additional pores from within the unreacted fly ash particles. The geopolymer materials prepared using low concentrations of NaOH had a more interconnected pore structure which facilitated the escape of moisture when heated. Consquently, materials prepared with higher concentrations of NaOH experienced greater deteriorations in strength compared to those prepared with lower concentrations after exposure to firing at 400°C.

4. The XRD results indicated that geopolymer showed similar peak intensity in fly ash-based geopolymers before and after exposure to 400°C: Class C fly ash was shown to have a mainly amorphous structure, while Class F fly ash had a considerably crystalline composition. In this study, the onset of crystal growth in the geopolymer-paste was not found at 400°C. This study demonstrated that a loss of compressive strength in fly ash-based geopolymer when exposed to firing was associated with a significant increase in the average pore size and total porosity percentages of the geopolymer paste specimens.

Recommendations

1. Future research should be concerned with water/binder ratios, higher NaOH and shrinkage in the geopolymer paste due to some shrinkage/expansion processes, which can occur during heating at high temperature, especially important in geopolymers containing aggregates with thermal expansion mismatch between binder and aggregate.

2. Study the addition of amount of calcium to fly ash geopolymers and the sodium silicate/NaOH ratio at high temperature.

3. Study crystal formation, crystal destruction and crystal structural changes at higher temperature.

4. Study the relation between the thermal resistance of the protection layer and the thickness of equivalent concrete protection due to geopolymers designed for high temperature applications which may be exposed to temperatures in excess of 400°C.

LITERATURE CITED

Barbosa, V.F.F. and K.J.D. MacKenzie. 2002. Synthesis and thermal behaviour of potassium sialate geopolymers. **Material Letters.** 4012: 1477-1482.

_____. 2003. Themal behaviour of inorganic geopolymers and composites derived from sodium polysialate. **Material Reseach Bulletin.** 38(2): 319-331.

_____ and C. Thaumaturgo. 2000. Synthesis and characterization of materials based on inorganic polymers of alumina and silica : sodium polysialate polymers. **International Journal of Inorganic Material.** 2(4): 309-317.

Bakharev, T. 2006. Thermal behaviour of geopolymers prepared using class F fly ash and elevated temperature curing. **Cement and Concrete Research** 36: 1134-1147.

Cheng, T.W. and J.P.Chiu. 2003. Chiu.Fire-Resistant Geopolymer Produced by Granulated Blast Furnace Slag, **Minerals Engineering** 16: 205-210.

Chindaprasirt, P., T. Chareerat and V. Sirivivatnanon. 2007. Workability and strength of coarse high calcium fly ash geopolymer. **Cement and Concrete Composite.** 29: 224-229.

Davidovits, J. 1982. Mineral polymers and method of making them. **United States Patent.** 4: 349, 386.

_____. 1987. Properties of geopolymer cements. **Concrete International** 9: 23-35.

_____. 1988. **Geopolymers of the first generation: Siliface-Process**. Geopolymer'88, First European Conference on Soft Mineralogy. Compiegne, France.

Davidovits, J. 1991. Geopolymers: Inorganic Polymeric New Materials. **Journal of Thermal Analysis.** 37: 1633-1656.

_____. 1994a. Properties of geopolymer cements, Vol.1 pp. 131-149. *In* **Proceeding of the First International Conference on Alkaline Cements and Concretes.** 1994, Scientific Research Institute on Binder and Materials, Kiev State Technical University, Kiev, Ukraine.

_____. 1994b. Global warning impact on the cement and aggregate industries. **World Resource Review.** 6(2): 263-278.

_____. 1999. **Chemistry of Geopolymeric System Terminology**. Geopolymere '99. Saint-Quentine, France.

_____. 2002. They have built the Pyramids. **Workshop Curtin University of Technolygy,** 12(8): 120-134.

_____. and C. James. 1988. Low temperature geopolymeric setting (LTGS) and Archaeometry. **Geopolymere '88.** First European Conference on Soft Mineralogy, Compiegne, France.

_____. and J.L. Sawyer. 1985. Early-high strength mineral polymer. **United States Patent.** 26: 1033-1041.

Dombrowski, K., A. Buchwald and M. Weil. 2007. The influence of calcium content on the structure and thermal performance of fly ash based geopolymers. **Journal of Material Science** 42: 3033-3043.

Hardjito, D., S.E. Wallah and B.V. Rangan. 2002. Study of engineering properties of fly ash based Geopolymer concrete. **Journal of the Australian Ceramic Society.** 38(1): 44-47.

Hardjito, D., S.E. Wallah, D.M.J. Sumajouw and B.V. Rangan. 2004a. Properties of Geopolymer concrete with fly ash as source material : effect of mixture composition. **The 7th CANMET/ACI International Conference on Recent Advances in Concrete Technology.** Las Vegas, USA.

_____. 2004b. On the development of fly ash based Geopolymer concrete. **ACI material journal.** 101(6): 467-471.

Hardjito, D. and M. Tsen. 2008. Strength and Thermal Stability of Fly ash Based Geopolymer Mortar, **3rd International Conference-ACF/VCA**, 2008: A.05

Kong.D.L.Y, J. G. Sanjayan, and K. Sagoe-Crentsil. 2007. Comparatve performance of geopolymers made with metakaolin and fly ash after exposure to elevated temperatures. **Cement and Concrete Research** 37(12): 1583-1589, 2007.

Palomo, A., M.T. Blanco-Varela, M.L. Granizo, F. Puertas, T. Vasquez and M.W. Grutzeck. 1999. Chemical stability of cementitious materials based on metakaolin. **Cement and Concrete Research** 29: 997-1004.

Xu, H. and J.S.J. Van Deventer. 2000. The geopolymerisation of alumino silicate minerials. **International Journal of Mineral Processing** 59(3): 247-266.

APPENDICES

Appendix A

Tables

Appendix Table A1 Mixture composition in terms of molar ratio

Mixture No	Concentration of NaOH (Mole)	Molar ratio			Water/binder ratio
		SiO_2/Al_2O_3	Na_2O/SiO_2	Na_2O/Al_2O_3	w/b
F1	4	6.11	0.14	0.84	0.38
F2	8	6.11	0.21	1.29	0.35
F3	12	6.11	0.28	1.74	0.31
F4	4	5.90	0.12	0.69	0.34
F5	8	5.90	0.18	1.06	0.31
F6	12	5.90	0.24	1.43	0.28
F7	4	5.72	0.10	0.57	0.30
F8	8	5.72	0.15	0.87	0.28
F9	12	5.72	0.20	1.17	0.25
C1	4	3.92	0.2	0.77	0.31
C2	8	3.92	0.29	1.12	0.29
C3	12	3.92	0.38	1.48	0.26
C4	4	3.74	0.17	0.64	0.28
C5	8	3.74	0.25	0.93	0.25
C6	12	3.74	0.33	1.22	0.23
C7	4	3.59	0.15	0.54	0.24
C8	8	3.59	0.21	0.76	0.22
C9	12	3.59	0.28	0.99	0.20

Appendix Table A2 Compressive strength of specimens after thermal exposure for class F fly ash

Specimens	Sample No.	Strength (ksc.)			
		Before firing	After firing (°C)		
			200	300	400
4F-50	1	144.52	144.56	55.24	48.85
	2	168.58	81.29	63.01	51.80
	3	173.09	134.12	68.90	54.72
	Average	162.06	119.99	62.38	51.79
8F-50	1	162.95	34.43	13.18	18.01
	2	183.53	29.45	-	20.52
	3	192.32	33.05	-	22.41
	Average	179.60	32.31	13.18	20.31
12F-50	1	97.52	23.91	9.86	7.58
	2	127.24	17.81	-	8.28
	3	117.54	19.76	-	9.01
	Average	114.10	20.49	9.86	8.29

Appendix Table A2 (Continued)

Specimens	Sample No.	Strength (ksc.)			
		Before firing	After firing (°C)		
			200	300	400
4F-55	1	164.70	149.14	55.37	96.53
	2	132.40	89.51	89.57	89.57
	3	182.60	119.34	55.47	125.55
	Average	159.90	119.33	66.80	103.88
8F-55	1	182.35	42.13	46.07	31.98
	2	182.13	32.91	43.18	46.01
	3	183.74	31.91	44.19	48.67
	Average	182.74	35.65	44.48	42.22
12F-55	1	230.44	23.91	13.74	12.53
	2	176.53	21.91	12.10	11.99
	3	234.97	23.63	15.64	12.86
	Average	213.98	23.15	13.83	12.46
4F-60	1	130.73	111.09	90.31	80.05
	2	111.81	101.92	119.65	87.44
	3	120.37	106.52	89.90	76.47
	Average	120.97	106.51	99.95	81.32
8F-60	1	295.27	126.71	76.71	90.54
	2	274.02	104.80	97.50	69.05
	3	319.40	115.77	89.33	35.89
	Average	296.23	115.76	87.85	65.16
12F-60	1	201.86	22.76	15.60	25.72
	2	254.74	21.04	19.45	28.31
	3	267.22	21.06	13.50	26.37
	Average	241.27	21.62	16.18	26.80

Appendix Table A3 Compressive strength of specimens after thermal exposure for class C fly ash

Specimens	Sample No.	Strength (ksc.)			
		Before firing	After firing (°C)		
			200	300	400
4C-60	1	198.41	80.65	36.83	43.21
	2	211.45	96.86	44.26	50.73
	3	195.93	95.28	65.87	52.01
	Average	201.93	90.93	48.99	48.65
8C-60	1	242.29	55.65	33.11	27.36
	2	212.98	37.93	23.73	45.09
	3	242.65	39.25	15.65	44.56
	Average	232.64	44.28	24.16	39.00
12C-60	1	320.49	31.20	14.64	12.41
	2	338.90	18.31	21.89	-
	3	303.15	22.16	17.89	-
	Average	320.85	23.89	18.14	12.41
4C-65	1	286.49	112.79	80.27	66.50
	2	273.55	90.23	109.96	72.81
	3	257.13	128.06	113.34	60.16
	Average	272.39	110.36	101.19	66.49
8C-65	1	375.97	154.23	144.36	111.87
	2	263.37	190.38	129.15	123.22
	3	275.07	219.42	128.55	123.53
	Average	304.80	188.01	134.02	119.54
12C-65	1	328.82	83.51	68.50	51.38
	2	323.69	85.31	49.74	50.73
	3	326.27	100.67	82.82	47.02
	Average	326.26	89.83	67.02	49.71
4C-70	1	308.86	99.29	121.94	137.35
	2	256.88	80.41	104.54	185.18
	3	312.87	117.39	97.10	98.85
	Average	292.87	99.03	107.86	140.46

Appendix Table A3 (Continued)

Specimens	Sample No.	Strength (ksc.)			
		Before firing	After firing (°C)		
			200	300	400
8C-70	1	352.74	177.16	127.70	140.50
	2	348.07	198.14	163.71	198.55
	3	367.95	234.21	138.10	176.71
	Average	356.25	203.17	143.17	171.92
12C-70	1	488.30	201.17	216.63	130.83
	2	504.15	274.00	195.43	161.49
	3	511.24	208.32	175.43	119.13
	Average	501.23	227.83	195.83	137.15

Appendix Table A4 Residual strength of specimens after thermal exposure for class F fly ash

Mixture No.	Concentration of NaOH (Mole)	Designation	Residual strength (%) After firing (°C)		
			200	300	400
F1	4	4F-50	74.04	38.49	31.96
F2	8	8F-50	17.99	7.34	11.31
F3	12	12F-50	19.70	9.48	7.97
F4	4	4F-55	74.63	41.78	64.97
F5	8	8F-55	21.16	26.40	25.06
F6	12	12F-55	11.44	6.83	6.16
F7	4	4F-60	88.05	82.62	67.22
F8	8	8F-60	39.08	29.66	22.00
F9	12	12F-60	8.96	6.71	11.11

Appendix Table A5 Residual strength of specimens after thermal exposure for class C fly ash

Mixture No.	Concentration of NaOH (Mole)	Designation	Residual strength (%) After firing (°C)		
			200	300	400
C1	4	4C-60	45.03	24.26	24.09
C2	8	8C-60	19.03	10.39	16.77
C3	12	12C-60	7.45	5.65	3.87
C4	4	4C-65	40.52	37.15	24.41
C5	8	8C-65	61.68	43.97	39.22
C6	12	12C-65	27.53	20.54	15.24
C7	4	4C-70	33.81	36.83	47.96
C8	8	8C-70	57.03	40.19	48.26
C9	12	12C-70	45.45	39.07	27.36

Appendix Table A6 Result of thermal conductivity testing after exposure for geopolymer-paste panels. Mix F1, 4M, Class F fly ash 50%

Time	T_{IN} (°C)		T_{OUT} (°C)	Thermal Conductivity
(min)	E119 Std.	Ave. Furnace	Ave. thermocouple	$W.m^{-1}.K^{-1}$
0	30	39	32	
1		475	63	0.268
2		570	82	0.248
3		621	93	0.239
4		638	99	0.237
5	538	650	100	0.235
6		669	107	0.232
7		679	127	0.234
8		683	158	0.240
9		688	186	0.245
10	704	703	215	0.249
11		713	239	0.252
12		717	261	0.257
13		720	282	0.261
14		724	304	0.266
15		722	323	0.272
16		721	341	0.278

Appendix Table A6 (Continued)

Time	T_{IN} (°C)		T_{OUT} (°C)	Thermal Conductivity
(min)	E119 Std.	Ave. Furnace	Ave. thermocouple	$W.m^{-1}.K^{-1}$
17		724	361	0.283
18		740	382	0.284
19		734	395	0.290
20		737	409	0.294
21		739	422	0.298
22		756	435	0.296
23		766	441	0.295
24		752	442	0.300
25		759	444	0.299
26		754	441	0.299
27		766	440	0.295
28		765	442	0.296
29		776	440	0.291
30	843	800	448	0.286
31		803	449	0.286
32		806	450	0.285
33		813	452	0.283
34		813	453	0.284
35		805	451	0.286

Appendix Table A7 Result of thermal conductivity testing after exposure for geopolymer-paste panels. Mix F2, 8M, Class F fly ash 50%

Time	T_{IN} (°C)		T_{OUT} (°C)	Thermal Conductivity
(min)	E119 Std	Ave. Furnace	Ave. thermocouple	$W.m^{-1}.K^{-1}$
0	30	35	31	
1		404	61	0.233
2		576	82	0.219
3		655	95	0.216
4		688	105	0.220
5	538	731	120	0.216
6		747	136	0.219

Appendix Table A7 (Continued)

Time	T_{IN} (^{o}C)		T_{OUT} (^{o}C)	Thermal Conductivity
(min)	E119 Std	Ave. Furnace	Ave. thermocouple	$W.m^{-1}.K^{-1}$
7		762	164	0.222
8		768	196	0.228
9		757	234	0.241
10	704	768	275	0.246
11		761	328	0.263
12		772	397	0.278
13		768	445	0.296
14		786	475	0.297
15		789	499	0.305
16		795	514	0.306
17		802	525	0.307
18		805	534	0.309
19		807	537	0.308
20		813	543	0.308
21		813	543	0.308
22		815	549	0.308
23		812	555	0.312
24		816	559	0.310
25		816	564	0.312
26		820	565	0.310
27		815	570	0.313
28		811	569	0.316
29		818	567	0.312
30	843	817	571	0.315
31		811	579	0.322
32		821	579	0.317
33		823	579	0.318
34		818	578	0.320
35		824	581	0.318

Appendix Table A8 Result of thermal conductivity testing after exposure for geopolymer-paste panels. Mix F3, 12M, Class F fly ash 50%

Time	T_{IN} (°C)		T_{OUT} (°C)	Thermal Conductivity
(min)	E119 Std	Ave. Furnace	Ave. thermocouple	$W.m^{-1}.K^{-1}$
0	30	31	32	
1		56	70	0.276
2		81	89	0.246
3		94	100	0.243
4		105	116	0.239
5	538	122	119	0.237
6		140	168	0.245
7		170	199	0.245
8		207	240	0.252
9		248	289	0.259
10	704	291	316	0.261
11		337	355	0.272
12		384	392	0.277
13		420	434	0.287
14		452	463	0.290
15		470	479	0.292
16		488	493	0.294
17		497	509	0.297
18		506	516	0.301
19		509	521	0.300
20		522	530	0.307
21		525	529	0.302
22		527	530	0.301
23		530	531	0.304
24		529	529	0.302
25		529	532	0.301
26		531	533	0.303
27		531	541	0.305
28		530	525	0.298
29		532	525	0.294
30	843	532	530	0.297
31		530	542	0.305
32		531	532	0.297
33		529	537	0.299
34		528	531	0.297
35		530	535	0.299

Appendix Table A9 Result of thermal conductivity testing after exposure for geopolymer-paste panels. Mix F4, 4M, Class F fly ash 55%

Time	T_{IN} (°C)		T_{OUT} (°C)	Thermal Conductivity
(min)	E119 Std	Ave. Furnace	Ave. thermocouple	$W.m^{-1}.K^{-1}$
0	30	40	33	
1		450	58	0.274
2		574	78	0.247
3		613	91	0.241
4		655	99	0.233
5	538	668	102	0.231
6		628	108	0.241
7		640	127	0.243
8		662	140	0.241
9		671	166	0.245
10	704	674	190	0.250
11		659	222	0.261
12		701	251	0.258
13		710	275	0.262
14		718	300	0.267
15		727	330	0.273
16		734	362	0.280
17		746	394	0.286
18		756	425	0.293
19		765	450	0.299
20		755	468	0.309
21		762	480	0.310
22		776	483	0.306
23		769	488	0.311
24		785	486	0.304
25		780	489	0.307
26		781	492	0.308
27		783	489	0.306
28		787	489	0.305
29		792	494	0.305
30	843	786	494	0.307
31		791	492	0.304
32		791	492	0.304
33		783	496	0.309
34		787	496	0.307
35		789	492	0.305

Appendix Table A10 Result of thermal conductivity testing after exposure for geopolymer-paste panels. Mix F5, 8M, Class F fly ash 55%

Time	T_{IN} (°C)		T_{OUT} (°C)	Thermal Conductivity
(min)	E119 Std	Ave. Furnace	Ave. thermocouple	$W.m^{-1}.K^{-1}$
0	30	46	38	
1		332	75	0.274
2		531	97	0.243
3		608	108	0.240
4		655	128	0.240
5	538	675	161	0.247
6		688	197	0.255
7		709	232	0.259
8		725	271	0.264
9		740	323	0.274
10	704	743	369	0.287
11		746	418	0.303
12		761	463	0.311
13		770	499	0.320
14		782	525	0.324
15		787	540	0.327
16		794	550	0.327
17		796	559	0.329
18		794	562	0.332
19		796	564	0.331
20		785	570	0.342
21		797	568	0.334
22		800	578	0.336
23		804	586	0.338
24		805	591	0.339
25		807	589	0.336
26		796	589	0.344
27		802	595	0.343
28		802	592	0.341
29		800	594	0.343
30	843	799	597	0.344
31		801	605	0.345
32		799	602	0.345
33		802	599	0.342
34		800	595	0.341
35		805	599	0.339

Appendix Table A11 Result of thermal conductivity testing after exposure for geopolymer-paste panels. Mix F6, 12M, Class F fly ash 55%

Time	T_{IN} (°C)		T_{OUT} (°C)	Thermal Conductivity
(min)	E119 Std	Ave. Furnace	Ave. thermocouple	$W.m^{-1}.K^{-1}$
0	30	42	31	
1		354	86	0.262
2		571	111	0.233
3		641	124	0.231
4		687	135	0.229
5	538	716	152	0.229
6		732	170	0.231
7		742	200	0.236
8		756	237	0.241
9		767	278	0.248
10	704	779	321	0.255
11		792	367	0.263
12		801	414	0.272
13		806	450	0.282
14		815	482	0.287
15		815	485	0.289
16		822	503	0.290
17		826	512	0.292
18		832	521	0.292
19		834	524	0.292
20		835	537	0.296
21		838	540	0.295
22		838	542	0.296
23		841	545	0.294
24		837	544	0.296
25		839	544	0.294
26		842	546	0.293
27		842	546	0.293
28		845	545	0.291
29		844	547	0.292
30	843	845	547	0.292
31		845	550	0.293
32		845	551	0.293
33		846	550	0.292
34		843	555	0.295
35		845	554	0.294

Appendix Table A12 Result of thermal conductivity testing after exposure for geopolymer-paste panels. Mix F7, 4M, Class F fly ash 60%

Time	T_{IN} (°C)		T_{OUT} (°C)	Thermal Conductivity
(min)	E119 Std	Ave. Furnace	Ave. thermocouple	$W.m^{-1}.K^{-1}$
0	30	34	32	
1		387	58	0.294
2		578	77	0.245
3		604	88	0.242
4		623	94	0.239
5	538	628	95	0.238
6		636	98	0.237
7		651	119	0.238
8		673	149	0.240
9		660	177	0.250
10	704	671	206	0.254
11		685	230	0.257
12		697	252	0.259
13		682	273	0.269
14		690	295	0.273
15		692	314	0.278
16		699	328	0.280
17		710	348	0.283
18		723	369	0.286
19		739	382	0.285
20		722	396	0.295
21		745	409	0.291
22		746	422	0.295
23		737	428	0.301
24		752	429	0.296
25		764	431	0.292
26		767	424	0.289
27		757	423	0.292
28		781	425	0.285
29		773	423	0.287
30	843	767	431	0.291
31		773	432	0.290
32		767	433	0.292
33		768	435	0.292
34		814	436	0.278
35		805	434	0.280

Appendix Table A13 Result of thermal conductivity testing after exposure for geopolymer-paste panels. Mix F8, 8M, Class F fly ash 60%

Time	T_{IN} (°C)		T_{OUT} (°C)	Thermal Conductivity
(min)	E119 Std	Ave. Furnace	Ave. thermocouple	$W.m^{-1}.K^{-1}$
0	30	31	35	
1		338	61	0.264
2		545	85	0.236
3		645	100	0.227
4		694	107	0.224
5	538	729	122	0.223
6		749	147	0.225
7		754	173	0.231
8		765	200	0.233
9		776	238	0.238
10	704	781	277	0.245
11		787	317	0.253
12		787	351	0.262
13		791	390	0.271
14		795	425	0.279
15		803	458	0.285
16		803	478	0.291
17		804	491	0.295
18		819	505	0.291
19		805	509	0.301
20		811	516	0.300
21		818	518	0.296
22		801	519	0.307
23		818	523	0.297
24		825	527	0.296
25		833	539	0.295
26		831	541	0.298
27		833	544	0.297
28		825	545	0.301
29		824	540	0.300
30	843	829	544	0.300
31		832	553	0.301
32		830	556	0.304
33		832	559	0.302
34		829	561	0.305
35		832	563	0.305

Appendix Table A14 Result of thermal conductivity testing after exposure for geopolymer-paste panels. Mix F9, 12M, Class F fly ash 60%

Time	T_{IN} (°C)		T_{OUT} (°C)	Thermal Conductivity
(min)	E119 Std	Ave. Furnace	Ave. thermocouple	$W.m^{-1}.K^{-1}$
0	30	32	31	
1		407	57	0.238
2		599	89	0.219
3		673	114	0.222
4		713	144	0.226
5	538	736	175	0.231
6		753	189	0.232
7		766	219	0.235
8		770	250	0.242
9		775	281	0.248
10	704	783	310	0.252
11		787	337	0.258
12		791	367	0.264
13		794	393	0.270
14		797	417	0.275
15		802	441	0.280
16		805	450	0.282
17		807	476	0.289
18		811	488	0.291
19		811	495	0.293
20		814	502	0.293
21		814	488	0.289
22		814	491	0.289
23		817	495	0.289
24		817	497	0.289
25		820	493	0.286
26		815	499	0.290
27		814	503	0.292
28		817	505	0.290
29		816	509	0.292
30	843	817	512	0.292
31		817	509	0.290
32		819	510	0.290
33		819	508	0.289
34		819	510	0.289
35		818	512	0.290

Appendix Table A15 Result of thermal conductivity testing after exposure for geopolymer-paste panels. Mix C1, 4M, Class C fly ash 60%

Time	T_{IN} (°C)		T_{OUT} (°C)	Thermal Conductivity
(min)	E119 Std	Ave. Furnace	Ave. thermocouple	$W.m^{-1}.K^{-1}$
0	30	34	32	
1		470	98	0.280
2		605	119	0.249
3		645	132	0.243
4		669	140	0.239
5	538	686	153	0.238
6		700	165	0.238
7		717	175	0.236
8		724	194	0.239
9		735	217	0.242
10	704	746	248	0.246
11		753	274	0.251
12		760	298	0.255
13		764	321	0.260
14		768	345	0.265
15		770	366	0.271
16		776	386	0.275
17		781	408	0.280
18		785	431	0.286
19		792	446	0.288
20		789	462	0.294
21		791	477	0.299
22		790	492	0.305
23		797	500	0.305
24		799	503	0.305
25		794	507	0.309
26		801	506	0.306
27		803	507	0.305
28		796	511	0.309
29		803	511	0.307
30	843	798	521	0.312
31		787	524	0.318
32		789	527	0.318
33		798	531	0.316
34		797	534	0.318
35		791	534	0.320

Appendix Table A16 Result of thermal conductivity testing after exposure for geopolymer-paste panels. Mix C2, 8M, Class C fly ash 60%

Time	T_{IN} (°C)		T_{OUT} (°C)	Thermal Conductivity
(min)	E119 Std	Ave. Furnace	Ave. thermocouple	$W.m^{-1}.K^{-1}$
0	30	33	30	
1		377	113	0.249
2		523	133	0.226
3		583	157	0.228
4		632	204	0.230
5	538	638	253	0.251
6		671	305	0.257
7		697	351	0.261
8		707	387	0.271
9		701	421	0.290
10	704	711	468	0.306
11		718	494	0.312
12		720	518	0.318
13		724	542	0.329
14		734	564	0.328
15		719	583	0.347
16		733	600	0.339
17		734	612	0.351
18		742	623	0.358
19		746	632	0.363
20		732	637	0.384
21		754	643	0.368
22		755	640	0.365
23		746	646	0.375
24		759	648	0.359
25		759	649	0.361
26		754	651	0.371
27		765	651	0.362
28		751	653	0.376
29		743	653	0.392
30	843	765	644	0.359
31		756	654	0.367
32		768	652	0.354
33		756	653	0.374
34		759	654	0.371
35		771	655	0.358

Appendix Table A17 Result of thermal conductivity testing after exposure for geopolymer-paste panels. Mix C3, 12M, Class C fly ash 60%

Time	T_{IN} (°C)		T_{OUT} (°C)	Thermal Conductivity
(min)	E119 Std	Ave. Furnace	Ave. thermocouple	$W.m^{-1}.K^{-1}$
0	30	31	30	
1		390	93	0.241
2		581	112	0.214
3		659	135	0.214
4		699	181	0.221
5	538	726	229	0.227
6		740	280	0.237
7		749	325	0.246
8		756	360	0.253
9		760	393	0.260
10	704	759	426	0.269
11		757	451	0.275
12		760	473	0.280
13		761	496	0.287
14		756	516	0.293
15		761	534	0.297
16		762	549	0.302
17		769	560	0.304
18		774	569	0.306
19		774	577	0.309
20		780	582	0.309
21		783	588	0.310
22		781	585	0.310
23		783	591	0.311
24		783	593	0.312
25		784	594	0.312
26		791	596	0.311
27		791	596	0.311
28		789	598	0.312
29		787	598	0.312
30	843	794	589	0.307
31		794	599	0.311
32		793	597	0.311
33		792	598	0.310
34		792	599	0.310
35		828	600	0.313

Appendix Table A18 Result of thermal conductivity testing after exposure for geopolymer-paste panels. Mix C4, 4M, Class C fly ash 65%

Time	T_{IN} (°C)		T_{OUT} (°C)	Thermal Conductivity
(min)	E119 Std	Ave. Furnace	Ave. thermocouple	$W.m^{-1}.K^{-1}$
0	30	50	33	
1		514	82	0.263
2		631	104	0.240
3		661	119	0.236
4		679	129	0.234
5	538	690	134	0.233
6		696	142	0.234
7		709	146	0.232
8		714	153	0.232
9		728	161	0.231
10	704	736	177	0.233
11		736	190	0.235
12		748	222	0.240
13		752	248	0.245
14		759	275	0.250
15		765	307	0.256
16		769	341	0.264
17		770	355	0.267
18		772	388	0.276
19		777	415	0.283
20		777	435	0.289
21		784	449	0.292
22		784	454	0.293
23		784	461	0.296
24		780	461	0.297
25		784	466	0.297
26		777	471	0.302
27		780	470	0.300
28		783	472	0.300
29		782	479	0.303
30	843	780	481	0.304
31		776	481	0.306
32		784	483	0.303
33		784	489	0.306
34		778	491	0.309
35		780	489	0.307

Appendix Table A19 Result of thermal conductivity testing after exposure for geopolymer-paste panels. Mix C5, 8M, Class C fly ash 65%

Time	T_{IN} (°C)		T_{OUT} (°C)	Thermal Conductivity
(min)	E119 Std	Ave. Furnace	Ave. thermocouple	$W.m^{-1}.K^{-1}$
0	30	34	35	
1		341	84	0.258
2		490	107	0.233
3		556	130	0.231
4		602	161	0.234
5	538	629	186	0.239
6		659	219	0.241
7		671	242	0.248
8		682	273	0.254
9		686	306	0.263
10	704	696	343	0.269
11		698	379	0.282
12		707	409	0.287
13		709	434	0.296
14		715	458	0.303
15		710	476	0.313
16		721	485	0.308
17		725	500	0.315
18		717	511	0.323
19		722	518	0.320
20		726	515	0.318
21		732	521	0.318
22		736	520	0.317
23		733	522	0.321
24		742	523	0.315
25		741	523	0.316
26		741	524	0.317
27		740	526	0.316
28		740	529	0.317
29		741	524	0.312
30	843	743	528	0.316
31		744	523	0.313
32		746	524	0.314
33		752	527	0.313
34		750	527	0.315
35		745	527	0.318

Appendix Table A20 Result of thermal conductivity testing after exposure for geopolymer-paste panels. Mix C6, 12M, Class C fly ash 65%

Time	T_{IN} (°C)		T_{OUT} (°C)	Thermal Conductivity
(min)	E119 Std	Ave. Furnace	Ave. thermocouple	$W.m^{-1}.K^{-1}$
0	30	35	41	
1		340	83	0.269
2		504	106	0.244
3		592	124	0.239
4		642	145	0.236
5	538	669	150	0.234
6		694	171	0.233
7		699	184	0.237
8		705	203	0.241
9		713	224	0.244
10	704	721	250	0.248
11		726	295	0.258
12		728	326	0.267
13		729	351	0.274
14		740	377	0.277
15		742	402	0.284
16		751	423	0.287
17		742	438	0.298
18		751	460	0.301
19		755	477	0.305
20		756	485	0.308
21		753	485	0.310
22		757	487	0.309
23		751	492	0.315
24		755	492	0.313
25		753	495	0.316
26		750	498	0.320
27		751	498	0.320
28		759	501	0.314
29		748	502	0.323
30	843	743	505	0.328
31		752	502	0.320
32		752	504	0.321
33		746	508	0.327
34		752	509	0.323
35		743	508	0.328

Appendix Table A21 Result of thermal conductivity testing after exposure for geopolymer-paste panels. Mix C7, 4M, Class C fly ash 70%

Time	T_{IN} (°C)		T_{OUT} (°C)	Thermal Conductivity
(min)	E119 Std	Ave. Furnace	Ave. thermocouple	$W.m^{-1}.K^{-1}$
0	30	31	35	
1		476	70	0.270
2		609	94	0.242
3		652	111	0.236
4		669	116	0.234
5	538	683	120	0.232
6		696	130	0.231
7		706	134	0.230
8		710	131	0.228
9		720	139	0.228
10	704	726	149	0.229
11		730	154	0.229
12		736	166	0.230
13		741	183	0.233
14		743	211	0.238
15		747	244	0.245
16		751	279	0.252
17		753	314	0.261
18		755	348	0.270
19		756	376	0.278
20		759	397	0.283
21		759	405	0.286
22		761	411	0.287
23		761	418	0.289
24		761	419	0.289
25		762	424	0.291
26		763	430	0.292
27		765	429	0.291
28		763	432	0.293
29		766	439	0.294
30	843	766	442	0.295
31		762	442	0.297
32		766	445	0.296
33		768	451	0.298
34		767	454	0.299
35		768	452	0.298

Appendix Table A22 Result of thermal conductivity testing after exposure for geopolymer-paste panels. Mix C8, 8M, Class C fly ash 70%

Time	T_{IN} (°C)		T_{OUT} (°C)	Thermal Conductivity
(min)	E119 Std	Ave. Furnace	Ave. thermocouple	$W.m^{-1}.K^{-1}$
0	30	33	33	
1		434	154	0.251
2		500	224	0.273
3		593	275	0.265
4		640	335	0.273
5	538	658	398	0.297
6		668	444	0.317
7		686	496	0.327
8		702	539	0.340
9		690	593	0.383
10	704	729	620	0.376
11		704	639	0.402
12		722	645	0.390
13		728	652	0.388
14		733	655	0.387
15		738	656	0.402
16		744	669	0.409
17		731	663	0.414
18		740	668	0.400
19		714	671	0.430
20		738	670	0.395
21		745	668	0.401
22		744	672	0.400
23		752	677	0.394
24		746	675	0.396
25		748	677	0.409
26		751	690	0.414
27		740	688	0.416
28		732	690	0.421
29		752	690	0.405
30	843	734	689	0.426
31		755	687	0.400
32		759	685	0.401
33		761	688	0.400
34		761	687	0.396
35		759	686	0.402

Appendix Table A23 Result of thermal conductivity testing after exposure for geopolymer-paste panels. Mix C9, 12M, Class C fly ash 70%

Time	T_{IN} (°C)		T_{OUT} (°C)	Thermal Conductivity
(min)	E119 Std	Ave. Furnace	Ave. thermocouple	$W.m^{-1}.K^{-1}$
0	30	32	33	
1		351	129	0.288
2		675	199	0.271
3		621	250	0.270
4		674	310	0.278
5	538	701	373	0.293
6		723	419	0.300
7		744	471	0.309
8		754	514	0.323
9		764	543	0.329
10	704	772	570	0.335
11		782	589	0.338
12		796	595	0.334
13		798	602	0.339
14		798	605	0.339
15		794	606	0.342
16		797	619	0.346
17		788	613	0.349
18		792	618	0.348
19		796	621	0.347
20		791	620	0.350
21		786	618	0.350
22		786	622	0.352
23		785	627	0.355
24		780	625	0.357
25		774	627	0.363
26		776	625	0.359
27		775	623	0.357
28		776	625	0.356
29		790	625	0.357
30	843	768	624	0.360
31		763	622	0.362
32		757	620	0.363
33		762	623	0.361
34		755	622	0.366
35		757	621	0.362

Appendix B

Figures

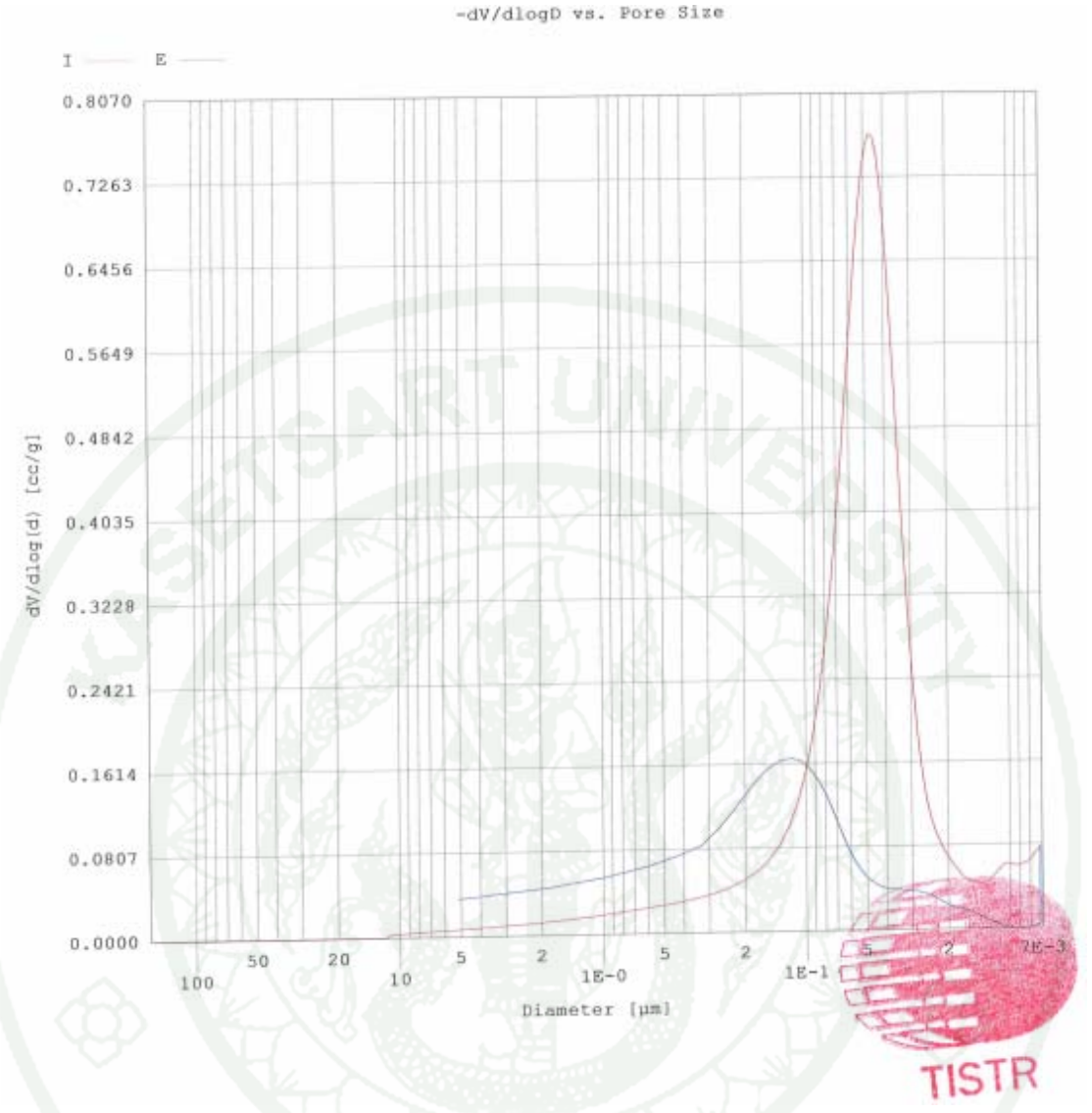

Appendix Figure B1 Pore size distribution in the MIP tests for the 4M geopolymer class F fly ash 60% before exposure to firing.

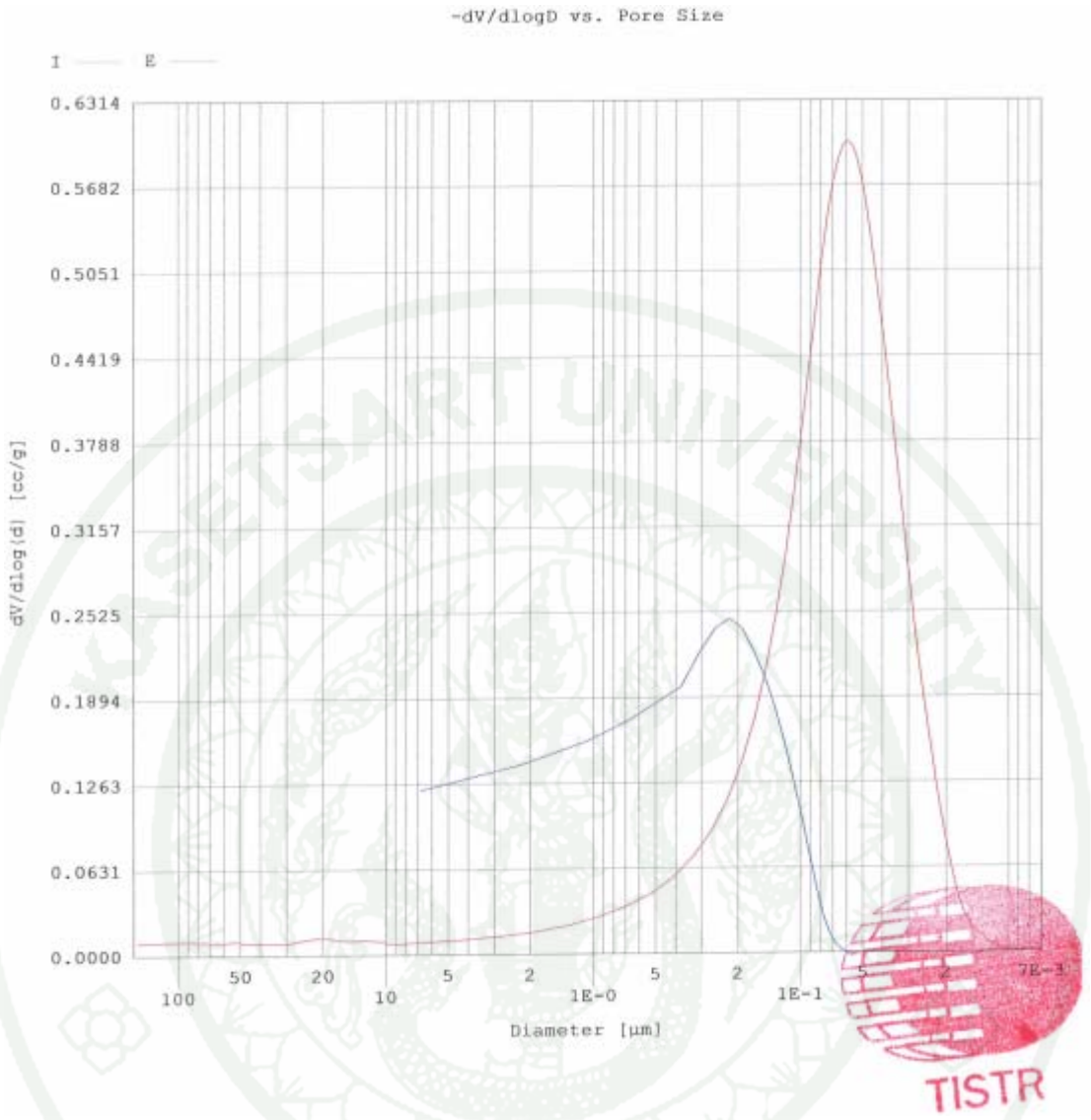

Appendix Figure B2 Pore size distribution in the MIP tests for the 4M geopolymer class F fly ash 60% after exposure to firing at 400°C.

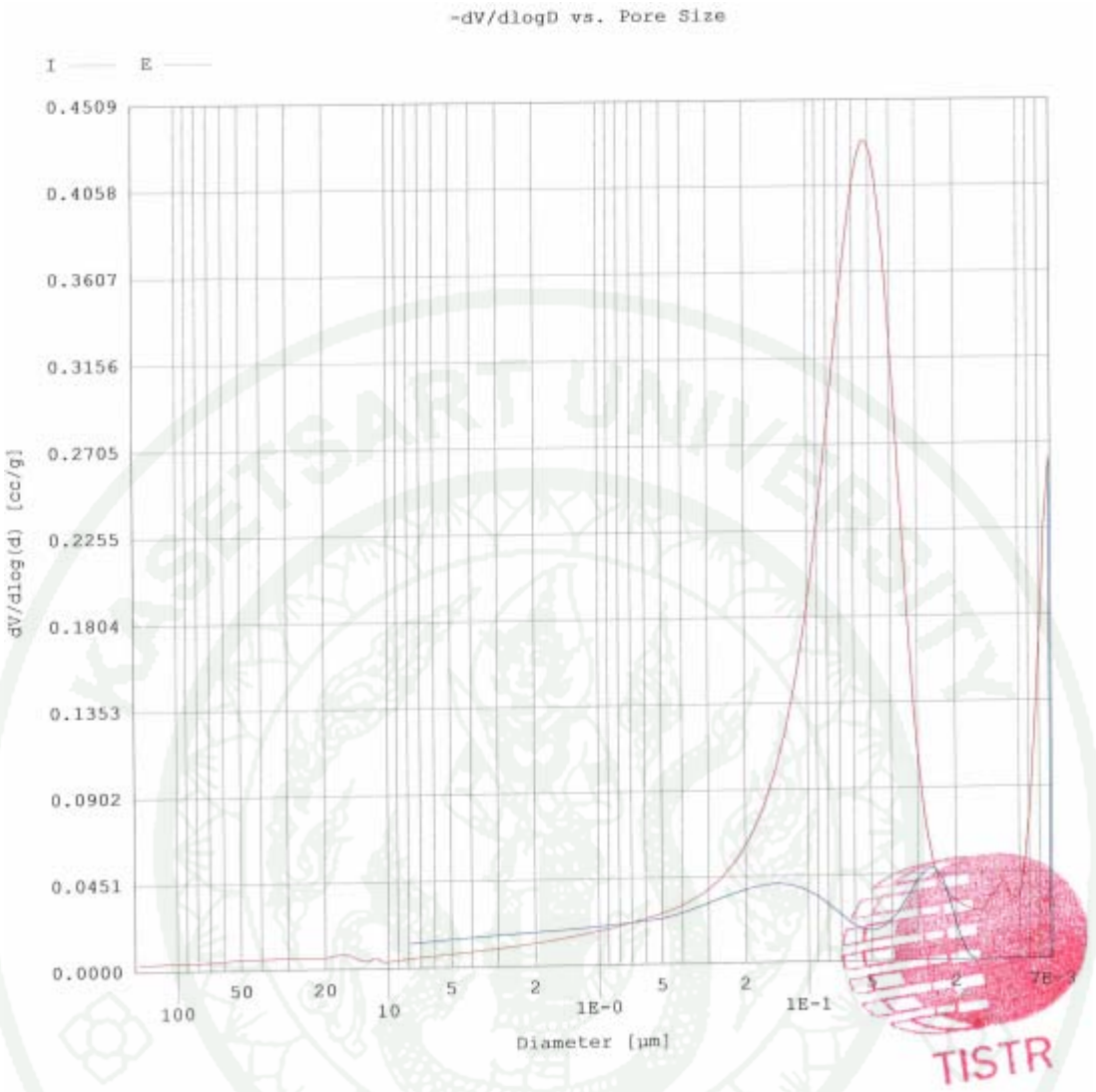

Appendix Figure B3 Pore size distribution in the MIP tests for the 8M geopolymer class F fly ash 60% before exposure to firing.

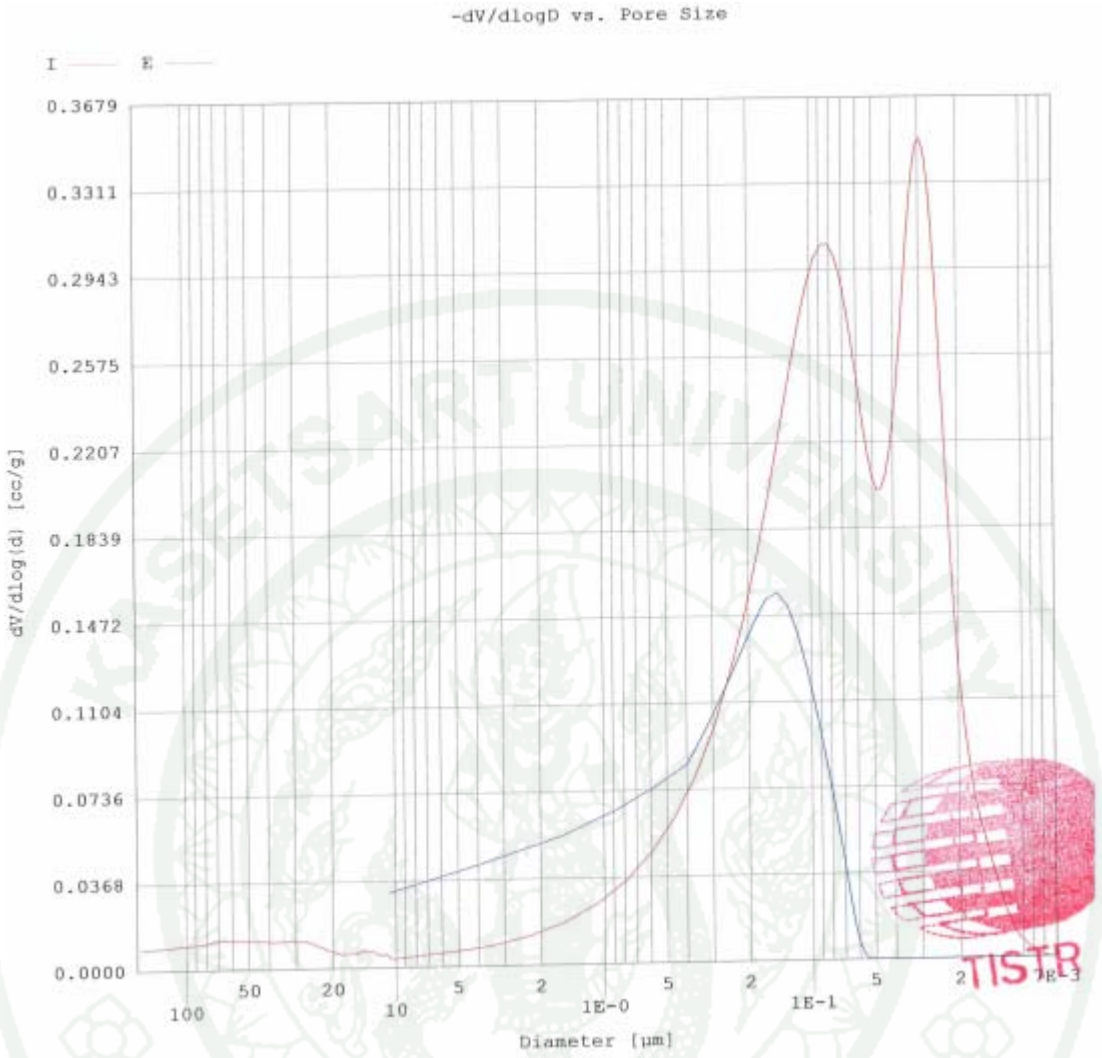

Appendix Figure B4 Pore size distribution in the MIP tests for the 8M geopolymer class F fly ash 60% after exposure to firing at 400°C.

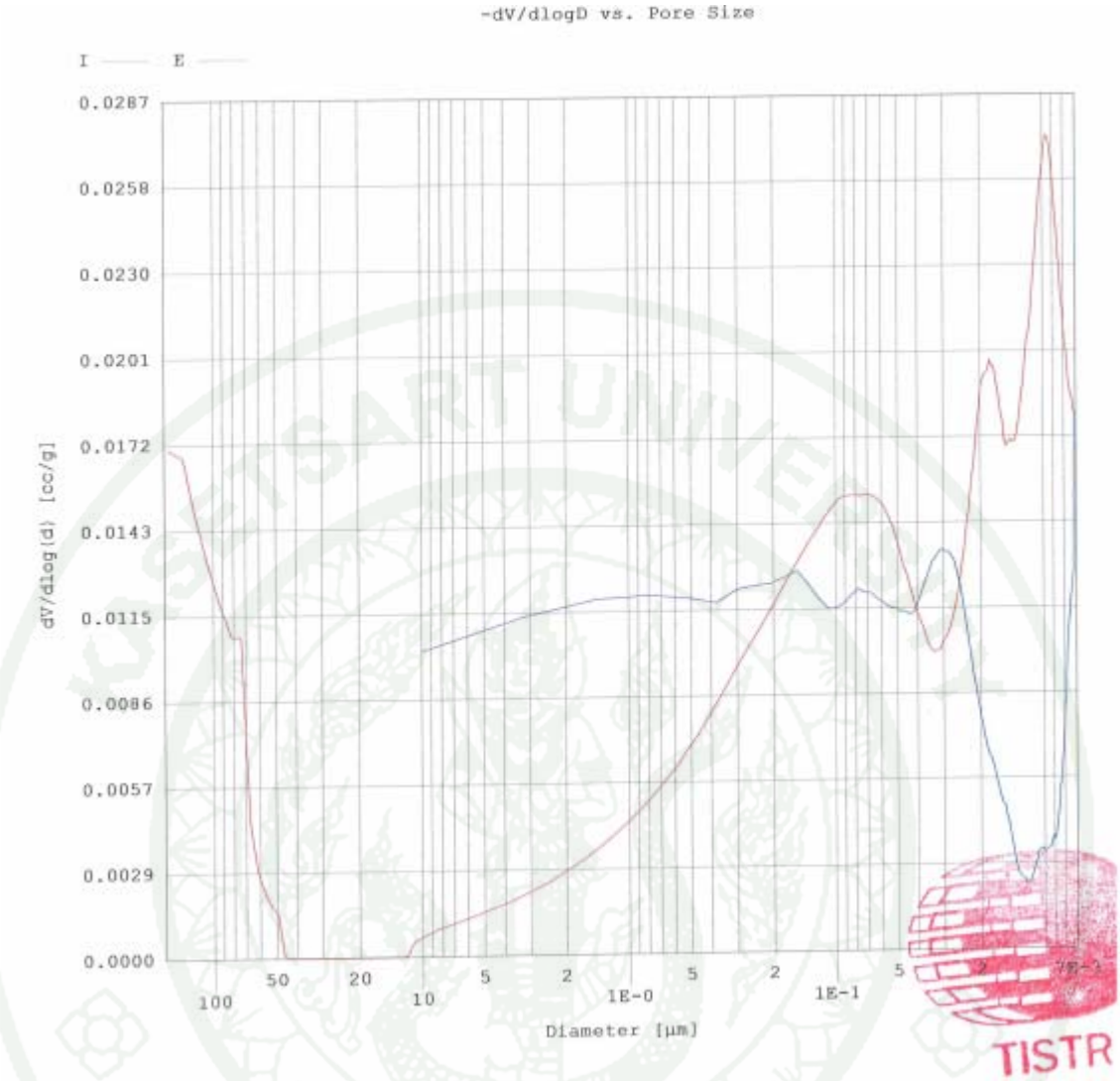

Appendix Figure B5 Pore size distribution in the MIP tests for the 4M geopolymer class C fly ash 70% before exposure to firing.

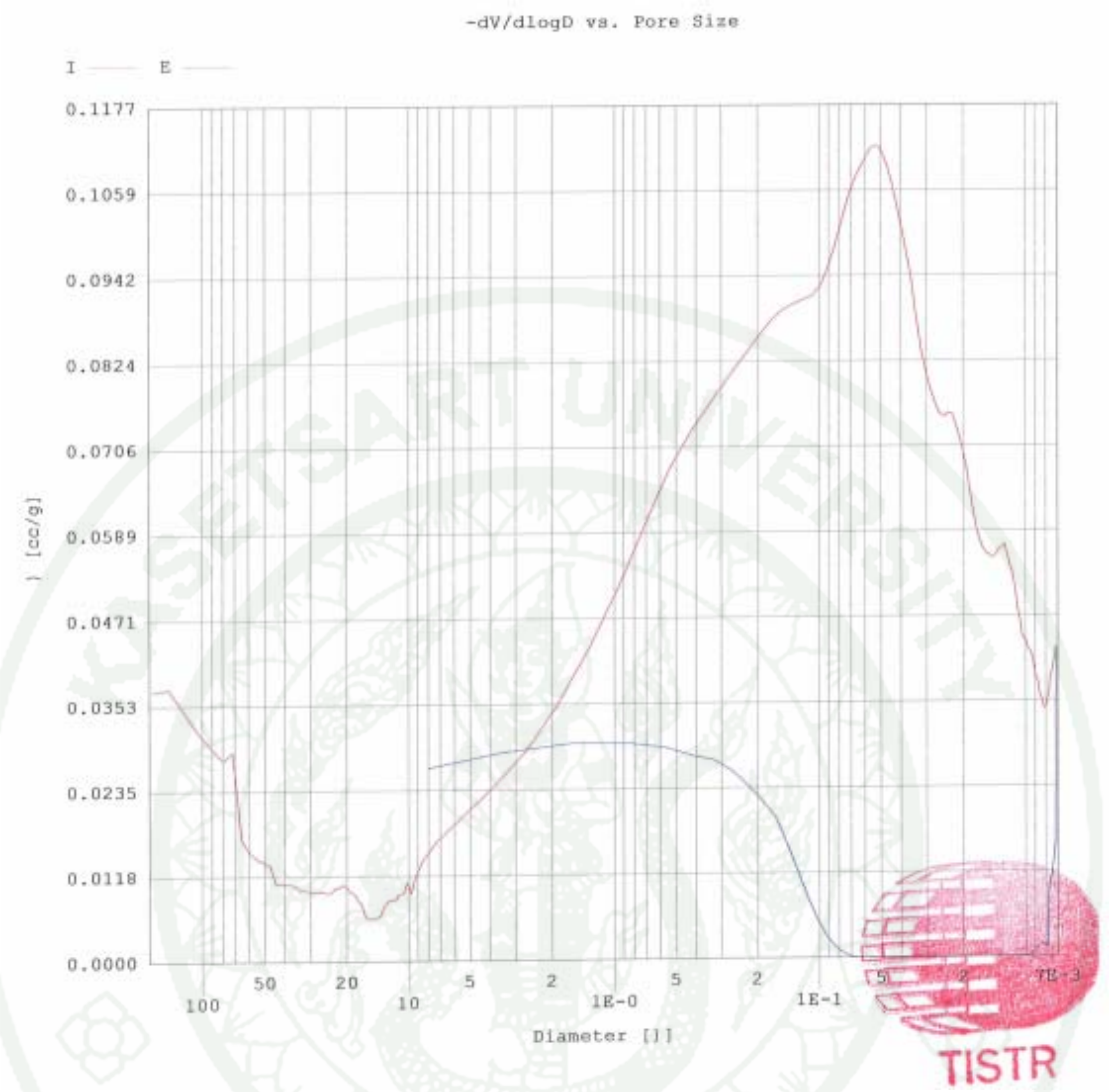

Appendix Figure B6 Pore size distribution in the MIP tests for the 4M geopolymer class C fly ash 70% after exposure to firing at 400°C.

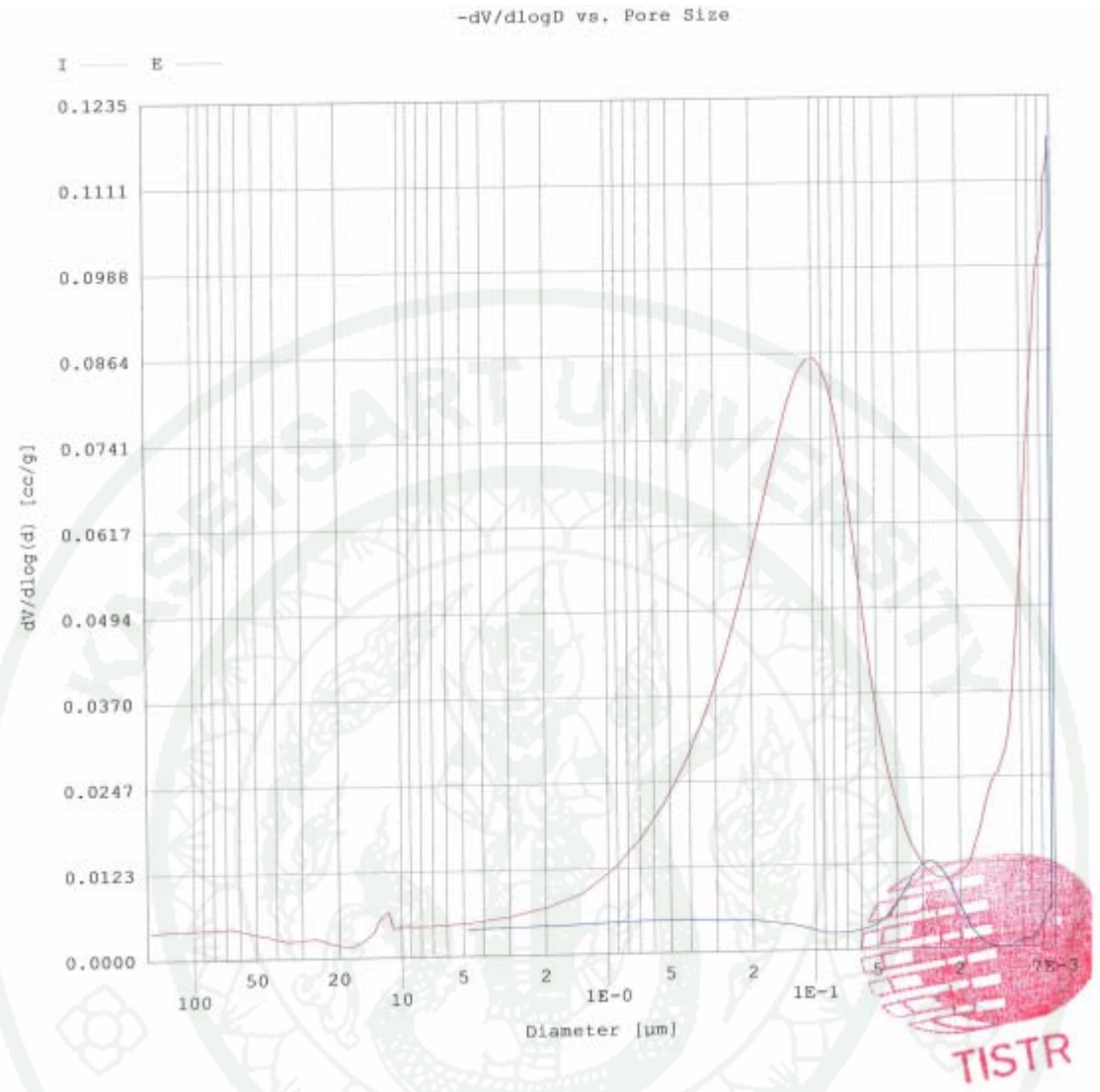

Appendix Figure B7 Pore size distribution in the MIP tests for the 12M geopolymer class C fly ash 70% before exposure to firing.

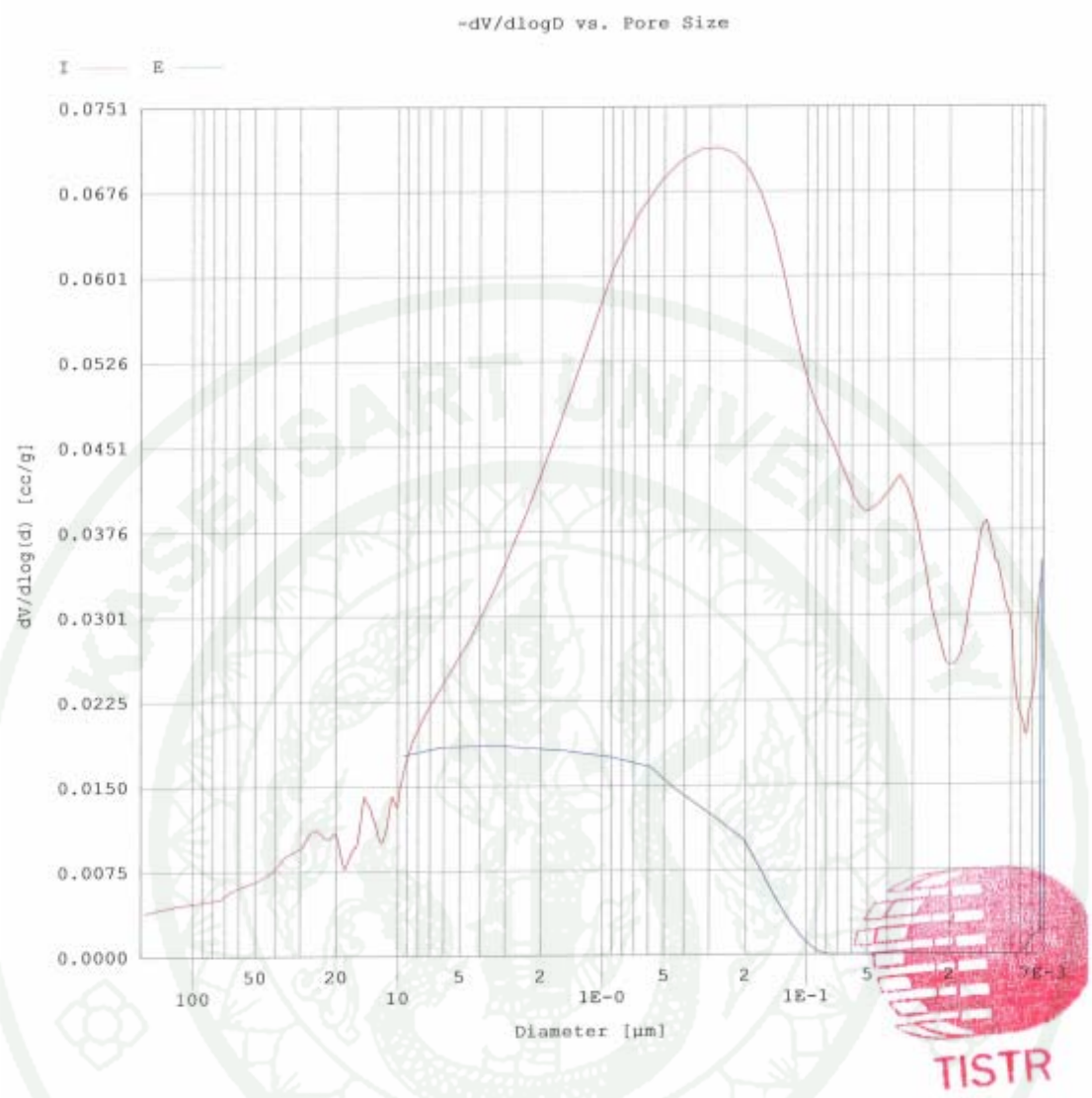

Appendix Figure B8 Pore size distribution in the MIP tests for the 12M geopolymer class C fly ash 70% after exposure to firing at 400°C.

Appendix Figure B9 Materials for experiment

Appendix Figure B10 Hobart mixer.

Appendix Figure B11 CWF1200 carbolite furnace.

Appendix Figure B12 Thermometer measurement and Regulator Flow-meter (LPG)

.

Appendix Figure B13 Result of thermal stability tests for class F fly ash mixed with 4M, 8M and 12M NaOH, post thermal exposure at 200°C.

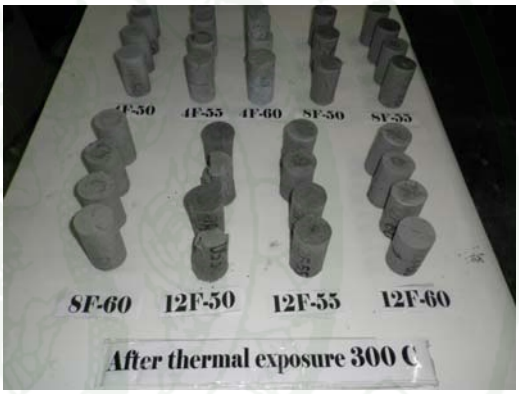

Appendix Figure B14 Result of thermal stability tests for class F fly ash mixed with 4M, 8M and 12M NaOH, post thermal exposure at 300°C.

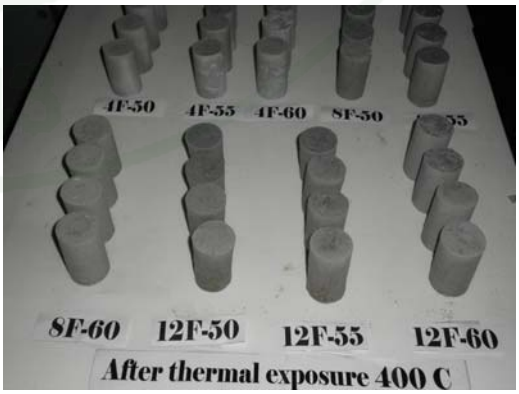

Appendix Figure B15 Result of thermal stability tests for class F fly ash mixed with 4M, 8M and 12M NaOH, post thermal exposure at 400°C.

Appendix Figure B16 Result of thermal stability tests for class C fly ash mixed with 4M, 8M and 12M NaOH, post thermal exposure at 200°C.

Appendix Figure B17 Result of thermal stability tests for class C fly ash mixed with 4M, 8M and 12M NaOH, post thermal exposure at 300°C.

Appendix Figure B18 Result of thermal stability tests for class C fly ash mixed with 4M, 8M and 12M NaOH, post thermal exposure at 400°C.

Appendix Figure B19 Result of fire-resistance tests after exposure for class F fly ash geopolymer-paste panels.

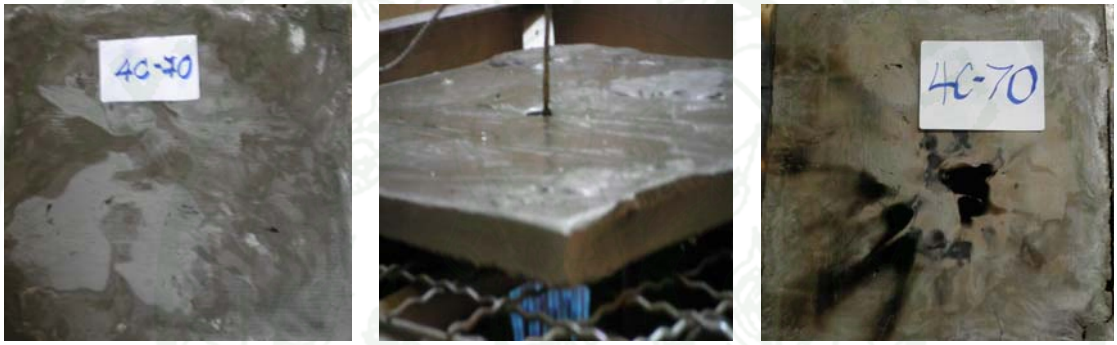

Appendix Figure B20 Result of fire-resistance tests after exposure for class C fly ash geopolymer-paste panels.

CURRICULUM VITAE

NAME : Mr. Tikumporn Thubpo

BIRTH DATE : March 29, 1977

BIRTH PLACE : Bangkok, Thailand

EDUCATION :

YEAR	INSTITUTE	DEGREE/DIPLOMA
2000	Kasetsart University	B.E (Irrigation engineering.)

POSITION/TITLE : Structure Engineer

WORK PLACE : Royal Irrigation Department